JPRS-CST-89-007
17 MARCH 1989

FOREIGN BROADCAST INFORMATION SERVICE

JPRS Report

Science & Technology

China

JPRS-CST-89-007

17 MARCH 1989

SCIENCE & TECHNOLOGY

CHINA

CONTENTS

CAS Approaches Reform of Basic Research

40080081b Beijing GUANGMING RIBAO in Chinese 9 Nov 88 p 3

[Article by Li Hongbing [2621 3126 0393] and Wang Yougong [3769 0642 1872]]

[Excerpt] Senior scientist Shi Changxu [1597 2490 4872] today called upon people to focus on basic scientific research in the Basic Research Work Conference of the Chinese Academy of Sciences. He said: "We have been saying all along that we will transform science and technology into production power, but if we still don't pay some real attention to basic research, we will not have research results to transform into production power years down the line." His words were enthusiastically applauded.

At a time when the basic research ranks are confused and affected by a number of external influences, the meeting held by the Chinese Academy of Sciences is undoubtedly an opportunity for the research officials of the branches to speak their minds. This afternoon they intently listened to a long speech by Academy President Zhou Guangzhao [0791 0342 0664].

Zhou believes that basic research must proceed steadily in the time of reform because it has revolutionary affects on the development of the society. He proposed that the principal goals of basic research at the Chinese Academy of Sciences should be as follows: The management of basic research should be conducted via optimization and competition, in the spirit of openness, exchange, and with the whole country in mind. A team of basic researchers led by middle-aged and young academicians should be gradually formed as the result of improved coordination and uniform planning. In a number of important frontier fields, active schools with international influence should be established to produce world-class research results. Basic research should contribute to the societal and economic development of China and provide senior personnel to the field of applied development.

President Zhou then stated adamantly that in basic research we must establish the thought of international competition and world standards. Phrases like "filling a void in China" and "advanced Chinese standards" should not be the goals of scientific researchers.

He said the research team should be "lean and mean" and must maintain stability in a changing time.

Zhou Guangzhao asked research leaders to have broad knowledge, a sharp mind, good organizational ability and a spirit of cooperation. While letting old scientists playing a directing role and middle-aged scientists be the main force of basic research, we must also discover and cultivate young talents. Special allocations should be made for a small number of superior young scientists with the potential of first-rate research outputs. In the meantime, encourage experienced basic researchers to go into applied research and development, or switch field and collaborate with other specialties to promote interdisciplinary activities.

Zhou also talked about careful selection of basic research topics and establish a limited number of targets. In the next 10 years the CAS should pay particular attention to rapidly evolving fields that require modest investment and topics with special natural environment characteristics of China. Examples are condensed matter physics, biochemistry, large molecule structure and function, global changes, etc.

When asked whether a basic research organization should keep instituting new systems in order to achieve the expected goals, Zhou answered affirmatively. He has a number of basic requirements on new systems: The system must face the nation and the world. It should have a liberal democratic and academic atmosphere conducive to competition, a flexible environment, superior facilities, and sound work conditions. The system should also have a highly efficient, reasonably staffed management force to coordinate the work.

Zhou said that the dozens of open laboratories established in recent years with openness, flexibility, and coordination represent a better organizational format for basic research institutes. Starting next year, national searches will be conducted for the directorships of the open laboratories so that these institutes may become advanced national science laboratories.

Zhou also revealed that the CAS is investigating reorganization of existing research and institutions so that a number of science centers can be established in the last 10 years of the century. The tentative plan calls for carefully selected outstanding young academic leaders to head these centers. Pre-doctoral and post-doctoral fellows will engage in the most dynamic frontier research in the science centers.

President Zhou pointed out that the CAS has a complete series of basic research institutes with considerable manpower and a variety of characteristics. They represent a team of highly skilled, experienced, and ambitious researchers capable of solving major problems of an integrated nature. [passage omitted]

Stimulating Basic Research Through Revamped Funding Program

40080068 Tianjin KEXUEXUE YU KEXUE JISHU GUANLI [SCIENCE OF SCIENCE AND MANAGEMENT OF S&T] in Chinese No 9, 88 pp 16-17

[Article by Jia Daping [6328 1129 1627] of the National People's Congress Education, Science, Culture, and Public Health Committee: "On China's Science Fund System"]

[Text] In 1982, the State Council approved establishment of the Chinese Academy of Sciences Science Fund and began conducting funding system experiments for basic scientific research. The State Natural Science Fund Commission was established in 1986, indicating a comprehensive shift in China to a funding system for basic and some applied scientific research.

Implementation of a science fund system and penetration of scientific research by competitive mechanisms are important ways to invigorate S&T progress in China as well as major reforms in S&T management systems. Their superiority over former level-by-level allocation of research funds by region and unit is becoming more apparent.

The basic methods involved in implementing a science fund system in China were: macro guidance, freedom in topic selection, and direct application for approval; appraisal by persons in the same trade or occupation, application for approval to a fund commission, and selection of the best topics for support; one-time appraisal and ratification, scheduled allocations, and special funds for special purposes; having applicants assume responsibility, with their units providing supervision and guarantees, and inspections and summarizations at fixed periods. The science fund system has the following advantages compared to the past method of allocations of administrative funds by bits and pieces:

First, it aids the state in carrying out macro guidance and management. In the past, basic scientific research topics usually were chosen by researchers themselves, which hindered state efforts to increase control and administration. This led to a great deal of low-level and redundant research in basic research and made it hard to concentrate the required manpower and capital for several major theoretical topics and basic research with important applicational prospects. In implementing the fund system, the state has used methods such as formulating the relevant regulations and

articles, compiling fund topic selection guides, appraisal by persons in the same trade or occupation, application and approval by a fund committee, and so on, which enabled it to improve effective direction and implement macro management for key research directions, spheres, and even topics.

Second, it has helped break down barriers between departments and regions and promote horizontal integration of S&T personnel in different units. In the past, restrictive and fractionated allocation of research expenditures by department and region often separated research personnel and hindered mutual integration to form more effective research systems. The fund system breaks down these barriers and enables people responsible for project applications to cooperate with those having common goals and organize structurally rational research collectives with matching tacit understandings.

Third, the fund system's implementation of "appraisal by persons in the same trade or occupation, selection of thebest topics for support" has brought competitive mechanisms into scientific research work. This has enabled scientific research personnel to struggle upward and strive to improve their own qualities and research levels. It has aided the state in using limited research funds for units and research personnel to enhance their research capabilities and working conditions, which in turn has improved the results of investments in research.

Fourth, it has aided in raising the sense of responsibility of units and research personnel. The state approves projects and funds, directly allocating them to the applicant or the unit in which they work, with responsibility by the applicants and the units providing supervision and guarantees. Applicants have rather full independence in decision making over project research personnel, fund utilization, and work arrangements. The result is direct responsibility for project completion and a much stronger sense of responsibility.

Of course, many problems remain in China's implementation of a science fund system.

1. There is a severe shortage of science funds, which requires that the state increase science funds.

Scientific research units in China, particularly those involved in basic research, have had insufficient funds for a long time and are in a state of instability. The situation has improved since the Natural Science Fund was established, but the science fund is far from adequate and there is an increasingly severe trend toward a lack of conditions. One prominent manifestation is the continual decline in the approval rate for topics and the strength of average project capital support over the years. The approval rate and average amount of capital support per project was 48.7 percent and 56,000 yuan, respectively, in 1982, but fell to 23.3 percent and 29,300 yuan in 1987. Most capital assistance funds for projects are allocated over 3 years, so the yearly amount per project is under 10,000 yuan. The approval rate for topic applications is less than

one-fourth. Experts feel, however, that these project applications are class A ones, meaning projects of rather great significance or value which should receive funding, and should account for more than one-third of project applications.

S&T expenditures in China as a proportion of GNP are low compared with many nations. State basic scientific research expenditures also comprise a small proportion of total S&T expenditures. This statistic in 1986 was 20.9 percent in France, 16 percent in England, 15.9 percent in Japan, 15.7 percent in Italy, 13.2 percent in the United States, and 10.7 percent in Hungary. In China, however, it was less than 5 percent, with the State Natural Science Fund providing less than 1 percent. Some research institutes involved mainly in basic research haveindicated that about 30 to 40 percent of their scientific research personnel were unable to proceed normally with their work because they failed to receive applied-for funds or had severely inadequate funds. Many scientific research units have complained of difficulties in obtaining funds from technology markets for applied research and research of a technical reserve nature, and in applying to the science fund. If this continues for very long, there is a latent risk of a steady reduction in S&T reserves. The state has decided that funding for scientific research activities eliminated or reduced during reforms can still be used to support and develop scientific activities. We feel that it is entirely necessary and feasible to deduct a portion of these and other state S&T appropriations to add to the science fund.

2. Establish personnel circulation personnel systems, strengthen cooperative research among different units.

Skilled people are the key to all undertakings. This is even more important in basic research, which is highly exploratory. It requires project leaders with substantial scholarly levels and organizational leadership capabilities as well as a lean, capable, and rationally organized research collective with matching tacit understandings. This type of research collective often must be composed of personnel from different regions and units. Thus, implementation of a science fund system should be combined with gradual establishment of a personnel system in basic research work to allow free circulation of scientific research personnel.

Implementation of the science fund system has opened the route to establish this type of cooperative research collective. However, many obstacles still exist. Examples include the departmental ownership system for personnel, barriers to administrative relationships, restrictions of working conditions, family problems, and so on. We must create the conditions to promote development of basic research and applied research in China and gradually solve these problems. This is especially true of the need to establish dual-position systems and visiting research systems to enable S&T personnel in other research units to encourage research personnel in different units to take matching dual positions, encourage visiting research, and establish open laboratories to absorb talented S&T personnel from all fields for cooperative research.

3. Strengthen science fund management and services.

Administrative personnel for science fund management work in China have problems of insufficiency, low quality, and other things, and many areas need improvement. Examples include research on scientific discipline policies, planning guide formulation, inspection and management of capital assistance projects, examination and acceptance of completed projects and evaluation of their results, development of international cooperative research, and so on. Several things in project administration, appraisal, examination and approval, allocation, and so on require improvement. Some units, for example, have complained of the long period between application for funds and their approval and allocation. In the area of allocations, some units require more funds to create working conditions during the initial stages of a research project, but the fund uses "one-time examination and approval" and basically allocates funds according to a yearly average figure, which cannot meet the real situation and needs of research work. Some units and scientific research personnel have indicated that channels for supplies of instruments, equipment, reagents, pharmaceuticals, laboratory animals, and other scientific research materials are not sufficiently open, which often affects smooth research progress. Some research requires purchases of small quantities of materials, pharmaceuticals, and reagents from abroad, but they are hard to obtain because they lack a small amount of foreign exchange. These problems have shown that reinforcement of science fund management work should be combined with a corresponding strengthening of service-type work.

4. Implement legislation for China's science fund system.

Many nations of the world with science fund systems have used the national situation in their particular country as a basis for state legislation to establish various science fund systems. For example, the National Science Fund established by law in the United States is an organ of the federal government which provides funding support to universities, research institutes, non-profit organizations, and so on. It is a key government mechanism for promoting the development of S&T. National laws also encourage the establishment of many non-governmental and non-profit private fund commission organizations, and these private funds play important roles in promoting development of scientific research activities in the United States.

As China continues to develop State Natural Science Fund work, many other forms of science funds and organs to administer them will be created. Examples include establishment of seismic and geological science funds according to disciplines, coal, machinery, and petroleum science funds according to industries, establishment of provincial and municipal technical development funds according to region, as in Shanghai, Shanxi, Guizhou, Guangdong, Chongqing, and other places, and establishment of science funds in many institutions of higher education and scientific research units. These different categories of science funds have played a very good role in promoting scientific and technical research in these disciplines, industries, regions, and units. The establishment of S&T funds of different

types and at different levels and the state's legislative recognition of their existence have promoted their development, and will benefit further motivation of initiative in all areas to show concern for and support S&T research and accelerate their development. The State Natural Science Fund Commission and other S&T fund organizations should use legislation to clarify their legal status, duties, and functions and give them sufficient independent functions and authority in applying for science funds, organizing expert appraisals, deciding on the amount of funds, examining research work in funded projects, and other areas and to remove any illegal interference by administrative organizations and other institutions. Legislation also should be used to clarify and coordinate interrelationships between them and other relevant organizations and individuals, to make stipulations on procedures for application, appraisal, examination, approval, allocation, inspection, and other things, to assure that science fund has a scientific, democratic, and legal nature.

(Responsible editor: Xu Jing [6079 7234])

Hunan Province Adopts "Torch Plan" Measures

40080087b Beijing JISUANJI SHIJIE [CHINA COMPUTERWORLD] in Chinese No 45, 23 Nov 88 p 1

[Article by Xiang Hanyuan [0686 3352 3293]: "Hunan Province Draws Up 'Torch Plan' That Will Focus on Microelectronics Information Technology"]

[Text] Concerned departments in Hunan Province are in the process of drawing up a "Torch Plan" for this province to stimulate the transformation of the achievements of high and new technologies and from phased results into commodities. The focus of the near-term goals will develop in three fields: microelectronics information technology, new materials technology, and biological technology. They have also applied to the State Science and Technology Commission for product development for the "Galaxy" supercomputer as one of the six projects for the state "Torch Plan."

This year, Hunan Province selected high-technology projects needing little funding, having a large insurance factor, and having high results to be their first steps toward implementing the "Torch Plan," after which they began full-scale efforts.

Hunan is preparing to work hard for three years to develop nearly 100 high- and new-technology products, among which one-third will be for export and the generation of foreign currencies; they will initiate 100 high- and new-technology enterprises; and they will train thousands of high- and new-technology entrepreneurs, managers, "Torch Plan" management personnel, and management personnel for S&T development experimental areas, who all will work toward an export-oriented economy and will participate in international competition.

Vice Minister Tells of Machinery and Electronics Outlook for 1989

40080087a Beijing ZHONGGUO JIXIE BAO in Chinese 24 Nov 88 p 1

[Article by Liu Jianguo [0491 1696 0948]: "'To Harness and Rectify' is Both an Impetus and an Opportunity"]

[Text] In the coming year, China's Ministry of Machine-Building and Electronics Industry (MMEI) will face up to a stern test, which is the unanimous view of experts in the machinery profession. In that situation, what are to be the circumstances and mission for the machine-building and electronics industries? A Vice Minister of this ministry, He Guangyuan [0149 0342 6678], recently spoke on this question at a meeting held in Beijing.

One Environment That Must Be Rectified

He Guangyuan said that beginning this year, production growth for MMEI units has been at a rapid pace. During the period from January through September, these industries continued the rapid growth of the previous year by continuing with about a 20 percent increase in growth, which was clearly higher than the growth rate for all industries throughout the country--17 percent--during the same period.

At the same time, the scale of fixed assets investment for the machinery industry has not declined, primarily due to the excessive number of projects outside state planning. To use this year's funding for technology transformation of the machinery and electronics industries as an example, 1.98 billion yuan was planned by the state for 1986, but 6.54 billion yuan was actually spent; 2.59 billion yuan was planned for 1987, but 7.6 billion yuan was actually spent. In these years, the volumes of fixed-asset funding for the machinery industry were two and three times that of state planning. There are about 200,000 machinery and electronics enterprises throughout the country at present, but new ones continue to spring up, and conditions of duplication of distribution, of construction, of production, and of importing have become serious. For example, 142 designated production facilities were planned for the electric wire and cable industries, but this has now grown to 3,000; nine production sites were designated throughout the country for video tape recorder production, but another nine provinces and municipalities have requested to be added, and color TV tubes and stored-program-controlled [telephone] exchanges have also become hot items.

He said that in general the current situation for the machinery and electronics industry is no different from that of the overheated economy at large, as the explosion in capital for industries throughout the country, their expenditure of funds, and their runaway loans have all been reflected in the machinery and electronics industry to one degree or other. We must seriously reflect on this and exert great effort to harness the economic environments of industry and rectify the economic priorities of those industries if we are to ensure the smooth progress of the restructuring and growth.

Harnessing and Rectification Are Beneficial to the Machinery and Electronics Industry

He Guangyuan said that as we harness the economic environment and rectify economic priorities throughout the country, as far as the machinery and electronics industries are concerned, as long as we are resolute and uncompromising in our implementation of the decisions made by the central authorities, we will be able to healthily develop and create an excellent economic environment and conditions for growth.

One, we must reduce the scale of capital construction and bring down the "investment fever" that is prevalent everywhere, which actions would without doubt benefit the investment of limited funds for the machinery and electronics industry in the major projects for industry growth. At the same time, it would also benefit the adjustment and optimization of commodity structures for the machinery and electronics industry, consequently making industrial and commodity structures throughout the industry more rational.

Two, we must reduce credit and control social demands overall, which can to some degree alleviate the tight situation regarding energy resources, transportation, and various goods and materials. Take steel products, for example. From the point of view of the 50 billion yuan in fixed-assets funding already clearly reduced by the state, if 800,000 tons of steel are needed for each 10 billion yuan of fixed assets, we then would reduce our consumption of steel by about 4 million tons, which could possibly allow the current shortage of steel for the machinery and electronics industry to turn for the better. By tightening up on finances, we could be quickening the pace of restructuring of the system of property rights, which would give impetus to the growth of a stock system and enterprise mergers. This would provide an excellent opportunity and conditions for the restructuring and optimization of organizational structures in the machinery and electronics industry, and it could also cause what wins and what loses to become more apparent, greatly forwarding the progress of the restructuring of all industries.

Three, we must bring down the pace of growth and extinguish the economic fever. This will help enterprises put the bulk of their energies into seeking a shift of output values toward improving economic results. This would fully release the potential held by enterprises and transform the quick results that are so difficult to maintain into reliable economic results.

Four, the Central Committee has clearly demanded that the inflation index for the prices of goods be clearly lower next year than this. This will relieve the heavy burden of machinery and electronics enterprises that derives from the great increases of prices for raw materials, and will aid the healthy development of the enterprise contract operations responsibility system.

Five, we must rectify economic priorities, and especially must rectify the confusion rampant in the realms of circulation. This would create a largely equal competitive environment for various kinds of enterprises, which undoubtedly would benefit the growth of the machinery and electronics enterprises, especially that of the medium to large key enterprises.

Six, on this occasion of harnessing the economic environment, we will comprehensively use the means of economic, administrative, legal, disciplinary, and ideological work, all of them in turn, to enhance and improve the overall control of economic activity. This will play a major role as we strengthen overall control and promote industrial management.

A Serious Test

He Guangyuan said that major trends for the state will benefit the restructuring and growth of the machinery and electronics industry. However, we should be well aware at the same time that this major decision by the Central Committee to harness the environment and rectify priorities will be a new serious test for the machinery and electronics industry.

The chief points to be dealt with first are: reducing scale and controlling demand, which means that the domestic market demand for electro-mechanical products will fall. Looking at the fact that beginning next year there will be a reduction in the scale of fixed-asset funding, funding for equipment will be reduced and orders for electro-mechanical equipment will drop correspondingly. This will affect the market for electro-mechanical products, bringing even fiercer competition to the marketplace.

Then, the trend to cut back will inevitably lead to anxiety about circulating capital for enterprises, credit will become more difficult, and some scientific research, production, and technology transformation projects will find it difficult to proceed because funds will not be secure. At the same time, slowing the rate of growth for production will effect the rise of enterprise profits, retention of said profits by enterprises will be reduced, there will be an increase in the number of them that fail, and economic results for all industries will be volatile.

Also, although suppressing demand and controlling scale might bring some relief to the situation of shortages of materials, conflicts in supply and demand for some non-ferrous metals and steel products will not be able to be resolved in the short-run.

In summary, the situation faced by the machinery and electronics industry is quite serious, for there are not only many beneficial factors urging us onward, but we are also faced with the tremendous pressure of various difficulties. Whether or not we can ride out this new situation will be a major test of the capacity and level of management for China's machinery and electronics industry.

The Primary Mission for the Machinery and Electronics Industry

He Guangyuan proposed that in the face of these conditions, we must become vigilant about many things, must maintain clear heads, and must take up the policies made for this new situation to better accomplish the major tasks that face us in these new circumstances.

First, we must take stock of our own real situations, must harness our economic environments, and must rectify economic priorities to form a new industrial environment and new priorities. Second, during the next two years as the machinery and electronics industry everywhere intensifies its restructuring: (1) we must strengthen overall control under the new circumstances, promoting industrial management; (2) we must invigorate the medium to large enterprises; and (3) we must transform organizational functions. Third, we must actively make the most of the new situation in which machinery is combined with electronics. Fourth, we must more closely integrate maintenance of an ongoing restructuring with the execution of development strategies for science, which would allow the entire industry to safely effect the replacement of old systems with new. Fifth, we must further expand the exports of electro-mechanical products to lighten the pressure that comes from the sagging domestic market for electro-mechanical goods. Sixth, we must develop high and new technologies to support the formation of new industries. Seventh, as products grow, we must make rational the relations between laying foundations, paying attention to important points, and striving for completeness. Eighth, we must make the most of political advantages and rely upon ideological and political efforts, as well as iron discipline to serve restructuring and development.

Vice Minister He Guangyuan pointed out that in general we can transform the enormous difficulties and pressures created by the objective factors--this occasion of controlling demand, reducing scale, slackening the pace, and reducing the money supply--into an impetus and opportunity to spur on the development of our industry. In consequence, this will allow our industry, even all industries, to experience a significant resurgence, enabling the restructuring and development of the entire industry to make great strides forward, finally realizing the flourishing of the machinery and electronics industry.

Greater Involvement in 'Torch Plan' Reported

Local Implementation Detailed

40080084 Beijing RENMIN RIBAO in Chinese 26 Oct 88 p 3

[Article by He Huangbiao [0149 7806 1753]: "The 'Torch Plan' Is Being Firmly Implemented Everywhere"]

[Text] Since the State Science and Technology Commission convened its first "Torch Plan" working session in August this year, many areas, departments, research institutes, and higher institutions throughout the country have drawn up plans and topics for consideration. They have also arranged for their scientists and technical personnel to involve themselves in research and development for the high-tech and new-tech industries.

Beijing Municipality, which is strong in skilled personnel and technology advantages, has worked out an outline for the "Torch Plan." It is their goal that within 3 years, 500 high- and new-technology enterprises will have begun operations, and they are encouraging these enterprises to form associations with medium to large enterprises and with township enterprises. They hope to develop about 500 high- and new-technology products, among which 70 percent can reach commercial production, that volume of operations for these high- and new-technology enterprises would reach 5 billion yuan, and that they can train some 2,000 operations, management, and international trade personnel.

The "Torch Plan" was first implemented in Tianjin Municipality. Nine specialized trades, 18 small groups, and 71 individuals formed a team of experts, which did a great deal of survey work and has undertaken the first phase of the screening for 1989-90 "Torch Plan" projects. They screened 93 projects in Tianjin Municipality for development, among which are microelectronics technology, computer and office-automation technology, fiber-optic communications technology, laser technology, new materials technology, biological engineering, electronic and mechanical consolidation technology, and new energy source and high efficiency energy conservation technology. Completion of these projects will see annual revenues from profits of 200 million yuan, and will fully realize the characteristics of high-level pricing for high- and new-technology products.

Some research institutes, S&T development companies, and institutions of higher learning that focus primarily on high and new technologies are following the principle of "having limited goals and outstanding points of emphasis" in accordance with the thought: "target the future and follow up enthusiastically" as they join in the "Torch Plan." Academy No 7 of the China State Shipbuilding Corporation, which has more than 20 institutes, more than 100 large-scale laboratories, and 12,000 middle and high-level technical personnel, applied for 209 projects at one time, but after careful screening, 10 of these were recommended to the state, and all were accepted. One among them, the high-precision numerically controlled well logging system, involves more than 60 specialties, such as acoustics, optics, electricity, electronics, nuclear technology, precision machinery, and information transmission and processing. A new-technology enterprise under citizen collective ownership that integrates scientific research, engineering, production, and technology trade--the Beijing Municipality Jinghai Computer Group Company, has established three specialty companies for the transformation of the results of scientific research and for development of high and new technologies, which next year will have turned 10 research achievements into products. Qinghua University, rich in skilled personnel, has mobilized nearly one-tenth its force of S&T personnel for participation in the "Torch Plan." Currently, they have applied for 41 projects, and some of the project groups are hurrying to produce samples. Some have developed multi-channel, varied lateral associations, have worked hard for foreign funding, and have broken into international markets.

It is said that areas like Shanghai, Guangzhou, Wuhan, Xi'an, and Shenyang have widely arranged for S&T personnel to become involved in the "Torch Plan."

Song Jian Spells Out Strategy

40080084 Beijing RENMIN RIBAO in Chinese 26 Oct 88 p 3

[Article: "We Will Create the Environment and Conditions Beneficial to the Development of High-Technology Industries"]

[Text] State Councillor and Minister of the State Science and Technology Commission Song Jian gave a talk recently on how to implement the "Torch Plan" in which he demanded that each relevant area and sector energetically create an environment and conditions conducive to the formulation of policies and measures necessary for the development of high and new technologies.

Song Jian said that in March of this year the party Central Committee and the State Council had put forth the demand that scientific and technical sectors make the most of S&T advantages and participate in the facilitation of the coastal development strategy, which demand occasioned a new outlook for scientific and technical endeavors. Many sectors and regions made provisions for an intense restructuring of the science and technology system, which enlivened the development of complementary policies and encouraging measures for the high- and new-technology industries. Countless S&T experts have responded to the call of the Central Committee, and are

leading S&T workers in the building of an economic entity where science and technology is at the forefront and is closely integrated with skilled workers and trade, to boldly welcome scientific and technical competition that is world-class in stature.

He said that at present in China, there are about 1.3 million scientific and technical personnel in science research organizations, higher institutions, and medium to large enterprises, and that aside from those engaged in basic research and applied basic research that are supported with state funds, those engaged in the "863" plan, and those engaged in key projects for the "Seventh 5-Year Plan," some two-thirds of the more than 1 million other scientific and technical personnel are underemployed. Therefore, if we are to make the most of China's scientific and technical advantages, their potential for participation in the coastal development strategy and for the development of foreign export-oriented high- and new-technology industries is great.

The goals of the "Torch Plan" are primarily to provide research organizations and higher level institutions throughout the country, medium-to-large enterprises and military-industrial enterprises that have stronger abilities in technology development, as well as tens of thousands of scientific and technical personnel, with safeguards in the form of policies as they become part of the coastal development strategy to develop high- and new-technology industries. The goals are also to organize leadership, train cadres, clear the channels for the rational organization of technology, capital, and skilled personnel, and to create a beneficial social environment both domestically and abroad that will foster an appropriate climate. The "Torch Plan" is similar to the "Spark Plan" in that it is not prescriptive planning solely concerned with arranging for commodities, ascertaining projects, and allocating funds, but rather is overall guidance planning. In the early stages, the particular facilitation measures for the "Torch Plan" are: to draw up policies and management methods that attract funds and skilled personnel, and that found high- and new-technology industries, and to establish high- and new-technology parks in areas where the conditions are ripe, to build a group of pioneering service centers, that is, incubators for high- and new-technology industries, and to provide various services for S&T enterprises and start-ups; to train skilled personnel for the high- and new-technology industries; and to seek out funds for S&T enterprises and start-ups, and clear the credit channels.

Song Jian pointed out that implementation of the "Torch Plan" will require placing an intensifying transformation at the forefront of all efforts. The facilitation of the coastal development policy and the "Torch Plan" will provide a powerful impetus for the restructuring of the science and technology system at major institutions, colleges and universities, and medium to large enterprises. The Central Committee and the State Council are placing their hopes in the S&T departments of all the ministries and commissions, and in the research organizations and higher institutions. We must not lose this rare historical opportunity. We must be daring and bold, must give full play to our own advantages in science and technology, must take the initiative in striking out [on our own], and must make these things part of our economy.

He said that looking at this from the view of the growth of science and technology, the "Torch Plan" will erect a bridge for the commercialization of technological achievements, and it will create an excellent environment and conditions for the entrance of achievements from the stages of the 863 and key project plans. Therefore, scientists and technical specialists involved with key project plans, 863 plans, and projects funded by the National Natural Science Foundation should make full use of the environment and conditions created by the "Torch Plan," no opportunity should be lost, and they should take the initiative to promptly present their own new achievements. Scientists engaged in basic research and in applied research should turn their attentions to discovering and getting hold of whatever new thinking, concepts, theories, technologies, or methods that have value as market commodities, which will provide a never-ending flow of new knowledge and information for the formation and development of new- and high-technology industries.

Song Jian proposed four basic principles to be followed in facilitating the "Torch Plan":

First, we must continue to walk on both legs. On the one hand, all ministries and commissions of the central government, all medium to large enterprises, all academies and institutes, and all financial organizations should initiate high- and new-technology industries in a planned way. On the other hand, they should also adopt all possible measures to forcefully maintain and encourage large academies and institutes, higher institutions, medium to large enterprises, and S&T personnel to generate their own funds and to take responsibility for their own gains and losses, which will create S&T enterprises of varied forms of ownership that merge the trade of technology and labor with the trade of technology and agriculture, where the marketplace is the goal for which to develop high- and new-technology commodities.

Second, each S&T plan funded and implemented by the state and by government departments at all levels, as for example the key projects plan and the 863 plan, should maintain the principle of making commodities of phased achievements. For all phased achievements that are possible to transform into commodities and that can occupy a share of the market, efforts should be made to carry out product development.

Third, in developing high- and new-technology industries, we must maintain the principle of opening up to the outside world, and when high technology and its products begin to have an international character, we must seek out ways to make them available abroad.

Fourth, in the building of high- and new-technology industries and the execution of the "Torch Plan," we must maintain a way to act where there is "painstaking leadership, awareness of strengths, a focus on breakthroughs, models to show the way, and a progressive opening up." We must not proceed blindly.

BRIEFS

Key Genetic Engineering Lab Completed--The construction of the State Plant Molecular Genetics Laboratory has been completed in Shanghai. Already checked and accepted by the State Planning Commission and the CAS, the laboratory will be engaged in basic research and the application of plant molecular genetic engineering and gene engineering. The laboratory is responsible for 24 national key projects including high-tech research projects and joint research with foreign experts. The study of such subjects as controlling factor of higher plant transposon and its expression, plant cell transformation, gene expression and control of plant cell division and its development will provide scientists better information for developing more disease and pest-resistant crops. /40081021 Shanghai JIEFANG RIBAO in Chinese 29 Oct 88 p 1/

Xichang Satellite Launch Center Detailed

40080109 Beijing SHIJIE DAODAN YU HANGTIAN [MISSILES AND SPACECRAFT] in Chinese No 10, Oct 88 pp 10-13

[Text] China's Xichang satellite launch center is a modern satellite launch and test facility with headquarters in Sichuan Province's Xichang City and the launch site located approximately 60 km northwest of the city. The launch center is divided into the following organizations: the launch site, the technical center, the command and control center, and the tracking stations. The tracking stations are located in Xichang and Yibin of Sichuan Province and in Guiyang of Guizhou Province.

The launch center can be easily reached by several different means of transportation: the Xichang Airport, which can accommodate large airplanes; the Chengdu-Kunming railroad and the Sichuan-Yunnan highway, both of which pass through the city of Xichang; and the dedicated railroads and highways which connect the launch center with the technical center, the launch site and the command and control center.

The launch center has been completed to conduct test launches and operational launches of various payloads carried by the Long March-3 launch vehicle (e.g., communications satellites, broadcast satellites, weather satellites, etc.). Specifically, four communications satellites have been launched from this launch center:

1. On 29 January 1984, an experimental satellite was launched;

2. On 8 April 1984, an experimental communications satellite was launched into a geosynchronous station at 125° East longitude above the Equator;

3. On 1 February 1986, an operational communications satellite was launched into a geosynchronous station at 103° East longitude above the Equator;

4. On 7 March 1988, another operational satellite was launched into a geosynchronous station at 87.5° East longitude above the Equator.

The last three operational satellites have now become China's valuable assets in satellite communication.

The Technical Center

The technical center is responsible for the disassembly, assembly, unit test and inspection, subsystem test, system integration, and overall inspection of the launch vehicle and the payload; it is also responsible for the test, inspection and installation of combustible products, the filling of hydrazine, and the temporary storage and relocation of the launch vehicle and payload. The center is equipped with the following facilities: test chambers, preparation rooms, filling chambers, final assembly hall and leakage inspection room for the payload; test chamber for the launch vehicle; test chamber for the apogee motor; and storage room and test chamber for cumbustible products. Also, under construction are a satellite preparation room, a propellant filling facility, a solid rocket engine room, a rocket cooling facility, and an X-ray facility.

The Launch Site

The launch site is where the launch vehicle and the payload are erected and joined, tested and inspected, adjusted for bearing, filled with propellant, ignited, and launched. It has a stationary launch tower with an underground channel to vent the exhaust gas and smoke; the preparation and launch operations are carried out above ground. The launch site includes the launch pad, the launch tower, and the control room. On top of the launch tower is an ultra-clean room which is at the same height as the third stage of the launch vehicle; it is here that the satellite is joined with the launch vehicle. The launch platform also has a 77-m, 11-story service tower; each story has a rotating service platform. On top of the tower is a crane with a 20-ton lifting capacity. There are 1,200 technical personnel working at the launch site.

The Command and Control Center

The command and control center is the "soul" of the launch center; it is responsible for integrated system test and for the overall command of each subsystem and the safety control of the launch vehicle during the launch operation. It contains many specialized equipment designed to carry out the following tasks: commanding, assignment, safety control, computing, display, recording, television monitoring, time synchronization, and data transmission. The electronic computer performs the functions of editing, optimizing, computing, and processing on the received information and sends it to the command console. The command, launch, inspection, and display operations are highly automated. For example, after lift-off of the Long March-3 rocket, the data received by the radar and the optical tracking stations in the Xichang area are sent to the computer of the command and control center, which steers the radar antenna and the tracking sensor to follow the ascending rocket. At the same time, the tracking data are also sent to the command center to derive various flight data including data for launch site safety. If a malfunction of the rocket is detected, the computer will calculate a point along its trajectory for self destruction to ensure that it will not fall back into an inhabited area.

Figure 1. Layout of the Xichang Satellite Launch Center

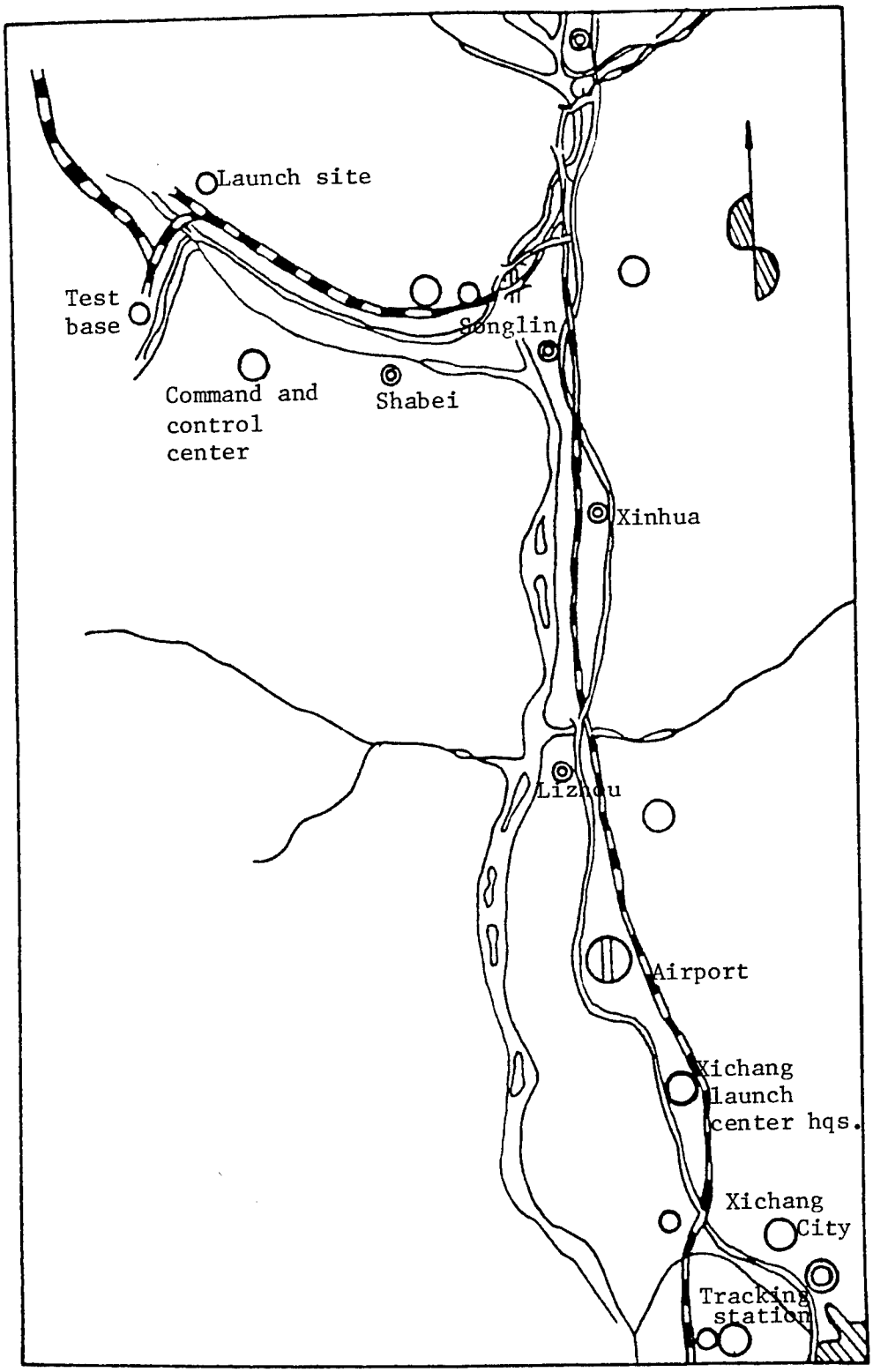

Figure 2. Locations of the Tracking Stations

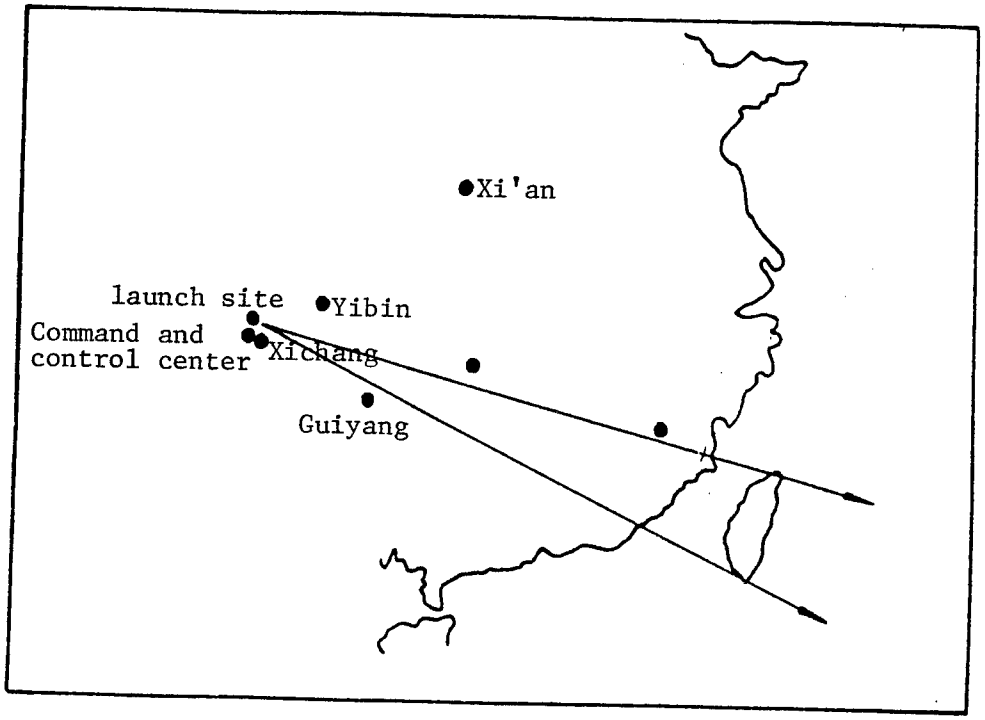

The Tracking Stations

The launch center has three tracking stations located respectively at Xichang, Yibin, and Guiyang. The tracking stations are equipped with laser digital transits, pulse radars, continuous-wave radars, continuous-wave interferometers, ultra-shortwave telemetry systems, and components of the guidance system; their function is to track the launch vehicle and the payload during powered flight, and to follow the payload along its trajectory after separation from the launch vehicle. The main tracking station of the rocket booster is located inside Xichang City; it has three dome-shaped tracking and telemetry facilities, two of which contain optical tracking systems, and one contains a radar tracking system. The optical system includes a laser tracking sensor, an infrared system, as well as television monitors and a computer system. The straight-line distance between the tracking station and the launch platform is approximately 40 km. Typically, the Long March-3 rocket travels in a southeast direction after launch. The first-stage separation, which occurs 130 seconds after lift-off at an altitude of 29 km, is monitored by the optical system; the second-stage separation, which occurs 262 seconds after lift-off, is monitored by the telemetry system.

Figure 3. Map of the Technical Center

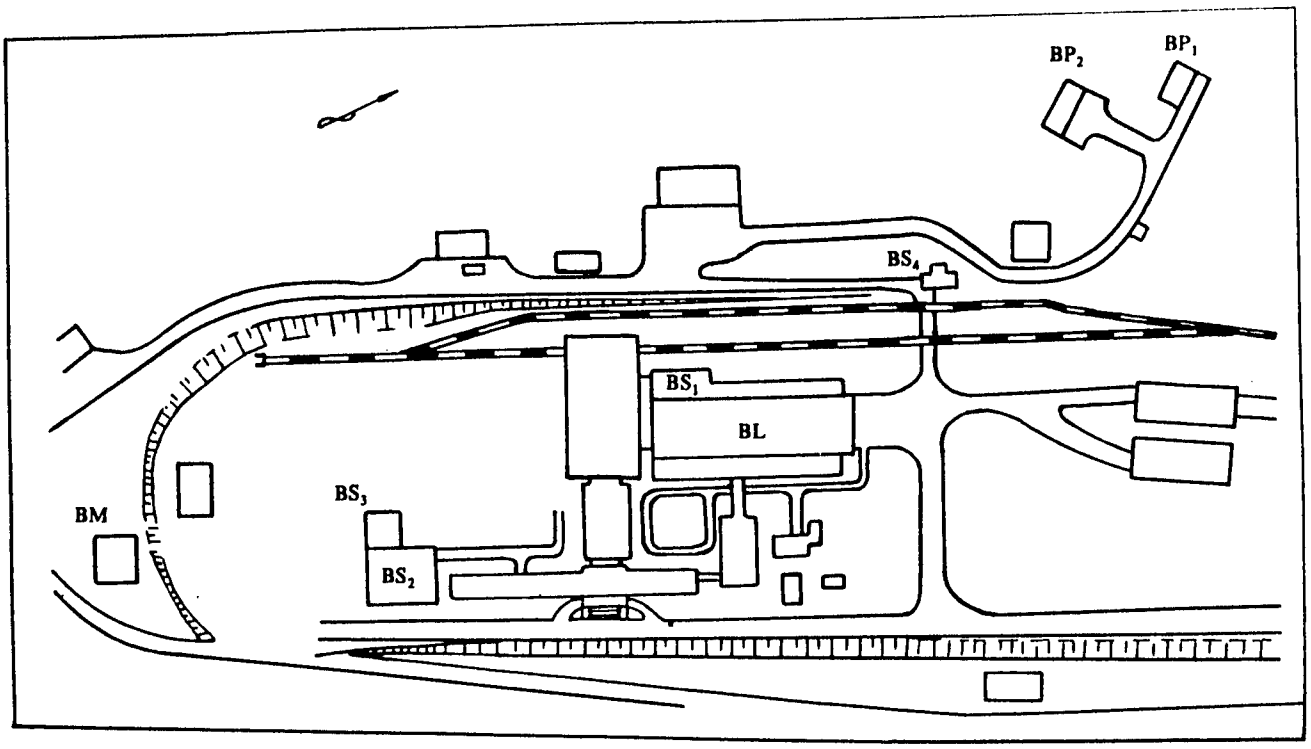

BL - launch vehicle test chamber
BS1 - payload test chamber
BS2 - payload preparation room
BS3 - payload filling and final assembly hall
BS4 - payload leakage inspection room
BM - apogee motor test chamber
BP1 - combustible products storage room
BP2 - combustible products test chamber

Figure 4. Map of the Launch Site

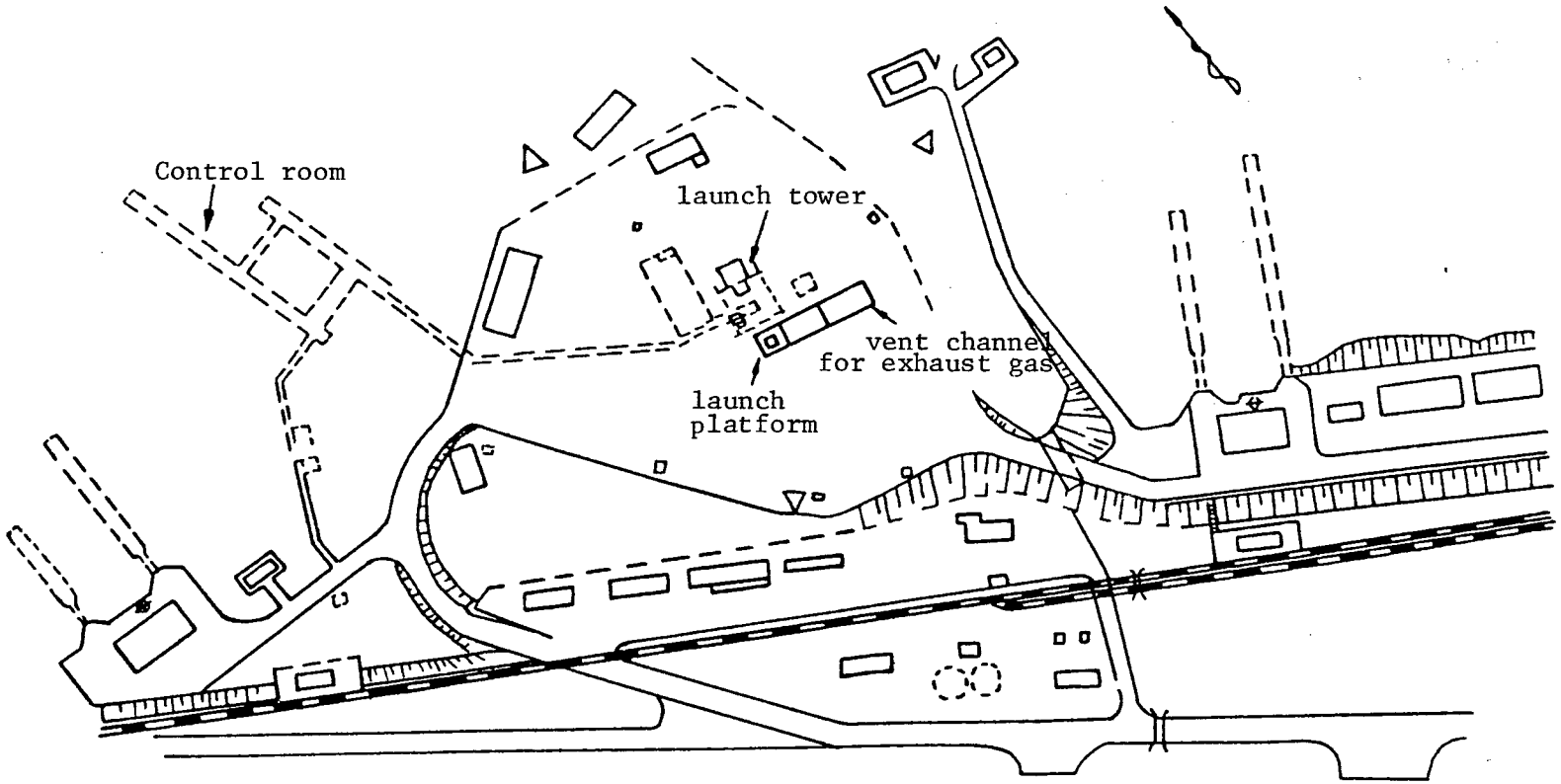

Figure 5. Tracking Station Coverage Diagram

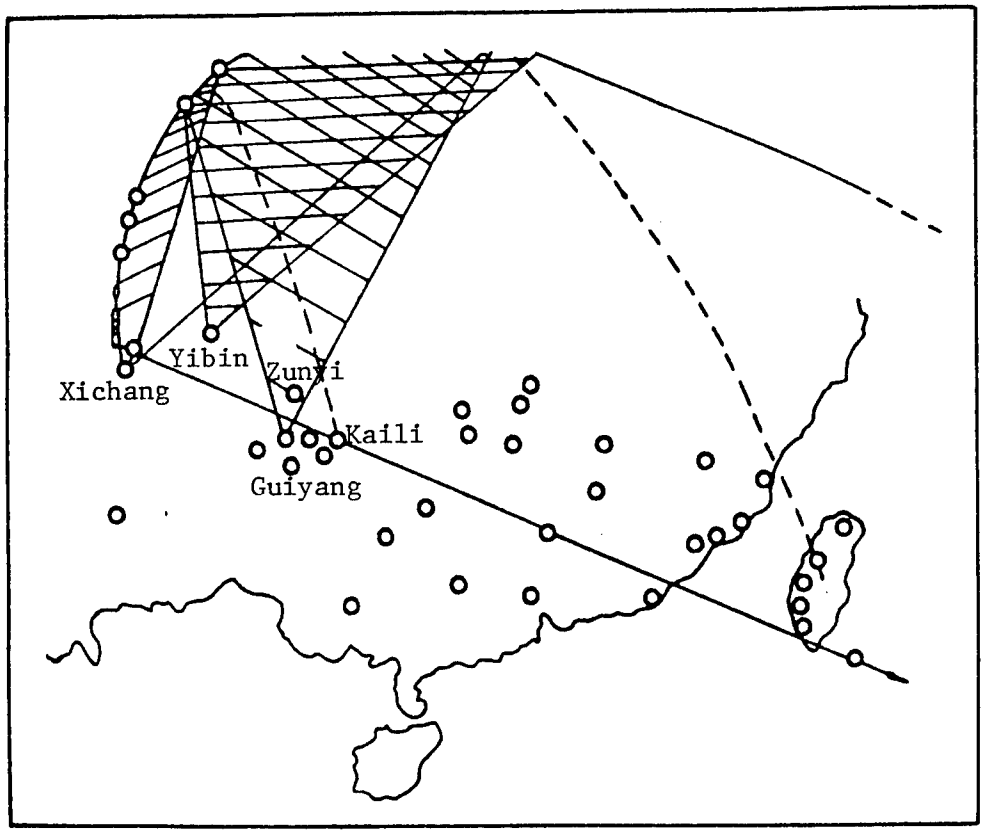

Communication and Time Synchronization

The real-time and service communications within the launch center and to the outside are accomplished by the following systems: the conventional communication system, the launch command communications system, the time synchronization unit, the data transmission unit, and the satellite communications system. A relay tower has been constructed between the satellite preparation room and the launch platform in order to transmit the test data back to the computer in the preparation room when the satellite is in its final phase of inspection.

Weather Monitoring

Geographically, the launch center is located in a sub-tropical region. The local temperature is generally above 0°C, with an average temperature of 16°C; there are many sunny days during the year, and the frost-free season is quite long; there is also a clear division between the dry season and the rainy season. During the rather long dry season, most days are clear, and precipitation and relative humidity are low; this is the ideal launch season.

The launch center has several weather stations, which collectively form a weather exchange network, a weather forecast network, a weather intelligence network, a micro-weather network and a thunder-storm monitoring network to provide accurate long-term, short-term, and intermediate weather forecast to support the launch activities.

Currently, a large-scale construction project is underway at the Xichang launch center; it is expected that the center will play a major role not only in meeting China's future aerospace needs, but also in meeting the needs of foreign countries to launch their satellites.

Development of Amphibious Ground-Effect Craft Outlined

40080107a Shanghai CHUANBO GONGCHENG [SHIP ENGINEERING] in Chinese No 6, 1 Dec 88 pp 18-21, 33

[Article by Hu Anding [5170 1344 1353]]

[Text] I. Introduction

It has been more than half a century since the Finnish engineer Toivo Kaario built the first successful ground-effect vehicle in 1935; during this period, progress in the development of ground-effect vehicles had been eratic. In the early 1960's, the invention of the air-cushioned ship renewed the interest of many countries in the research of ground-effect vehicles. The United States, Finland, Japan, Sweden and the Soviet Union have devoted considerable resources in theoretical studies, as well as in wind tunnel tests and water-tank tests, and had built a large number of test craft; more than 30 of these test craft have been reported in the open literature. Unfortunately, because of the dynamic stability problems associated with these vehicles in the ground-effect region, this new craft has never been developed into a practical transportation vehicle. In 1963, in building the X-112 ground-effect vehicle and the subsequent models, the X-113 and X-114, the German engineer Alexander Lippisch demonstrated that the dynamic stability problem can be solved. At the same time, important contributions were also made to the theory of dynamic stability of ground-effect vehicles by the British engineer P. E. Kumar and the German engineer Rolf Stanfenbiel. However, if a ground-effect craft were to take off and land by gliding over the water surface like a seaplane or by taking advantage of the propeller slip stream, it must be able to overcome very large hydraulic drag. To meet this requirement, the engine thrust must be increased and the wing loading must be reduced; also the structure must be strengthened in order to withstand the huge impact from ocean waves. As a result, the overall performance of the ground-effect craft was limited, and its development and application remained stagnant. In the mid 1970's, the principle of the "power-augmented ram wing-in-ground effect" was proposed in the United States, and at the same time, the new concept of "powered aircushion" was proposed in this country. Through theoretical calculations, wind tunnel tests and unmanned model tests, it was shown that this principle can be successfully applied to develop a take-off and landing system for the ground-effect vehicle. Thus, the future of the ground-effect vehicle was revived.

There are three basic types of ground-effect vehicles:

1. the flying-wing type, which the Soviet Union calls the "Ekranoplan";

2. the airplane type, which the Soviet Union calls the "Ekranolet"; and

3. a transition model between the two.

The flying-wing type ground-effect vehicle can operate within the ground effect region; we call it the ground-effect flying ship because its characteristics are similar to those of a conventional ship. The airplane type ground-effect vehicle primarily travels at higher altitudes where ground effect does not exist; the United States calls it the ground-effect seaplane.

In 1977, we proposed the design of an amphibious ground-effect craft which combines the features of the powered aircushion and the ground effect wing; since that time, a large number of wind tunnel tests[2,3] and unmanned model tests have been conducted. In May 1987, the successful test of the 750 twin-seat amphibious ground-effect craft demonstrated the feasibility of designing an amphibious, airworthy, and stable ground-effect vehicle. This test laid a solid foundation for developing the amphibious ground-effect craft into a practical transportation vehicle.

II. Key Technical Problems in Developing the Ground Effect Craft

1. The Amphibious Take-Off and Landing System

The early ground-effect craft developed prior to the 1960's basically used the gliding take-off and landing system of a conventional seaplane. Such a system has several disadvantages; for example, it is difficult to take off or land on a rough sea due to the large impact force of ocean waves; it also adds to the weight of the craft and reduces the payload capability and wing loading. For this reason, American experts F. H. Krause and R. W. Gallington believe that it is not possible for the ground-effect vehicle to achieve high performance with a conventional take-off and landing system even though very high lift-to-drag ratio may be obtained in wind tunnel tests.

A potentially very promising approach to solve the take-off and landing problem is to apply the principle of power augmentation and the principle of powered aircushion developed independently by the United States and China in the mid 1970's. The two principles are basically the same, i.e., by directing the high-speed jet stream from the forward engine into the cavity between the ground-effect vehicle and the earth surface, thereby converting dynamic pressure into static lift force in the form of an aircushion. There are three types of cavity designs: 1) the wing type powered aircushion design, where the cavity is formed by the lower surface of the wing, the flaps, and the two end plates; 2) the airduct type design, where the cavity is formed by the lower surface of a specially designed, small-aspect-ratio wing, the flaps, and the two end plates (we call it the airduct); during cruise flight, the airduct also provides part of the

aerodynamic force; 3) the fuselage type design, where the cavity is formed by the lower part of the fuselage and the two end plates; no aerodynamic force is provided by the cavity during cruise flight.

In 1977, we applied the principle of powered aircushion to the design of an amphibious ground-effect craft. First, we built and tested an unmanned model with a wing type take-off and landing system (Figure 1). Subsequently, we conducted a series of tests on more than 30 airduct designs to study the effect of different shapes and dimensions of the airduct and the relationship between the jet stream and the airduct. Figure 2 shows an airduct model being tested in a wind tunnel. Part of the test results can be found in Reference 3.

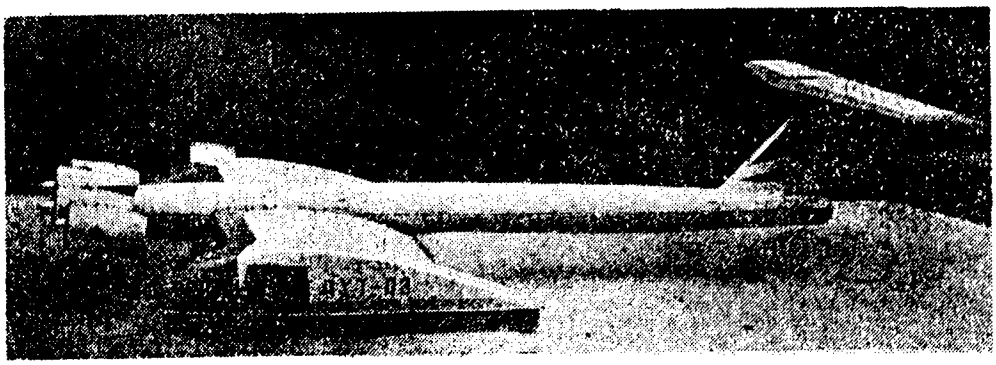

Figure 1. An Unmanned Model With Wing Type Powered Aircushion Take-off and Landing System

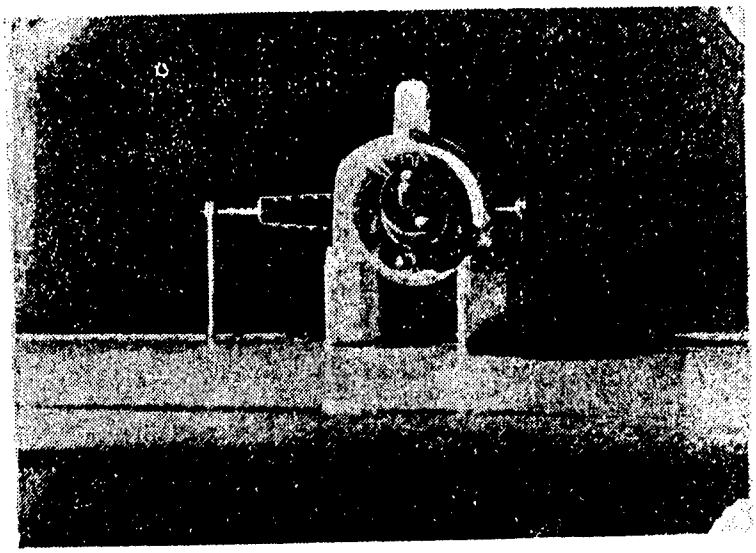

Figure 2. An Airduct Model Being Tested in Wind Tunnel

The lift characteristics of a powered aircushion take-off and landing system can be expressed in terms of four non-dimensional parameters:

The powered aircushion lift to thrust ratio $\eta_L = \frac{L}{T}$

The thrust recovery ratio $\eta_T = \frac{T - D}{T}$

The thrust loss ratio $\eta_D = \frac{T_0 - T}{T_0}$

The center of pressure $\bar{X}_{DC} = \frac{X_{DC}}{L_D}$

where L is the lift of the powered aircushion, T is the assembled engine thrust, T_0 is the single engine thrust, D is the airduct drag, X_{DC} is the distance between the center of pressure and the leading edge of the airduct, and l_D is the length of the airduct.

Extensive wind tunnel tests and unmanned model tests, and the recent test of the twin-seat prototype ground-effect craft showed that the airduct type powered aircushion take-off and landing system not only raised the lift-to-thrust ratio to more than 8, but also had the capability of lifting a ground-effect craft from land into water and from water onto land. This was a major breakthrough in ground effect flight technology.

2. The Flight Stability Problem

An amphibious ground-effect craft generally undergoes transitions through three different stages of motion: the first transition from conventional water-repelling motion to the powered aircushion motion, and the second transition from the powered aircushion motion to the ground effect motion (Figure 3 [not reproduced]). The dynamics of each stage of motion are very complicated, and the longitudinal stability of the motion is a key issue that must be carefully studied. During the transition regions, the positions of the center of buoyancy, the center of hydrodynamic forces, the center of pressure of the powered aircushion and the ram aircushion, and the center of aerodynamic forces are all nonlinear functions of the flight speed and the flight altitude; furthermore, since the thrust varies with speed, the longitudinal moment generated by the thrust about the center of gravity also varies. This is an important factor which cannot be ignored in analyzing longitudinal stability.

In order to solve the above problems, the following measures have been taken:

(1) The shape of the float and the longitudinal position of the center of buoyancy of the ground-effect craft have been designed to provide favorable take-off attitude and to reduce the peak drag during take-off.

(2) The arrangement of critical aerodynamic components(e.g., the ground-effect wing, the airduct and the horizontal tail etc.) and the placement of the thruster are chosen to ensure longitudinal stability of the ground-effect craft. The effect of downwash is also considered in choosing the location of the horizontal tail. The airfoil design of the ground-effect wing has been modified to minimize the variation of the aerodynamic center as a function of flight altitude. The airfoil design is also chosen with consideration given to the overall longitudinal stability of the vehicle and to its effect on the lift-to-drag ratio, and on the strength of ground effect.

(3) Because of the design consideration to improve the craft's loiter capability over ocean, which implies survivability and operations under adverse weather conditions, and because of structural considerations, we have chosen a very small aspect ratio (less than 1.0) for the wing design. This presents a difficult lateral stability problem during flight. We solve the stability problem by using a double airduct design at the wingtips and by operating the craft primarily in the ground effect region.

(4) Because the airfoil design and the airduct design both produce strong ground effects, the amphibious craft has good vertical stability within the ground-effect region. In order to design an airfoil with not only strong ground effect but also good performance, theoretical and experimental studies have been conducted on a large number of ground-effect wings with large thickness and end plates[2]. If the strength of ground effect is expressed in terms of the derivative of lift coefficient with respect to the flight altitude, C_L^h, then the airfoil used in this design, the QY14-15, has a C_L^h of -0.96, which is 6 times stronger than that of the KLARK YM-11 design.

3. Jet Stream for Powered Aircushion

In order to produce the powered aircushion, it is necessary to generate a high-speed jet stream to provide the suction effect at the leading edge of the airduct; the slip stream produced by a conventional propeller is not sufficient. An ideal source of the jet stream is a turbofan engine or a turbojet engine. Since China currently does not have a small engine of this type, we have specially designed the "DT-30" ducted thruster (Figure 4) [not reproduced], which uses a single-vaporizer aircraft engine to drive a stationary propeller. The propeller blade and the duct are both made of fiberglass material. In order to prolong the engine life and to provide sufficient reserve power for take-off under stormy conditions, the maximum design power was chosen to be 83 percent of the engine rated power.

4. Ultra-Light Structural Design

In order to reduce the vehicle weight, we use a light-weight, easy-to-form fiberglass composite material with a polystryene foam core; the areas with local stress concentration are reinforced with aircraft sandwiched plates. The specific gravity of the polystryene foam is only

20 km/m^3; the total weight of the main wing, the horizontal tail and the vertical tail is only 7 percent of the take-off weight. This ultra-light structure meets the specification for weight constraint, but also proved to be sufficiently strong to survive more than 40 flight tests over the past two years.

III. Key Performance Parameters of the Twin-Seat Amphibious Ground-Effect Craft

1. Overall Performance Parameters

(1) Weight

take-off weight	745 kg
payload weight	172 kg

(2) Dimensions

length	8.47 m
width	4.80 m
height	2.34 m

(3) Take-Off Performance

A) Under the conditions of wind intensity level of 4-5 and 0.5 m waves, the take-off time is approximately 30 seconds, and the take-off distance is approximately 160 m.

B) The take-off speed is approximately 45 km/hr.

(4) Cruising Speed and Range

A) The cruising speed is 132 km/hr; the corresponding cruising altitude is approximately 0.5 m.

B) The range is 130 km.

(5) Flight Performance

It has the capability to meet the following performance requirements: to take off, to maintain level flight, and to make high-speed turns under the conditions of 0.5-0.7 m waves and wind intensity level of 4-5 or gust level of 6. During level flight, the average longitudinal roll angle is 0.3°, and the average lateral roll angle is 0.52°. The maximum impact acceleration at landing is approximately 1.54 g.

(6) Amphibious Performance

A) It can use the powered aircushion to lift itself from land into water.

B) It can also use the powered aircushion to land from water.

C) It can travel over uneven grassland.

(7) Control Performance

A) At low speed, it can make turns in a hovering position.

B) At high speed, it can maneuver in a zig-zag pattern.

C) At high speed, it can make a complete turn in approximately 2 minutes 30 seconds, and the turning radius is approximately 600 m.

2. Flight Test of the Amphibious Craft

Flight test of the twin-seat amphibious ground-effect craft began in March 1985. By June 1987, more than 40 tests had been completed; they included: on-land static aircushion lift test; aircushion lift test from land into water; water-repelling motion test; on-water aircushion lift test; cruise flight test over water (Figure 5) [not reproduced]; aircushion lift test from water onto land; and low-speed test over uneven grassland.

IV. Future Prospects

1. Because of its low-flying ability, its loitering capability, its good flight performance and amphibious performance, the amphibious ground-effect craft has definite military value.

2. As a commercial transportation vehicle, the amphibious ground-effect craft has several desirable features: safety, speed, efficiency, and comfort.

A) Safety. Although the speed of the amphibious ground-effect craft is close to that of a low-speed aircraft, it is a relatively safe vehicle because it cruises at less than 10 m above the water surface. Even an engine failure or some other trouble occurs, the craft can safely land on water without suffering damages to the vehicle or injuries to the passengers.

B) Speed. The amphibious ground-effect craft travels at 200-300 km/hr (100-160 knots), which is 5-8 times faster than a water-repelling passenger ship, or 2.4-4 times faster than a high-speed boat (a hydrofoil or an aircushion vessel). Hence travel time is significantly reduced.

C) Efficiency. Because of the high lift-to-drag ratio (15-20) of a ground-effect craft, its fuel consumption is very low; for example, to carry a one-ton load over a distance of 1 km requires only 0.2-0.4 kg of fuel. Such high efficiency makes it a very competitive transportation vehicle.

D) Comfort. Under the conditions of 0.5-0.7 m waves, wind intensity level of 4-5, and gust level of 6, the average longitudinal roll angle is 0.3° in level flight, the lateral roll angle is 0.52°, and the maximum impact acceleration at during is approximately 1.54 g. These performance parameters reflect the degree of comfort provided by this craft as a passenger ship.

3. During the course of designing the amphibious ground-effect craft, considerable amount of technical data have been accumulated, and several techniques have been developed to carry out theoretical analysis and performance estimation. This valuable experience will contribute a great deal toward building a practical amphibious ground-effect vehicle in the future.

4. Finally, I would like to express my sincere thanks to the comrades who have participated in and provided support to the development of the amphibious ground-effect craft.

References

2. Hu Anding, Ma Ruren, "Aerodynamic Characteristics of Thick Ground-Effect Wings With End Plates," CHINA SHIP BUILDING, 1980 Vol 4.

3. Hu Anding, "Powered Aircushion Research," CHINA SHIP BUILDING, 1982 Vol 2.

Prototype 902 Single-Seat Ram Surface Effect Craft Said Successful

40080107b Shanghai CHUANBO GONGCHENG [SHIP ENGINEERING] in Chinese No 6, 1 Dec 88 pp 22-26

[Article by Li Shuming [2621 3219 2494] and Li Kaixie [2621 7030 3610]]

[Text] I. Introduction

It is known from the history of ship development that the speed of a ship traveling in water is limited by the wave drag and the air bubbles. One way to overcome this difficulty and achieve higher speed is to let the ship rise above water. The ram wing craft is a vessel designed to travel close to but above the water surface by using the high pressure aircushion between the wing and the surface to support the vessel.

The main challenge in designing a ram wing craft is to solve the longitudinal stability problem at different heights above the water surface. The surface effect causes the center of pressure of the wing to move forward as height increases. When the wing is next to the surface, the center of pressure is located approximately 1/2 chord length from the leading edge; when the craft leaves the surface, the center of pressure moves forward to 1/4 chord length from the leading edge, which creates a problem of longitudinal instability. Furthermore, the presence of surface effect also causes the aerodynamic characteristics of the ram wing to be highly non-linear, and induces coupling between the vertical motion and pitch motion. As a consequence, the problem becomes much more complicated.

In 1979, the China Marine Science Research Center began development of the 902 ram wing craft; through theoretical and experimental research, it succeeded in solving the longitudinal stability problem. The craft was completed in 1983, and flight test results showed that it had good performance both inside and outside the surface effect region. The success of the 902 craft provided the technical foundation for developing a practical ram wing craft.

II. Design of the 902 Ram Wing Craft

The configuration of the 902 ram wing craft is similar to that of a conventional airplane, as indicated in Figure 1. Specifically, it has

the following components: the main pontoon, the main wing, the double vertical tails, the horizontal tail, a pair of small lateral wings, and a pair of small pontoons. The craft is powered by two 20-hp piston engines located at the leading edge of the main wing[2].

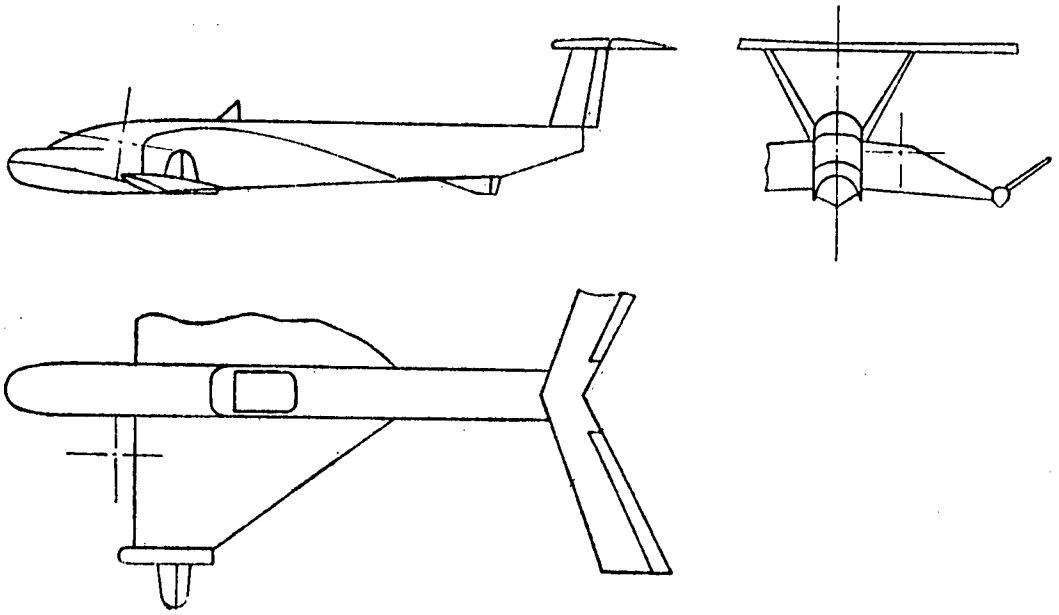

Figure 1. Three Views of the 902 Single-Seat Ram Wing Craft

This craft is primarily designed for operation in water. In the mid section of the wing is a seaplane type main pontoon[6] which provides the static buoyancy force for docking and the hydrodynamic lift force for take-off. To overcome the stability problem, we selected an inverted delta wing design with a twisted and drooped airfoil section. At the wingtips is a pair of narrow pontoons to maintain lateral attitude during docking or take-off and also to serve as end plates for the main wing. The small pontoons are equipped with lateral wings which can be extended outward or rotated upward to ensure lateral stability and to provide maneuverability. At the rear of the craft is a large-aspect-ratio, swept-back horizontal tail to provide longitudinal stability and control. The craft also has a pair of vertical tails which are used to support the horizontal tail and provide bearing stability and control. The bottom of the craft has a rudder which provides turning control when the craft is gliding in water.

The key technical data of the 902 single-seat ram wing craft are as follows:

Dimensions:

length:	9.55 m
width:	5.80 m
height:	2.30 m

Weight:

total weight:	385 kg
empty weight:	280 kg
payload:	105 kg

Power Plant:

two HS-350A piston engines with a maximum power of 20 hp x 2; constant-pitch air propellers.

Performance:

take-off speed:	75 km/hr
cruising speed:	120 km/hr
cruising altitude:	0.6 m
take-off distance:	150 m
landing distance:	100 m

III. Model Experiments

The design of the 902 ram wing craft depends heavily on the results of extensive model experiments. In particular, a large number of wind tunnel tests were conducted to arrive at a stable aerodynamic configuration[5].

The main objective of the wind tunnel tests was to explore various designs of the main wing and the horizontal tail in order to solve the longitudinal stability problem. We have tested a number of conventional airplane configurations and finally decided on the inverted delta wing design of the 902 craft. The horizontal tail was chosen to be an elevated large-aspect-ratio, swept-back wing design to provide longitudinal stability.

Figure 2 shows the test results of this model craft which include the lift coefficient, the drag coefficient, and the lift-to-drag ratio. It can be seen that when the craft is traveling next to the surface, the lift-to-drag ratio increases noticeably; the peak lift-to-drag reaches as high as 20. This phenomenon can be explained as follows: As a result of the twisted and drooped wing design, the wingtip on each side effectively bends downward; also, the narrow pontoons at the wingtips serve as end plates which block the outward flow of air from underneath the wing when the craft is traveling within the surface-effect region and the pontoons are very close to the water surface. This enhances the two-dimensional effect which in turn produces higher lift-to-drag ratio. Of course, these results apply only to the model test. In the case of the 902 ram wing craft, the actual lift-to-drag ratio is adversely affected by the lack of attention to surface finish when building the craft and by the open cockpit design.

Figure 3 shows the model test results of the longitudinal moment coefficient. The longitudinal moment coefficient m_z (θ, h) has a significant effect on the craft's stability. It can be seen from Figure 3a) that

the curves of moment coefficient versus pitch angle for different altitudes do not intersect; in fact, they form a family of nearly parallel lines. Also, the slopes of the curves m_z^{θ} (θ, h) change very little with altitude; they are approximately straight lines. Clearly, this type of longitudinal moment characteristics greatly improves the non-linearity caused by the surface effect and reduces the coupling between the vertical motion and the pitch motion. More importantly, for most flight conditions, the value of $m_z^{\bar{h}}$ (θ, h) of this craft is negative. As shown in Figure 3b), inside the region $-6° \leqslant \theta \leqslant 4°$ for all flight altitudes and inside the region $6° \geqslant \theta \geqslant 4°$ for $\bar{h} > 0.2$, all values of $m_z^{\bar{h}}$ (θ, h) are negative. The only region in which $m_z^{\bar{h}}$ (θ, h) has a small positive value is where $6° \geqslant \theta \geqslant 4°$ and $\bar{h} < 0.2$. Undoubtedly, longitudinal moment characteristics such as this is desirable for solving the stability problem.

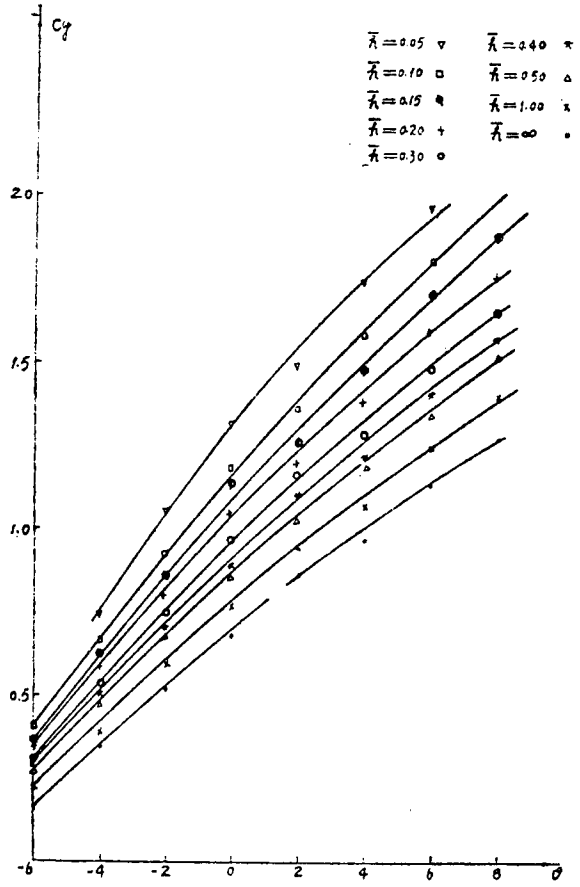

Figure 2a). Lift Characteristics of 902 Single-Seat Ram Wing Craft

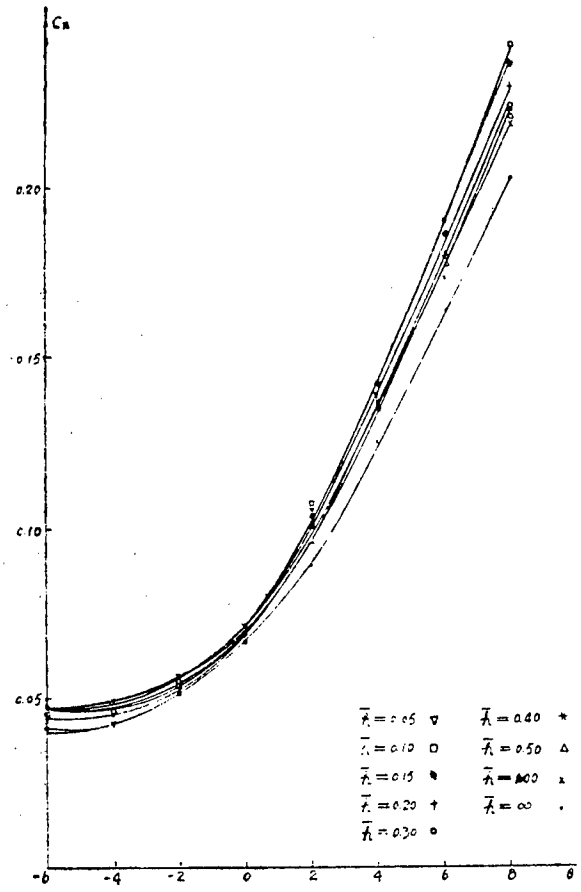

Figure 2b). Drag Characteristics of 902 Single-Seat Ram Wing Craft

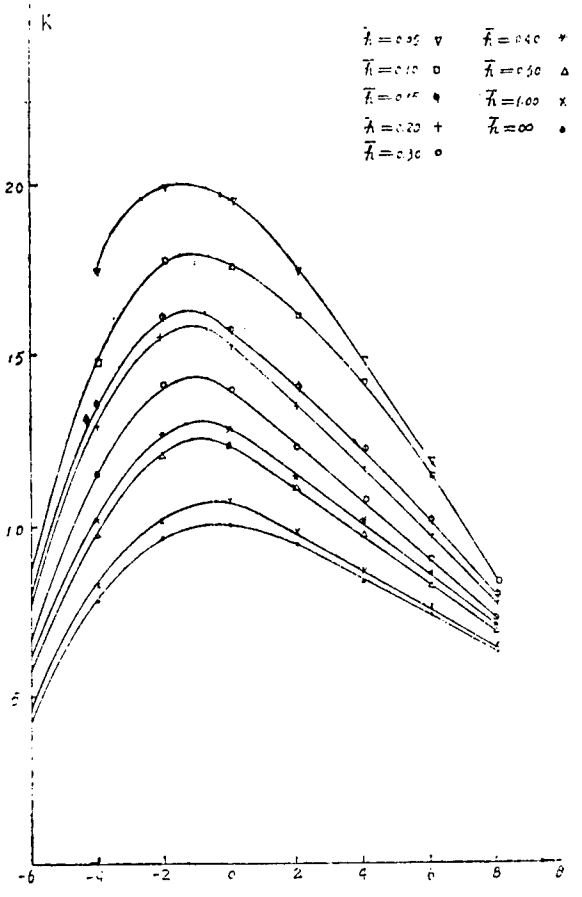

Figure 2c). Lift-to-Drag Ratio of 902 Single-Seat Ram Wing Craft

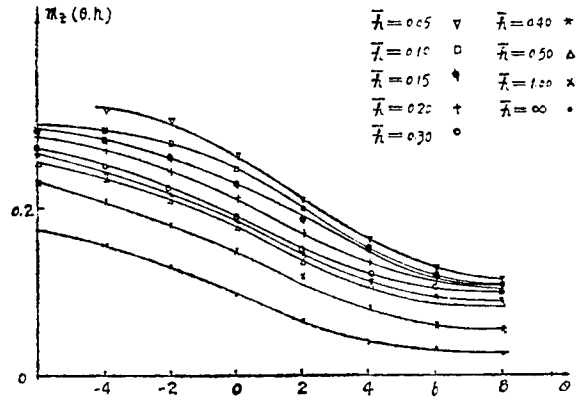

Figure 3a). Moment Coefficient Versus Pitch Angle for 902 Single-Seat Ram Wing Craft

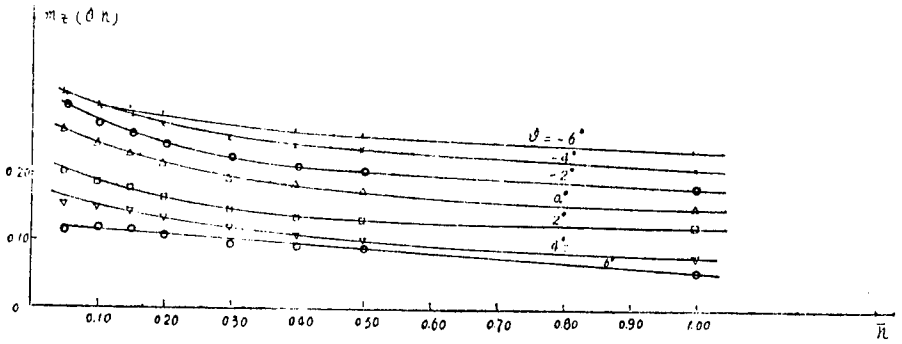

Figure 3b). Moment Coefficient Versus Altitude for 902 Single-Seat Ram Wing Craft

The performance of the 902 ram wing craft is primarily determined by the main wing design and the horizontal stabilizer design. The inverted delta wing has the inherent property that its lift coefficient curves for different flight altitudes do not intersect. This may lead to a family of parallel curves for the longitudinal moment coefficients. In addition, the twisted and drooped wing design enhances the surface effect, which tends to increase the separation between the lift curves for different altitudes, and makes it possible to achieve negative $m_z^{\bar{h}}(\theta, h)$ under most conditions. Now let us look at the design of the horizontal tail. Since the lift of the horizontal tail produces a negative pitch moment on the entire craft, if a wing configuration with strong surface effect were chosen for the horizontal tail, then it would accentuate the effect of decreasing moment with increasing altitude. This is clearly undesirable from the point of view of achieving uniformly negative $m_z^{\bar{h}}(\theta, h)$. For this reason, we have designed a high horizontal tail with small angle of incidence and a large-aspect-ratio, swept-back wing configuration to minimize the surface effect.

The 902 single-seat ram wing craft has been designed to maintain stable flight under most flight conditions. Even when the craft is traveling inside the surface-effect region at a large angle of attack, the positive moment generated by the main wing can be balanced by a small lift force provided by the horizontal tail. Outside the surface-effect region, the increase in downwash from the main wing may cause the condition $m_z^{\bar{h}}(\theta, h) < 0$ to be violated; but by choosing a large-aspect-ratio, swept-back design for the horizontal tail, it is possible not only to avoid the downwash inside the wing span region but also to take advantage of the upwash outside the wing span region. In the event an obstacle is encountered on the water surface, the craft can immediately pull up to fly over it. Therefore, the 902 ram wing craft has demonstrated good stability both inside and outside the surface-effect region[4].

IV. Flight Test Results of the Prototype Ram Wing Craft

On 12 November 1984, the first flight test of the 902 prototype craft was successfully conducted by the designer, who piloted the craft himself. The flight test results are summarized below:

When the wind intensity level is 6-7, it can take off from water under 0.4-0.5 m waves, and then maintain stable flight inside the surface-effect region. It can also maintain stable flight at different altitudes from 0.6m - 8.0m without the aid of any stabilizing devices. In short, it is completely stable both inside the surface-effect region and in free space.

The craft has excellent obstacle-avoidance capability; when encountering an obstacle on water, it can immediately pull up to fly over it. It also has good maneuverability; inside the surface-effect region, it can execute a turn maneuver at a 30° bank angle.

In the event that one engine or both engines fail during flight, the craft will be able to land softly without tilting or falling into the water[3]. Figure 4 [not reproduced] shows the actual photographs taken of the 902 single-seat ram wing craft when flying inside and outside the surface-effect region and when making a large-bank-angle turn inside the surface-effect region.

V. Concluding Remarks

The design of the 902 single-seat ram wing craft has been full verified by actual flight tests; in particular, the stability problem and the control problem have been resolved. Its performance has met all the design specifications[1]. Based on the success of the 902 prototype craft, we have begun development of two surface-effect craft for practical use: the XTW-1 and the XTW-2. The XTW-1 was completed in late 1987, and has been used as a high-speed transport vehicle on in-land rivers and lakes; it is capable of docking either in water or on land. It has completed all the scheduled flight tests with excellent results. It is powered by two 40-hp piston engines and has a maximum take-off weight of 950 kg; it can carry 2-3 passengers (not including the pilot) and travel at a speed of 110-130 km/hr. In addition, preliminary design of the 15-passenger XTW-2 ram wing craft had been completed; when built, this craft can be used in high-speed patrol along the coast or as a commuter boat or pleasure boat between islands. Figure 5 shows a photograph of the XTW-1 craft in flight.

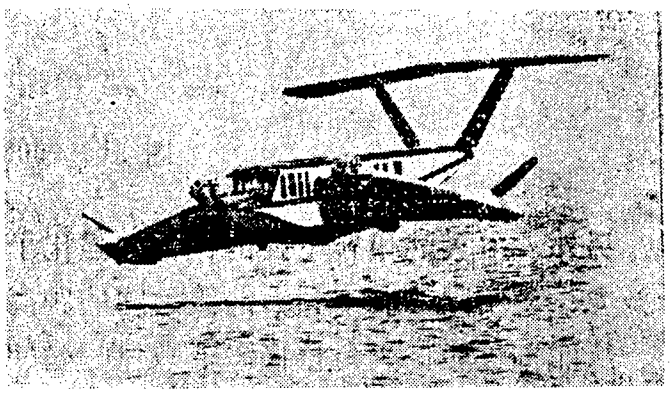

Figure 5. The XTW-1 Ram Wing Craft Flying Inside the Surface-Effect Region

References

1. Li Shuming, "Final Report of the 902 Single-Seat Ram Wing Craft," China Marine Science Research Center Technical Document 1985.10.

2. Li Kaixie, "Design Report of the 902 Single-Seat Ram Wing Craft," China Marine Science Research Center Technical Document 1986.5.

3. Li Kaixie, "Flight Test Report of the 902 Single-Seat Ram Wing Craft," China Marine Science Research Center Technical Document 1985.10.

4. Li Shuming, "Stability Research of Ram Wing Craft," China Marine Science Research Center Technical Document 1984.12.

5. Li Kaixie, "Wind Tunnel Test Report of the 902 Single-Seat Ram Wing Craft," China Marine Science Research Center Technical Document 1981.12.

6. Huang Kaisen, "Water Tank Test Report of the 902 Single-Seat Ram Wing Craft," China Marine Science Research Center Technical Document 1983.9.

Briefs

Computerized Centrifugal Impeller Technology--Computer-aided manufacturing of single-piece [zhengti] titanium-alloy centrifugal impellers, a new technology developed in a 6-year effort by Research Institute 608 (at Zhuzhou [Hunan Province]) of the Ministry of Aeronautics & Astronautics Industry, passed ministry-level technical certification in Zhuzhou at the end of last year. Specialists at the certification agreed that this new high-tech achievement is a major breakthrough for China's aerospace industry. The centrifugal impeller is a key component in small-to-mid-sized aircraft engines, and only a small number of developed countries have mastered this advanced technology. [Summary] [40080126a Beijing JISUANJI SHIJIE [CHINA COMPUTERWORLD] in Chinese No 1, 4 Jan 89 p 1]

Standardized Clock System--A model of H303-standardized clock-control-system equipment passed accreditation in Chengdu at the end of last year. This equipment, an essential component in space science experiments, in modern weapons research, and in the launching of guided missiles and artificial satellites--as well as in other areas such as meteorology and seismic forecasting--provides a standardized clock signal and frequency signal. This project, contracted out to the state-run Xinghua [2502 5478] Instrument Plant by the Commission of Science, Technology and Industry for National Defense in July 1987, has resulted in a product with the following specifications: the quartz[-resonator] frequency stabilization is $1 \times 10^{-9}/10$ms, and 1×10^{-11}/s; recurrence frequency [i.e., repetition rate] is 1×10^{-8}. [Summary] [40080126b Beijing ZHONGGUO DIANZI BAO in Chinese 13 Jan 89 p 3]

Piezoelectric Rate Gyroscope Developed--The TYSK-65 piezoelectric angular-rate gyroscope, developed by Research Institute 26 of the Ministry of Machine-Building & Electronics Industry (MMEI) with the assistance of MMEI Institute 207, Institute 23 of the Ministry of Aeronautics & Astronautics Industry, and the Shanghai Wired Telecommunications Plant, passed ministry-level design finalization on 21 December 1988 in Chongqing. This new high-tech vibrational inertia [zhendong guanxing] device, widely used in control systems for aerospace, navigation, and transportation, will replace mechanical gyros. The device's main technical indicators meet current advanced international standards, and the indicator for [precision in] null-setting repeatability [ling wei chongfuxing] exceeds those standards. [Summary] [40080126c Beijing DIANZI SHICHANG [ELECTRONICS MARKET] in Chinese 19 Jan 89 p 1]

More Major Successes in Crystal Materials Research Claimed

40080093 Beijing GUANGMING RIBAO in Chinese 17 Dec 88 p 1

[Article by Sang Hongchen [2718 3163 5256]]

[Excerpts] A delicate small box contained three small pieces of crystals that look like organic glass, but the price is several tens times that of gold because these are the new nonlinear optical crystals lithium boron oxide (LBO) developed by Fujian Materials Structure Research Institute. This research product is certified today by the Chinese Academy of Sciences. Experts believe that the development of LBO indicates that China still leads the world in the materials research of inorganic nonlinear optical crystals.

In 1984, research scientist Chen Chuangtian [4151 0857 6932], now Deputy Director, of Fujian Materials Structure Research Institute led a group and first developed barium boron oxide (BBO). This discovery shook the academic world and the high tech industry and is still regarded as the world's best ultraviolet nonlinear crystal. Famous companies of the United States, Japan, and West Europe rushed in their orders and the demand exceeded supply. [passage omitted]

Prestige and status in science did not make Chen's group stop their research. In order to make wider use of nonlinear optics technology and further development laser applications, they worked hard on the limitations of BBO in actual applications. Using ion group theory in nonlinear optics, they carefully investigated for 6 years different group structures in borates and calculated their frequency doubling coefficient, birefringes, and absorption edges. Through synthesis, phase diagram analysis, and measurement of nonlinear optics parameters, they finally developed the LBO crystal in 1987.

LBO overcame the shortcomings of BBO. It has a wide angular tuning half-width, a small divergence angle and very high damage threshold. It also has the advantages of chemical stability and is not deliquescent. It is now the world's best frequency doubling and frequency tripling materials for Nd:YAG (YAP) lasers. It is also a frequency doubling and summing

material for dye lasers and a nonlinear optics crystal for triple frequency pumping of the optical parametric oscillator in a Nd:YAG laser. It can be expected that LBO crystals will replace some of the commonly used KTP crystals.

Development of the LBO crystal is another major achievement in China's research on crystalline materials. Patents have been applied for in China, the United States, and in Japan. [passage omitted]

Effects of Task-Unrelated Stimuli on Frontal Neuron Responses in Delay Period of Performing Monkeys

40091015 Shanghai SHENGLI XUEBAO [ACTA PHYSIOLOGICA SINICA] in Chinese Vol 40 No 5, Oct 88 pp 452-463

[English abstract of article by Liu Jinlong [0491 6027 7893], et al., of the Institute of Space Medico-Engineering, Beijing]

[Text] The effects of task-unrelated novel stimuli on frontal neuron responses in delay periods were studied on conscious monkeys (Macaca mulatta) during performing delayed discrimination tasks and simple discrimination tasks. The duration of the delay periods of both tasks was set pseudo-randomly between 1-4 s in order that the monkey could watch the signal panel attentively to make a correct response. In the delayed discrimination task, the monkey had to remember the cue signal throughout the entire delay period, but this was not required in the simple discrimination task. Of the 203 task-related neurons recorded, a total of 70 showed changes in the discharge rate during the delay period (41 during the delayed discrimination task, 29 during the simple discrimination task). The features of the neuron responses in both tasks were similar. The monkey performed an incorrect response when he was distracted by visual, auditory, tactile or pain stimuli unrelated to the tasks, with decreased responses during the delay period in most neurons. However, facilitation was also observed in a few neurons. In some cases, facilitation and inhibition appeared even in the same neurons, depending on the sensory modalities of unrelated stimuli, suggesting that the effects could be somewhat modality specific. Moreover, in some neurons, different effects could be produced with the same task-unrelated stimuli applied during the delay period or during an intertrial interval. Most neurons studied were located in a circumscribed area medial to the superior ramus of the arcuate sulcus in the frontal cortex. It is suggested that the neuron responses during the delay period may be involved in selective attention. The dorsomedial portion of the frontal cortex, including the prefrontal and premotor areas, may play an important role in attention control.

References

1. Jacobsen, C.F., "Functions of the Frontal Association Area in Primates," ARCH NEUROL PSYCHIATRY, Vol 33, 1935 pp 558-569.

2. Jacobsen, C.F., "Studies of Cerebral Function in Primates. I. The Functions of the Frontal Association Areas in Monkeys," COMP PSYCHOL MONOGR, Vol 13, 1936 pp 3-60.
3. Jacobsen, C.F., "Studies of Cerebral Function in Primates. IV. The Effects of Frontal Lobe Lesions on the Delayed Alternation Habit in Monkey," J COMP PHYSIOL PSYCHOL, Vol 23, 1937 pp 101-112.
4. Fuster, J.M., "The Prefrontal Cortex," Raven Press, New York, 1980.
5. Kubota, K., Niki, H., "Prefrontal Cortical Unit Activity and Delayed Alternation Performance in Monkeys," J NEUROPHYSIOL, Vol 34, 1971 pp 337-347.
6. Fuster, J.M., Alexander, G.E., "Neuron Activity Related to Short-term Memory," SCIENCE, Vol 173, 1971 pp 652-654.
7. Fuster, J.M., "Unit Activity in Prefrontal Cortex During Delayed Response Performance--Neuronal Correlates of Transient Memory," J NEUROPHYSIOL, Vol 36, 1973 pp 61-78.
8. Kubota, K., Iwamoto, T., Suzuki, H., "Visuokinetic Activities of Primate Prefrontal Neurons During Delayed Response," J NEUROPHYSIOL, Vol 37, 1974 pp 1197-1212.
9. Kojima, S., Goldman-Rakic, P.S., "Delay-Related Activity of Prefrontal Neurons in Rhesus Monkeys Performing Delayed Response," BRAIN RES, Vol 248, 1982 pp 43-49.
10. Kubota, K., "Neuron Activity in the Dorsolateral Prefrontal Cortex of the Monkey and Initiation of Behavior." In Ito, M., Tsukahara, N., Kubota, K., Yaki, K., ed., "Integrated Control Functions of the Brain," Kodansha, Tokyo, 1978 pp 407-417.
11. Roland, P.E., "Cortical Regulation of Selective Attention in Man: A Regional Cerebral Blood Flow Study," J NEUROPHYSIOL, Vol 48, 1982 pp 1059-1078.
12. Matono, N., et al., "Manufacture of Platinum-Iridium Electrode by Glass Coating," SEITAI NO KAGAKU, Vol 26 No 2, 1975 pp 183-186.
13. Suzuki, H., Azuma, M., "A Glass-Insulated 'Elgiloy' Microelectrode for Recording Unit Activity in Chronic Monkey Experiments," EEG AND CLIN NEUROPHYSIOL, Vol 41, 1976 pp 93-95.
14. Liu Guanlong, et al., "Observation of Neural Multiple Sensory Activity in Prefrontal Lobe and Premotor Cortex of Awake Monkeys," ACTA PHYSIOLOGICA SINICA, Vol 36 No 4, 1984 pp 311-321.
15. Kendler, H.H., "Basic Psychology," 3rd Edition, W.A. Benjamin, Inc., Massachusetts, 1975.
16. Posner, M.I., "Current Research in the Study of Selective Attention." In Dunchin, E., Ed., "Cognitive Psychology--Event-Related Potentials and Study of Cognition," The Carmel Congress, Vol 1, Lawrence Erlbaum Associates, Hillsdale, New Jersey, 1984.
17. Hillyard, S.A., Kutas, M., "Electrophysiology of Cognitive Processing," ANN REV PSYCHOL, Vol 34, 1983 pp 33-61.
18. Niki, H., "Prefrontal Unit Activity During Delayed Alternation in the Monkey--I. Relation to Direction of Response," BRAIN RES, Vol 68, 1974 pp 185-196.

19. Niki, H., Watanabe, M., "Prefrontal Unit Activity and Delayed Response: Relation to Cue Location Versus Direction of Response," BRAIN RES, Vol 125, 1976 pp 78-88.
20. Von Bonin, G., Bailey, P., "The Neocortex of Macaca Mulatta," University of Illinois Press, Urbana, 1947.

Crystal Structure of New Diterpene Lactone--Chilobolide A

40091019a Beijing HUAXUE XUEBAO [ACTA CHIMICA SINICA] in Chinese Vol 46 No 11, Nov 88 pp 1055-1061

[English abstract of article by Han Yuzhen [7281 3768 4176], et al., of the Institute of Physical Chemistry, Beijing University; Su Jingyu [5685 6975 1225] of the Department of Chemistry, Zhongshan University, Guangzhou]

[Text] Chilobolide A, $C_{22}H_{30}O_5$, M_r = 374.5, orthorhombic, space group $P2_12_12_1$, a = 8.753(2), b = 8.887(3), c = 54.247(14) Å, V = 4220(2) $Å^3$, Z = 8, D_x = 1.17 $g \cdot cm^{-3}$, F(000) = 1616 e at room temperature. The structure was solved by direct methods with diffractometer data measured with CuK α radiation, and block-full-matrix least-squares refinement converged at R = 0.064 for 1805 observed reflections. Both molecules in an asymmetric unit have similar conformations. The molecular skeleton is a bicyclic system in which an envelope form γ-lactone ring is cis-fused to a cyclotridecadiene ring, the latter ring is in [-+-+-++++-+--] asymmetric conformation; the methyl groups attached to 4-C and 13-C are situated on an E-type double bond, the acetyl group is in equatorial orientation at 10-C and the acetoxy group is in axial orientation at 9-C.

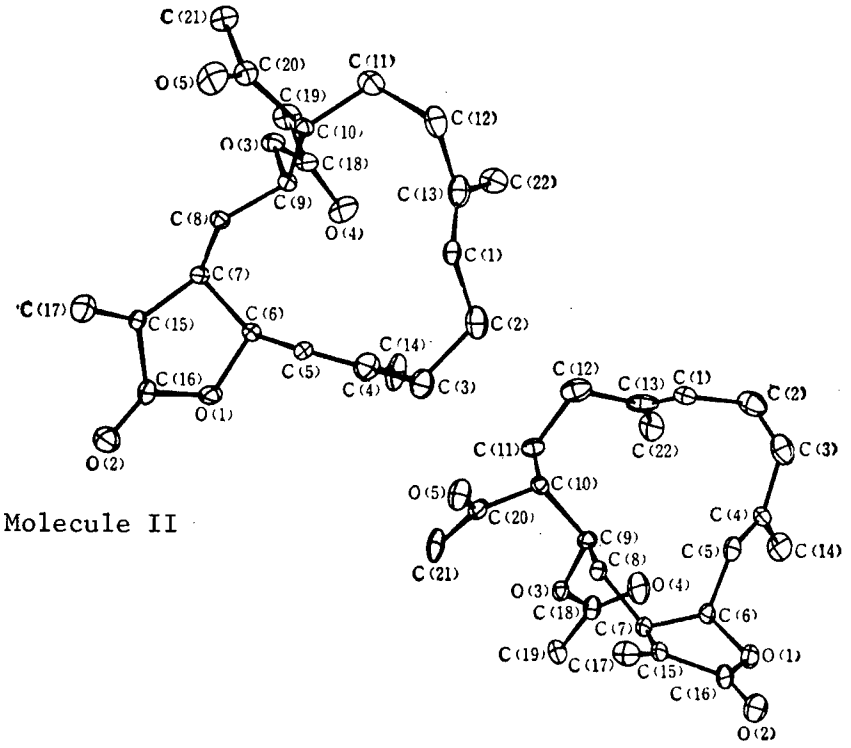

Stereostructures and atom numbers of the two molecules in Chilobolide-A crystal's asymmetric unit

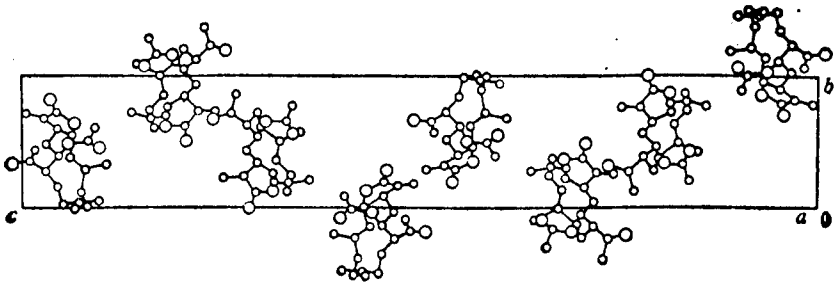

Molecular conformation of the crystal (a view from b direction)

Chilobolide-A, a substance extracted from soft coral from the South China Sea, is a natural product toxic to living cells.

References

1. Long Kanghou, et al., JOURNAL OF SUN YATSEN UNIVERSITY (NATURAL SCIENCES EDITION, Vol 2, 1981 p 8.
2. Bowden, B.F., Coll, J.C., Mitceu, S.J., Stokit, G.J., AUST J CHEM, Vol 31, 1978 p 1303.

3. Yao, J.X., ACTA CRYST, Vol A37, 1981 p 642.
4. Bixon, M., Lifson, S., TETRAHEDRON, Vol 23, 1967 p 769.
5. Dale, J., J CHEM SOC, 1963 p 93.
6. Dale, J., ACTA CHEM SCAND, Vol 27, 1973 p 1115.

Computer-Assisted Carboxypeptidase Method for C-Terminal Sequencing of Proteins, Polypeptides

40091019b Beijing HUAXUE XUEBAO [ACTA CHIMICA SINICA] in Chinese Vol 46 No 11, Nov 88 pp 1125-1133

[English abstract of article by Wang You [3076 3731], et al., of Shanghai Institute of Organic Chemistry, Chinese Academy of Sciences; Gu Tianjue [7357 1131 3635] of the Department of Biochemistry, Shanghai Medical University]

[Text] Upon further study of the computer-assisted carboxypeptidase method for C-terminal sequence determination of proteins or peptides, two computer programs--DPS and CPA--were successfully developed on the VAX-11/780 computer and tested with some synthetic peptides and degradation fragments of natural protein as model substrates. The C-terminal sequence of CB-3, one of the CNBr degradation fragments of trichosanthin, a protein abortifacient, was first determined by this method as -SerAlaSerAlaAlaLeuHseOH, which was later confirmed by other sequencing methods. This method can not only extend the C-terminal sequencing up to seven amino acid residues, but is also useful for determining the C-terminal sequence with some amino acid residues appearing in repetition.

References

1. Bailey, J.L., BIOCHEM J, Vol 60, 1955 p 173.
2. Meuth, J.L., Harris, D.E., Dwalet, F.E., Crowl-Powers, M.L., Gurd, F.R.N., BIOCHEMISTRY, Vol 21, 1982 p 3750.
3. Khorana, H.G., J CHEM SOC, Vol 228, 1952 p 2081.
4. Miller, M.J., Loudon, G.M., J AM CHEM SOC, Vol 97, 1975 p 5295.
5. Parham, M.E., Loudon, G.M., BIOCHEM BIOPHYS RES COMMUN, Vol 80, 1978 p 7.
6. Morris, H.R., NATURE, Vol 286, 1980 p 447.
7. Morris, H.R., Taylor, G.W., Panico, M., Dell, A., Etienne, A.T., McDowell, R.A., Judkins, M.B., "Methods in Protein Sequence Analysis," Clifton, NJ, Humana, 1982 p 243.
8. Ambler, R.P., METHODS IN ENZYMOLOGY, 1972 pp 25, 143, 262.
9. Zhang Linhua, MA Thesis, Shanghai Institute of Organic Chemistry, Chinese Academy of Sciences, 1981.
10. Wang, Y., Qian, R.Q., Gu, Z.W., Jin, S.W., Zhang, L.Q., Xia, Z.X., Tian, G.Y., Ni, C.Z., PURE AND APPLIED CHEMISTRY, Vol 58, 1986 p 789.

11. Wang You, et al., ACTA CHIMICA SINICA, Vol 46, 1983.
12. Petra, P.H., METHODS IN ENZYMOLOGY, Vol 19, 1970, p 460.
13. Hayashi, R., METHODS IN ENZYMOLOGY, Vol 45, 1976 p 568.
14. Stewart, J.M., Young, J.D., "Solid Phase Peptide Synthesis," San Francisco, CA, 1969.
15. Pravda, Z., Poduska, K., Blaha, K., COLLECTION CZECH CHEM COMMUN, Vol 29, 1964 p 2626.
16. Sun Xiaojian, PhD Dissertation, Shanghai Institute of Organic Chemistry, Chinese Academy of Sciences, 1986.
17. Roberts, D.V., "Enzyme Kinetics," Cambridge University, 1977.

Studies of Biosynthesis of Arteannuin. III. Arteannuic Acid As a Key Intermediate in Biosynthesis of Arteannuin, Arteannuin B

40091019c Beijing HUAXUE XUEBAO [ACTA CHIMICA SINICA] in Chinese Vol 46 No 11, Nov 88 pp 1152-1153

[English abstract of article by Wang You [3076 3731], et al., of Shanghai Institute of Organic Chemistry, Chinese Academy of Sciences]

[Text] [15- H] Arteannuic acid (1a) was incorporated into the biosynthesis of arteannuin (2a) and arteannuin B (3a) in a Qinghao plant (Artemisia annua L.) homogenate system. The experimental results show that arteannuic acid (1) is a key intermediate in the biosynthesis of both arteannuin (2) and arteannuin B (3) from MVA by Qinghao.

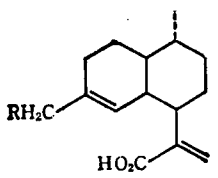

1 R=H;
1a R=T

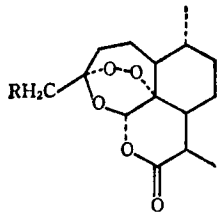

2 R=H;
2a R=T

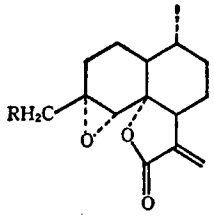

3 R=H;
3a R=T

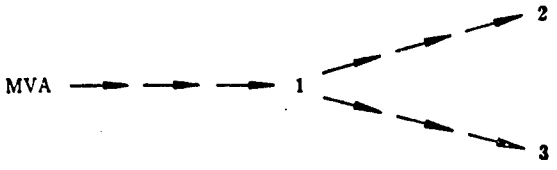

Qinghaosu from a Qinghao plant (Artemisia annua L.) has been proven to be a very effective traditional Chinese medicine for malarial treatments. Therefore, Chinese scientists have been closely studying the biosynthesis pathway of the drug in order to find a substitute for the expensive, natural one.

References

1. Huang, J.J., Zhou, F.Y., Wu, L.F., Zhen, G.H., ACTA CHIM SINICA (English Edition), in press.
2. Jermic, D., Jokic, A., Behbud, A., Stefanovic, M., TETRAHEDRON LETT, 1973 p 3039.
3. Huang, J.J., et al., publication pending.
4. Williams, B.L., Wilson, K., "Principles and Techniques of Practical Biochemistry," Edward Arnold, London, 1975.
5. Akhila, A., Thakur, R.S., Popli, S.P., PHYTOCHEMIST, Vol 26, 1987 p 1927.
6. Kudakasseril, G.J., Lam, L., Staba, E.J., PLANTA MEDICA, Vol 53, 1987 p 280.

Neuron Model Developed for Computer Simulation of Neural Nets

40080083a Beijing ZIDONGHUA XUEBAO [ACTA AUTOMATICA SINICA] in Chinese
Vol 14 No 6, Nov 88 pp 424-430

[Article by Wang Deliang [3076 1795 0081], Institute of Computing Technology, Chinese Academy of Sciences, and Xu Zhuoqun [6079 0587 5028], Beijing University: "A Neuron Model for Use in Computer Simulation." Manuscript received 24 November 1986.]

[Text] Abstract: This paper proposes a model for single neurons that can better resolve the problems of the relation between universality and precision demanded by computer simulation languages. By introducing an S-shaped curve to describe a memory value on the synapse, we can provide a uniform depiction of short-term memory and long-term memory, and we can also simulate the four basic study models: habituation, sensitization, conditioning, and facilitation.

I. Introduction

There has been great progress since McCulloch and Pitts proposed the first neuron mathematical model for single-neuron control theory. These efforts can roughly be seen to be of two categories: studies of single neurons and studies of neural networks.

In the simulation of single neurons there has been a greater emphasis on using mathematical forms to describe the biological nature of neurons, and especially on the electrophysiology. The goal of neural network research is to express the overall nature of the networks, but even in simulating neural networks one must model single neurons. This means that the neuron model that is designed will invariably be a more precise depiction of the various natures of the neurons, while ignoring other characteristics that are not relevant to the overall nature. Among the more typical are: those used in "perceptron" neuron models [14], where the perceptron is a device in a categorical diagram distinguishing learning and learned; those used in "cognitron" neuron models, where the cognitron can accomplish the task of completing recognition and association of a particular scale [5]; and the amphibian neuron model designed by Arbib et al., where neural networks based on this model can effectively emulate the preying and escape behaviors of amphibians [1,3].

We propose in this paper a new neuron model, the goal of which is to provide a finer basic neuron model for a general-purpose neural network modeling language called SLONN. SLONN is a system that is able to describe neural network structures, and that also can simulate network dynamic behavior on the computer. In order to suit multifaceted research on neural simulation, this neuron model should be rather accurate and general-purpose. We have solved these problems in two ways: one, under the premise of not introducing excessive complexity, to the greatest extent possible we allow the model that has been constituted to reflect the existing results of neurobiology, and two, by introducing some neuron parameters that can be adjusted by the user, this can be adapted to various needs. These are the primary characteristics of our model.

II. The Mathematical Model

Figure 1 is a graphic representation of a neuron model. $S_1,\ldots,S_m$ is the mth synapse connected to neuron N; $x_i(t)$ (where $i = 1,2\ldots,m$) is the input of synapse S_i during the time t, and where that value is either 0 or 1. Zero represents no pulse, and 1 indicates there is a pulse; W_i is used to represent the connecting strength of synapse S_i, and $-1 \leq W_i \leq 1$. When W_i is greater than zero, this means that S_i is an excited synapse; when W_i is less than zero, S_i is an inhibited synapse; when W_i equals zero, this indicates that S_i is not a factor.

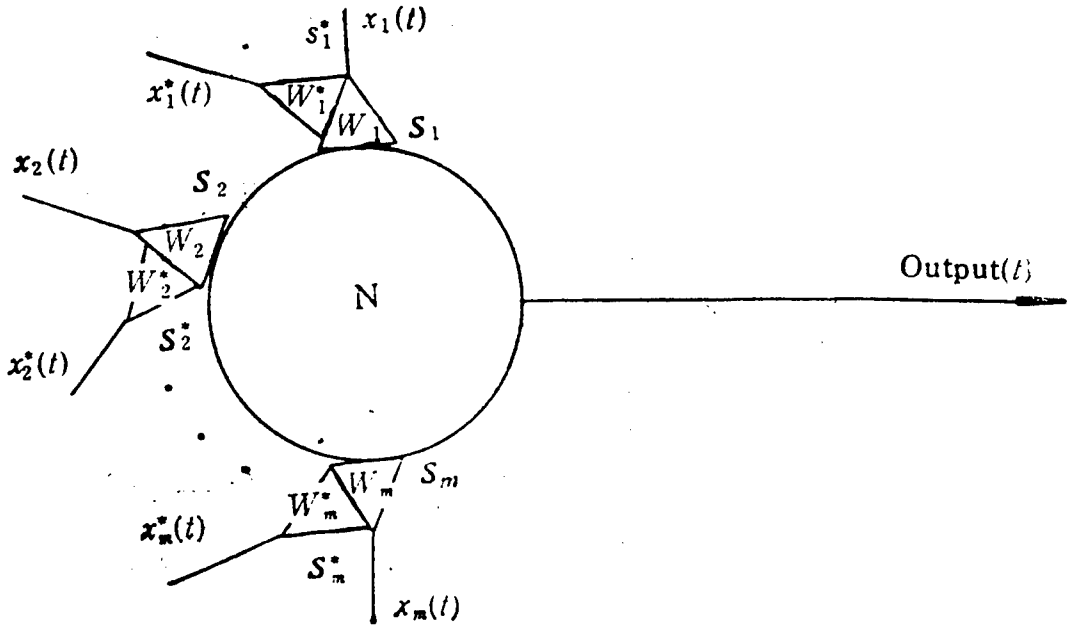

Figure 1. Diagram of the Neuron Model

When synapse S_i^* is placed under synapse S_i ($1 \leq i \leq m$), this method of connection is called a "synapse fore-connection," or it is said that S_i^* is the fore-synapse of the S_i synapse; $x_i^*(t)$ is the input of S_i^* at time t, where the value is either 0 or 1. W_i^* shows the strength of the connection at synapse S_i^*, where the scope of values is $-1 \leq W_i^* \leq 0$ or $W_i^* = 1$.

Output (t) is the output of neuron N at time t, and it is also a two-valued parameter, 0 and 1. Zero indicates that N is not generating a pulse, and 1 indicates that N is generating a pulse.

The neuron mathematical model includes a group of neuron parameters N_e and a group of system parameters N_i. The parameters in N_e are for the most part provided by the user, while the system parameters are realized by the SLONN system, where some of those parameters can be adjusted by SLONN management personnel.

$$N = \{N_e, N_i\}, \tag{2.1}$$

$$N_e = \{\theta, E, he, hi, \overrightarrow{lat}, \vec{W}, \vec{W}^*, \overrightarrow{ltype}\}, \tag{2.2}$$

$$N_i = \{pt, f_E(s), f_I(s), \vec{M}(t), \vec{L}(t)\}. \tag{2.3}$$

where θ represents the extension threshold of the neuron; E is the resting potential of neuron N; he and hi are the height values, respectively, of the resulting potential EPSP of the excited synapse generated by a single pulse arriving at the synapse and the potential IPSP coming from the inhibited synapse. All synapses are the same regarding the relationship of he and hi to N. Each component of the vector $\overrightarrow{lat}$ represents the delay time lat of each synapse as it affects the pulse before the synapse; $\vec{W}$ comprises the components $W_1,\ldots,W_m$, and $\vec{W}^*$ comprises $W_1^*,\ldots,W_m^*$; $\overrightarrow{ltype}$ indicates the learning category of each memory synapse at N. $\vec{W}$, $\vec{W}^*$, and $\overrightarrow{ltype}$ must be provided by the user, while the user need not provide the other parameters in equation (2.2), as the system will fill in the missing values.

Before resolving N_i, we input the time τ that is the uniform clock interval of the neurons. Using τ to represent the arrhythmic time of the neurons corresponds to the time intervals between the two successive pulses on the axon. Given that τ is the same for all neurons, let the durations of EPSP and IPSP both be pt.

To describe the time response parameters of EPSP and IPSP, we use $f_E(s)$ and $f_I(s)$, respectively, and the argument is time s.

$$f_E(s) = \begin{cases} \dfrac{he}{\tau}(s - lat), & lat \leqslant s \leqslant lat + \tau, \\ he \cdot e^{-\lambda_1(s-lat-\tau)}, & lat + \tau \leqslant s < lat + c\tau, \\ 0, & \text{other.} \end{cases} \tag{2.4}$$

$$f_I(s) = \begin{cases} -\dfrac{hi}{\tau}(s - lat), & lat \leqslant s < lat + \tau, \\ -hi \cdot e^{-\lambda_2(s-lat-\tau)}, & lat + \tau \leqslant s < lat + c\tau, \\ 0, & \text{other.} \end{cases} \tag{2.5}$$

where c = pt/τ, and λ_1 and λ_2 are the decay factors for EPSP and IPSP, respectively. The output of neuron N is given by the following equation:

$$\text{Output}(t) = H_\theta\left(\sum_{i=1}^{m}\sum_{r=1}^{c} u_i^r(t) + E\right). \tag{2.6}$$

where E is the resting potential and H_θ is the threshold parameter

$$H_\theta(x) = \begin{cases} 1, & \text{for } x > \theta, \\ 0, & \text{for } x \leqslant \theta. \end{cases}$$

$u_i^r(t)$ is the contribution of the input $x_i(t-r\tau)$ of the synapse S_i before the beat r (relative to time t) on the synapse post-potential. The expression $u_i^r(t)$ has two conditions: ordinary synapse and memory synapse. What we mean by "ordinary synapse" is where synapse strength W_i does not change. In contrast, what we call "memory synapse" is where the memory strength is $W_i(t)$.

1. For the ordinary synapse

$$u_i^r(t) = \begin{cases} W_i \cdot x_i(t-r\tau) \cdot f_E(r\tau), & \text{for } W_i \geqslant 0,\ W_i^* = 0, \\ -W_i \cdot x_i(t-r\tau) \cdot f_I(r\tau), & \text{for } W_i < 0,\ W_i^* = 0, \\ \text{Max}\,(W_i \cdot x_i(t-r\tau) \cdot f_E(r\tau) & \\ \quad + W_i^* \cdot x_i^*(t-r\tau) \cdot f_I(r\tau), 0) & \text{for } W_i > 0,\ W_i^* < 0, \\ \text{of no significance,} & \text{other conditions.} \end{cases}$$

In the $u_i^r(t)$ equation, the two preceding conditions were when there was no synapse fore-connection ($W_i^* = 0$), and for the excited synapse, introducing $x_i(t-r\tau)$ forms one EPSP, the value for which EPSP at time t is $f_E(r\tau)$; for the inhibited synapse, introducing $x_i(t-r\tau)$ forms one IPSP, the value for which IPSP at time t is $f_I(r\tau)$. The third condition, when W_i is greater than zero and W_i^* is less than zero, simulates the synapse pre-inhibition in the biological nerve system, which is to say that the input of $x_i^*(t-r\tau)$ inhibits (reduces) the contribution of the input of $x_i(t-r\tau)$ on the neuron extension. There is no biological evidence for other conditions, so we do no other simulation in this model.

2. For the memory synapse

$$u_i^r(t) = \begin{cases} W_i(t-r\tau) \cdot x_i(t-r\tau) \cdot f_E(r\tau), & \text{for } W > 0, \\ \text{of no significance,} & \text{other conditions.} \end{cases}$$

where $W = W_i(0)$, that is, the initial synapse strength.

The rules of change for $W_i(t)$ follow. Take a memory synapse (S_i, S_i^*) (see Figure 1). The memory is manifest as changes in the connecting strength $W_i(t)$ of the synapse S_i, where at this time the function of S_i^* is an

adjustment function for the memory function, that is, $W_i^* = 1$ is the constant. The memory input for remembering S_i is $z_i(t)$, where the generation of $z_i(t)$ is related to $x_i(t)$, $x_i^*(t)$, and the learning category.

When describing $W_i(t)$, we enter the memory parameter M(t) (a component of $\vec{M}(t)$ in equation (2.3)). A string of consecutive memory input $z_i(t)$ will cause M(t) to increase; otherwise, M(t) will attenuate. There are two kinds of attenuation: the two forget mechanisms of short-term memory and long-term memory, respectively. To this end, we input the status variable L(t) for the memory synapse (a component of $\vec{L}(t)$ in equation (2.3)). When L(t) equals zero, this indicates that the synapse is in a "training state" (also called the "short-term memory state"), while when L(t) equals one, this is called a "knowing state" (also called the "long-term memory state").

In order to more accurately simulate the research results of and hypotheses put forward by neurobiology, we consider memory to be of four kinds:

1. For habitual learning (ltype = habit), let:

$$W_i(t) = \text{Max}\,(W - M(t), 0), \quad z_i(t) = x_i(t). \tag{2.7}$$

We can see from this description that we solve for habitual learning by inputting $x_i(t)$ for S_i (at this time $x_i^*(t)$ makes no contribution to memory values). The sustained stimulus $x_i(t)$ will cause M(t) to increase, causing the value of $W_i(t)$ to drop, consequently forcing the sensitivity of the synapses to subsequent stimuli to drop.

2. For sensitized learning (ltype = sensi), let:

$$W_i(t) = \text{Min}\,(W + M(t), 1), \; z_i(t) = x_i^*(t). \tag{2.8}$$

This kind of learning is only solved for by inputting $x_i^*(t)$ for S_i^*. The arrival of any kind of disturbing stimulus $x_i^*(t)$ will cause $W_i(t)$ to rise, which strengthens the results to stimuli to S_i.

3. For conditioned learning (ltype = condi), let:

$$W_i(t) = \text{Min}\,(W + M(t), 1), \; z_i(t) = x_i(t) \cdot x_i^*(t). \tag{2.9}$$

Only when the stimulus $x_i(t)$ on S_i appears coincidentally with the stimulus $x_i^*(t)$ on S_i^* will this type of learning be generated. At such times, $W_i(t)$ will rise, which strengthens the effects of subsequent stimuli $x_i(t)$ on S_i.

4. For facile learning (ltype = facil), let:

$$W_i(t) = \text{Min}\,(W + M(t), 1), \quad z_i(t) = x_i(t) \cdot \text{Output}\,(t). \tag{2.10}$$

If stimuli on S_i can cause the entire neuron to extend, then Output(t) = 1, which strengthens the response effects of this synapse to subsequent stimuli ($W_i(t)$ rises).

We give below the mathematical format for M(t) and L(t). Our task is to provide the rules for obtaining $M(t + \tau)$ and $L(t + \tau)$ when M(t) and L(t) are already known. We provide initial values of M(0) = 0 and L(0) = 0. For this purpose we introduce the special coefficients f_m, f_s, and f_l; $f_m(t)$ satisfies the S-curve of differential equation (2.11), as shown in Figure 2.

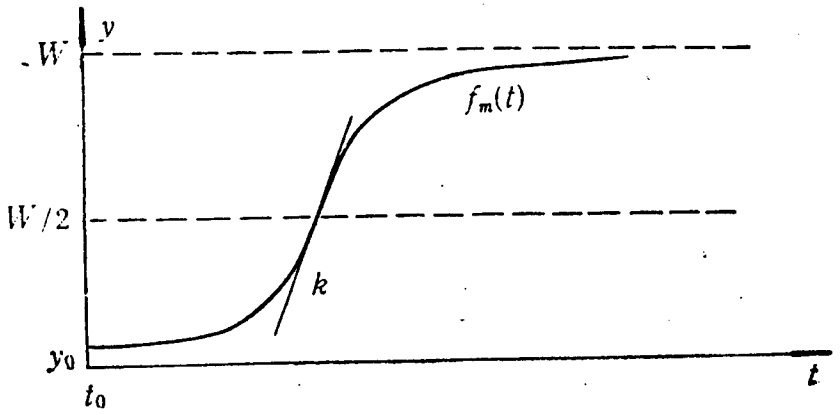

Figure 2. Diagram of the S-curve $f_m(t)$

Here, k and the initial values (when $t = t_0$, $y = y_0$) can be selected in accordance with a particular applications environment, and W is the degree of initial synapse strength. f_s and f_l are curves of exponential decay, with particular forms omitted.

$$dy/dt = \frac{4k}{W} \cdot y - \frac{4k}{W^2} y^2 \tag{2.11}$$

A total of three lines are used to describe the growth rules for M(t) and the rules for decay in short-term memory and in long-term memory.

To this end, we can provide:

$$M(t+\tau) = \begin{cases} h_m(M(t)), \text{ if } z_i(t) = 1, \\ h_l(M(t)), \text{ if } z_i(t) = 0,\ L(t) = 1, \\ h_s(M(t)), \text{ if } z_i(t) = 0,\ L(t) = 0, \end{cases} \tag{2.12}$$

$$L(t+\tau) = \begin{cases} 0, \text{ if } L(t) = 0,\ M(t+\tau) \leqslant \frac{W}{2}, \\ 1, \text{ other.} \end{cases} \tag{2.13}$$

where

$$h_m(y) = f_m(f_m^{-1}(y) + \tau), \tag{2.14}$$

$$h_l(y) = f_l(f_l^{-1}(y) + \tau), \tag{2.15}$$

$$h_s(y) = f_s(f_s^{-1}(y) + \tau). \tag{2.16}$$

Argument y indicates the memory value of the memory synapse.

L(t) is affected by the value of M(t). After M(t) exceeds W/2 (the inflection point of f_m), L(t) is set to 1, that is, it becomes a learned state. We can see from the equation above that as soon as L(t) becomes a learned state, it will not return to a learning state.

III. An Analysis and Explanation of the Model

We can see by analyzing equation (2.6) that: 1) the summation of the inner layer, i.e., $\sum_{r=1}^{c}$, is a simulation of the entire time at the synapse; the summation of the outer layer, i.e., $\sum_{i=1}^{m}$, is a summation of space for all synapses of N. 2) Inputting $f_E(t)$ and $f_I(t)$ allows each pulse arriving at the neuron synapse to generate a post-synapse potential in accordance with the type of synapse. 3) The user can fix beforehand the resting potential E for the neuron. If E is set near the threshold, this will simulate the phenomenon of self-electrical generation within the nervous system. 4) Setting the synapse delay $\overrightarrow{lat}$ determines the length of delays for N synapses. $\overrightarrow{lat}$ may also be used to represent the time consumed as a pulse is transmitted from one neuron to another neuron.

The synapse fore-connection is a common phenomenon in the nervous system. Consideration of this condition has brought our model closer to biological neurons. At the same time, because we see the synapse fore-connection as the controller of the learning type of memory synapses--which means that it can represent synapse expectancy and the four learning types (the habitual, the sensitized, the conditioned, and the facile) at the level of the synapse--this allows our neuron model to reflect various learning processes. Experiments by Kandel [7] have supported this model.

A description of synapse expectancy can basically be divided into two types: one is of a linear mode, i.e., the memory value grows or decays in a linear mode, for which see reference [17]. The other type is an exponential mode, as described in references]2, 10]. This model uses an S-curve to indicate the growth of memory values, which then has the following two advantages:

1. Long-term and short-term memory can be seen as a uniform process, which completely coincides with experimental results from small nervous systems [7], as well as with the modern view of psychology regarding short-term memory [16].

2. How can we use a uniform format to integrate the two processes of short-term memory and long-term memory? The S-curve resolves this problem. Because the S-curve has two processes of change, as well as a special breakpoint--the inflection point--this means that it can naturally express these two memory processes within a single curve.

IV. Conditions of Implementation

The neuron model just described has been partially realized on a Fortune 32:06 system in the SLONN language (see our other paper for details). To determine the parameters of our model, we will divide parameter selection into two levels:

1. Users. By the programmed SLONN routines and system communications, users can select various parameters for N_e in equation (2.2) from among those routines. The user must give synapse strength and the learning model for memory synapses.

2. System programmers. System programmers have the authority to allocate missing values for the various neuron parameters in equation (2.2). In addition, they can also determine the particular configuration for each curve input by this model, as for example k in equation (2.11). Tables 1 and 2 provide model-selected values for a typical experiment.

Table 1. Missing Values From Neuron Parameters

θ	E	he	h_i	$\overrightarrow{lat}$
30mV	0mV	50mV	-5mV	0

Table 2. Parameters for Each System Curve (equations (2.4), (2.5), and (2.11))

λ_1	λ_2	τ	c	t_0	y_0	k
0.25	0.167	2ms	7	10	$\frac{W}{2}$	$\frac{W^2}{8}$

A couple points should be made regarding actual implementation of this system:

1. The entire system is a discrete system, so choose discrete time values. The length of each beat equals τ.

2. In principle, at each beat, memory values for memory synapses will change in accordance with (2.12). Actually, the effects of each pulse on memory values for a synapse are inconsequential. In the implementation, each seven beats will generate the calculation of memory values, that is, the length of memory beats is 7τ. Accordingly, calculations for the forgetting of long-term memory will be made once each hundred memory beats.

References

1. Arbib, M. A., Lara, R., A Neural Model of the Interaction of Tectal Columns in Prey-Catching Behavior, Biological Cybernetics, 44(1982), 185-196.

2. Barto, A. G., et al., Neuron-like Adaptive Elements That Can Solve Difficult Learning Control Problems, IEEE Trans. System. Man. Cybernetics, SMC-13(5) (1983), 835-846.

3. Cervantes, F., Lara, R. and Arbib, M. A., A Neural Model of Interactions Subserving Prey-predator Discrimination and Size Preference in Anuran Amphibia, Journal of Theoretical Biology, 113(1985), 117-152.

4. Fukushima, K., Neucognitron: A Self-Organizing Neural Network Model for a Mechanism of Pattern Recognition Unaffected by Shift in Position, Biological Cybernetics, 36(1980), 193-202.

5. Fukushima, K., A Hierarchical Neural Network Model for Associative Memory, Biological Cybernetics, 50(1984), 105-113.

6. Hebf, D. O., The Organization of Behavior, Wiley Press, 1949.

7. Kandel, E. R., Small System of Neurons, Scientific American, 241(3), (1979), 67-76.

8. Lara, R., et al., Mathematical Models of Synaptic Plasticity, Journal of Neurology Research, 2(1980), 1-18.

9. Lara, R., Arbib, M. A., A Neural Model of Interaction Between Pretectum and Tectum in Prey Selection, Cognition and Brain Theory, 5(2) (1982), 149-171.

10. Lara, R., Arbib, M. A., A Model of the Neural Mechanisms Responsible for Pattern Recognition and Stimulus Specific Habituation in Toads, Biological Cybernetics, 51(1985), 223-237.

11. McCulloch, W. S., et al., A Logical Calculus of the Ideas Immanent in Neuron Activity, Bulletin of Mathematical Biophysics, 5(1943), 115-133.

12. Parlov, I. P., Lectures on Conditional Reflexes, International Publishers, 1982.

13. Peterson, L. R., et al., Short-Term Retention of Individual Verbal Items, Journal of Experimental Psychology, 58(1959), 193-198.

14. Rosenblatt, F., The Perceptron: A Probabilistic Model for Information Storage and Organization in the Brain, Psychological Review, 65(1958), 386-407.

15. Stein, R. B., A Theoretical Analysis of Neuronal Variability, Biophysical Journal, 5(1965), 173-194.

16. Wingfield, A., Byrnes, D. L., The Psychology of Human Memory, Academic Inc., 1981.

17. Barto, A. G., et al., Associative Search Network: A Reinforcement Learning Associative Memory, Biological Cybernetics, 40(1981), 201-211.

Latest Developments in Computer Networks

Embargoed Controller Now Chinese-Made

40080097 Beijing JISUANJI SHIJIE [CHINA COMPUTERWORLD] in Chinese 7 Dec 88 p 2

[Article by Gao Lihua [7559 7787 5478]: "X.25 Communications Controller Goes On Market, Filling Domestic Void"]

[Text] This reporter learned recently while at Southeast University (formerly Nanjing Engineering Institute) that an X.25 communications controller capable of connecting small mainframes, minicomputers, and microcomputers to public packet switching data networks passed its provincial technical evaluation in Nanjing on 8 November. More than a month ago, this controller had passed an interconnection test successfully held between the public packet switching network CNPAC belonging to the Nanjing Telecommunications Bureau and the Ministry of Posts and Telecommunications, and the private packet switching data network of a certain division of the central government, which test saw the first network communication within China by a domestically-produced communications controller.

The X.25 communications controller is responsible for the relay of high-level information. On one end it executes the three-level regulations of the CCITT/X.25 (1984) DTE [data terminal equipment], and on the other end uses asynchronous connection with each host. Aside from functions connecting it with the packet switching DCE [?data circuit-terminating equipment] equipment, some standard regulations having to do with the ISO 8028 DTE indirect connections have also been implemented, which means that different kinds of computers can be part of public packet switching data networks through telephone exchange lines or dedicated hookups. This fact directly affects the building of municipal area networks and long-distance information systems, as well as the efficiency of use for public data networks. There has been an embargo and blockade of this equipment and technology by foreign countries toward China. A research group at Southeast University was assigned this key S&T project of the Seventh 5-Year Plan in 1986. In keepingwith the project requirements as set forth by the provincial science and technology commission for "a description of a communications network protocol format" and "the Nanjing municipal area network," this group absorbed advanced foreign

technology and thinking, and after more than 2 years of hard work finally successfully developed this microprocessor-based communications network equipment. This equipment uses the Intel 8085 and 8273 chips, contains X.25 three-layer protocol software, and provides for the host interface logical servicing code that is completely in accordance with the OSI [open systems interconnection] network layered-service definitions as proposed by the International Standards Organization (ISO). It both regularizes host computers, and also provides a uniform reference base for the development of host interface software. After the release of this equipment, it passed tests by uniform testing software of the American NBS [National Bureau of Standards].

The evaluation considered that this new achievement fills a domestic void, and that it plays a leading role domestically in realizing the integration, standardization, and protocol engineering of the X.25 protocol. They felt that this equipment is a basis for application and commercialization, and that it has great value for dissemination. It will play an important role in stimulating the development of China's data communications and computer network efforts. It is understood that at present this new achievement has drawn the attention of domestic communications and banking systems, and that enterprises such as the Nanjing Wired Telecommunications Equipment Plant and the Changzhou Computer Plant have requested rights to transfer the technology.

National Defense S&T Document Library

40080097 Beijing JISUANJI SHIJIE [CHINA COMPUTERWORLD] in Chinese 7 Dec 88 p 2

[Text] As commissioned by the National Defense S&T Information Computer Network, software to enter bibliographic data bases into the National Defense S&T Information Computer Network was recently successfully developed by the Institute of Electronic S&T Information of the Ministry of Machine-Building and Electronics Industry. This software was developed in accordance with the uniform standards of the bibliographic data base recording formats formulated within the network, and this will serve an active role in promoting the building of national defense S&T bibliographic data bases and the sharing of data.

There are 26 units in Beijing currently part of China's National Defense S&T Information Network. Having many different types of computer systems, the recording formats for these bibliographic data bases developed by each unit are not always the same, which poses problems for future data base interconnection efforts. To ensure that China's rich national defense bibliographic data can be shared, it is imperative that uniform data entry standards be drawn up immediately. In April this year, the National Defense S&T Information Computer Network officially announced the recording format standards for bibliographic data bases, and they determined the design requirements for entry of working cells and recording software for various kinds of bibliographic data. Because of bidding considerations, it was determined to commission the data entry software of the Institute of Electronic S&T Information of the Ministry of Machine-Building and

Electronics Industry, which software is the "electronic working cells" necessary at the time of library creation. All software had been developed by the end of October this year [1988]. This software has powerful data checking functions, which will improve the reliability of entered data, and the data definitions are convenient and flexible; the system allows self-defined phrases, which will speed data entry; and the recorded data can be converted to standard floppy recording formats, which will allow data conversion with microcomputer systems.

The experts considered that this software satisfies the functions determined by the design requirements, that the design of the software is reasonable, flexible, general purpose, and that the materials included with it are complete, and that it is ready to be used. It is now being formally disseminated by the National Defense S&T Information Computer Network for use by units within the network.

Macintosh-Driven Network Goes Into Operation

40080097 Beijing JISUANJI SHIJIE [CHINA COMPUTERWORLD] in Chinese 7 Dec 88 p 18

[Text] The China MAC Development Center, set up with the aid of the American Apple Company at the Computer Research Institute of the National Defense University of Science and Technology, will use Ethernet to connect the center's Apple Talk local area network (there are several dozen different kinds of Macintosh and IBM microcomputers attached to this LAN) to the campus network, which has as its core the Galaxy 100MIPS supercomputer. This network is made up of DECnet and Ethernet networks, which include hundreds of mini and mainframe computers and microcomputers, and is officially on-line and being used for real applications.

On this basis, the MAC Development Center is successfully using the Macintosh microcomputer to build a remote computer network from Changsha to Guangzhou. There are various computers on this network, among them computers from the Macintosh series, IBM PC/XT and ATs, Great Wall 0520-CHs, and MicroVAX-IIs, and it has allowed exchanges among all the nodes on the network. The performance of this remote network is good, it costs little to develop, and the economic results are outstanding. At present, this remote network is being further improved, and it is about to begin formal application.

Briefs

New 32-Bit Supermicrocomputer Workstation--A key project in the Seventh 5-Year Plan, the development of the Model 0600 32-bit general-purpose supermicrocomputer engineering workstation--jointly perfected by Institute 6 of the Ministry of Machine-Building & Electronics Industry (MMEI), the University of Electronic Science & Technology (formerly Chengdu Institute of Telecommunications Engineering), and Nanjing Plant 734--passed MMEI-level technical accreditation and design finalization on 15 December [1988] in Beijing. The 0600 will also be known as the Hua Sheng [5478 0524] 3000 series; so far, this includes the Hua Sheng 3100 (monochrome) and the HS 3160 (color). Independently designed elements include the central processing unit, the graphics control card, the tape equipment interface card, the mother board, the external frame, and the power supply. The UNIX operating system, high-level language(s), graphics, windows, network software and database software have all been Sinicized [i.e., converted for running with Chinese characters], and the system is fully Chinese-English compatible. The 3000-series models, which are priced 25-43 percent below comparable foreign workstations and which are now in small-batch production, will provide a useful tool for CAD/CAM, software engineering, and artificial intelligence technology [development]. This is the first time such [functionally] complete Chinese-character processing software has been domestically developed for a supermicrocomputer workstation. [Summary] [40080120a Beijing JISUANJI SHIJIE [CHINA COMPUTERWORLD] in Chinese No 50, 28 Dec 88 p 1]

Galaxy-II Supercomputer Software Finalized--After a one-year effort, the National Defense University of Science & Technology's Computer Research Institute has formalized plans for the YH-II [i.e., Galaxy-II] software systems, and in late 1988 held a "YH-II Software Scheme Examination & Approval Conference." At the conference, held in Changsha and attended by over 80 specialists from 20 units including the State Meteorological Administration, the institute delivered a report on various aspects of the plan. The complex, large-scale YH-II software systems, which use the FORTRAN language, will have a functionally distributed operating system, with functions such as multiprocessor support, batch processing, and interactive processing; a tape subsystem and high-speed input/output are included. The system has automatic vector recognition, supports multitasking, and has a cache memory and a large internal memory. The assembler separates code data and work space, provides program reentry, and supports assembly-level multitask program design. Library routines utilize advanced parallel algorithms; the graphics library uses the international graphics standard GKS [graphics kernel system]. The heterogeneous network of the high-speed local area network system uses the ISO/OSI [International

Standards Organization's open systems interconnection] standard. Conference participants offered suggestions on software functions, testing, maintenance, tools, performance parameters, and standardization, and expressed hopes for further development of a YH-UNIX environment. [Summary] [40080120b Beijing JISUANJI SHIJIE [CHINA COMPUTERWORLD] in Chinese No 50, 28 Dec 88 p 1; see also JPRS-CST-89-004, 2 Feb 89, p 48]

Improved Taiji Superminicomputer--A new 2000-series Taiji superminicomputer, the model 2230, was recently introduced. Compared to the Taiji 2220 superminicomputer [see JPRS-CST-88-016, 29 Aug 88, p 52], the new model has the following characteristics: processing speed (now 2.7 MIPS [million instructions per second]) is 200 percent higher, main memory capacity [i.e, real storage] has doubled to 32Mbytes, the parity-check error-correcting code has been improved, system disk storage has increased from 86Mbytes (model 2220A) to 766Mbytes (model 2230A) and from 500Mbytes (model 2220B) to 1000Mbytes (model 2230B), and recording density for the industrial[-standard] tape drive has increased from 1600 BPI [bits per inch] to 3200 BPI and 6250 BPI. The Taiji 2230 comes with a 1Mbyte floppy disk [compared to 800Kbytes for the 2220]; a 95Mbyte cassette tape drive with a recording-density selection of 1600, 3200, or 6250 BPI; a 383Mbyte or 500Mbyte Winchester disk drive; and two operating systems: TJVMS [Taiji Virtual Machine System] and ULTRIX. There are two kinds of databases: database management systems and relational databases. Languages include FORTRAN77, COBOL, C, PASCAL, BASIC, ADA, and MACRO. [Summary] [40080120c Beijing JISUANJI SHIJIE [CHINA COMPUTERWORLD] in Chinese No 50, 28 Dec 88 p 11]

Marketing of Taiji 2230--With the formal signing of a contract for a US$4.5 million World Bank loan under the supervision of the State Education Commission, the Taiji Computer Company (North China Computing Technology Research Institute) has manufactured 64 fourth-generation-technology 32-bit Taiji 2230 superminicomputers, soon to be installed in 40 institutes and universities in 26 provinces, municipalities, and [autonomous] regions. With a performance meeting mid-to-late-eighties international standards, this computer is targeted to capture one-eighth of the Chinese market demand for superminicomputers. [Summary] [40080120d Beijing DIANZI SHICHANG [ELECTRONICS MARKET] in Chinese 12 Jan 89 p 1]

Naval Institute Develops New Simulator--The Institute of Naval Engineering has developed a model of a three-degrees-of-freedom (lateral rolling, vertical movement, and bow rolling) simulation system to reduce warship rolling of up to 40 degrees in a Force-8 storm down to four degrees or less--a reduction of over 90 percent. Systems to reduce rolling (and thereby provide stabilization) along three axes--a topic of research in only a few advanced countries--are of interest because severe waves can cause serious illness to personnel, threaten the life of the ship, and make weapons difficult to use. At present, Chinese warships have damping devices with only one degree of freedom--reduction of lateral rolling for light warships. In an effort lasting several years, Associate Professor Ren Xuepei [0117 1331 3099] led a team of over 10 researchers in the development of this computerized simulation system, which incorporates fuzzy control theory and which can also be used for naval confrontation exercises and other training exercises, for demonstrations of actual damping devices, for performance estimates, and for fault diagnosis. [Summary] [40080120e Beijing JISUANJI SHIJIE [CHINA COMPUTERWORLD] in Chinese No 1, 4 Jan 89 p 1]

Simulator for Daya Bay Nuclear Station--An [imported] basic-principles analog machine [i.e, control-unit simulator] for the Daya Bay Nuclear Power Station--China's first such simulator--became operational in November 1988. Plans for the Daya Bay Station, China's largest commercial nuclear power station, with a 2x900-megawatt installed capacity and an initial power-generation target date of 1992, also include importing of a full-range analog machine, for more advanced instruction. The basic-principles analog-machine system, designed and manufactured by France's CEA/CENG [Commissariat à l'Energie Atomique/Centre d'Études Nucléaires de Grenoble] as a relatively simple model of a 900-megawatt pressurized-water-reactor [control] unit, will be used for initial instruction of station personnel so that they can master various physical processes arising in the operation of the station. After personnel are trained on the basic-principles simulator, they will progress to the full-range analog machine for mastery of the principles of safe and reliable operation under normal and abnormal conditions. Hardware for the basic-principles simulator consists of a Gould Concept 32/6742C computer system, an analog control station, an instructor control station, an HP [Hewlett-Packard] graphics workstation, a PERICOM monitor, an instrument for recording operational curves [i.e., for taking the log], a plotter, and other components. Over 50 accidents and situations (including emergency shutdown and steam-turbine tripping) can be handled, and 39 alarm indicators are built into the system, which includes simulation software for both the G and A operational modes at the Guangdong Daya Bay station. [Summary] [40080120f Beijing JISUANJI SHIJIE [CHINA COMPUTERWORLD] in Chinese No 2, 11 Jan 89 p 1]

Military Expert Systems Conference--The first [Chinese] Military Expert Systems and Artificial Intelligence Conference concluded the other day at the PLA Engineering Corps' Engineering Institute. After over a decade of experimentation and practice, research in computerized military expert systems and artificial intelligence systems for battlefield simulation and combat decision-making is entering a new phase [see also JPRS-CST-89-005, 23 Feb 89, pp 64-70]. In addition to battlefield simulation and tactical training, experts agree that the new technologies can also be applied to strategic decision making, weapons control, [fault] diagnosis, etc. Organizations represented at the conference include the China Systems Engineering Institute, the Military Systems Engineering Commission, the China Artificial Intelligence Institute, and others. [Summary] [40080120g Beijing ZHONGGUO DIANZI BAO in Chinese 13 Jan 89 p 2]

Briefs

Multifunctional CNC Gas Cutting Machine--The model 5200A multifunctional microcomputer numerically controlled (CNC) gas cutting machine, jointly perfected by Design Institute 9 of the China State Shipbuilding Corporation, the Jiangsu [Province] Changzhou Electric Locomotive Plant, and the plant attached to Shanghai Jiaotong University, recently passed technical certification. Development of this CNC oxyacetylene machine, which has biaxial and other high-speed cutting functions and a precision which meets the "WES6601-1980 Japanese NC cutter precision test standard," will reduce imports and be of great value to the shipbuilding and machinery industries. [Summary] [40080117d Tianjin ZHONGGUO JISHU SHICHANG BAO [CHINA TECHNOLOGY MARKET NEWS] in Chinese 18 Jan 89 p 1]

Prospects for Stealth, Counter-Stealth Technologies

40080088 Beijing DIANZI KEXUE JISHU [ELECTRONIC SCIENCE & TECHNOLOGY] in Chinese Vol 18 No 11, Nov 88 pp 2-4

[Article by Ruan Yingzheng [7086 4481 6927] and Lin Weigan [2651 3634 1626], University of Electronic Science & Technology [formerly Chengdu Institute of Telecommunications Engineering]]

[Excerpts] I. Introduction

Stealth technology is a complex and sophisticated technology which has been developed in recent years to reduce the scattering and emission of energy from military targets (e.g., aircraft, missiles, ships, tanks, etc.) over a wide range of spectrum: microwave, infrared, light-wave and sound wave. [Passage omitted] Currently, the key stealth technology centers around evasive measures against radars, but to truly achieve the objective of stealth, one must also control the emission and scattering of energy in the form of heat, sound, light, and electricity. [Passage omitted]

The United States, the Soviet Union, Japan, and many European countries have devoted a large amount of human and material resources over the past 20 years toward research on stealth and counter-stealth technologies. Since the 1980's, major breakthroughs have been achieved in stealth technology[1]; in particular, it has advanced from basic theoretical research to prototype development. A variety of low-visibility stealth bombers, fighters, cruise missiles, helicopters and reconnaissance airplanes have been developed. [Passage omitted]

II. A Review of Stealth Technology in the United States

The United States was the first country to study stealth technology; it is also the country which has invested the largest amount of financial and human resources in stealth research. As early as the 1950's, it had developed the U-2 high-altitude reconnaissance airplane and the P2V-7 low-altitude reconnaissance airplane, and subsequently the A-12, the D-21 and the SR-71, all of which used radar-absorbent materials to reduce their radar characteristics. Since the Vietnam war and the Middle-East war, with better understanding of weapon survivability, the United States realized that stealth technology combined with active or passive interference

techniques will play a key role in modern warfare. [Passage omitted] Subsequently, stealth technology has been applied in the design of weapon systems of all three armed forces: strategic bombers, cruise missiles, fighter aircraft, reconnaissance airplanes and helicopters. It is estimated that the United States has already invested 30 billion dollars in stealth technology.

The U.S. stealth bomber development plan includes the B-1 which went into service in 1986, the recently developed B-2 long-range bomber, and the ATB advanced bomber which is scheduled to be ready for service in 1991. The B-1 is a successor to the B-52 strategic bomber; by using stealth technology, its effective radar cross section in the forward direction is only 1 m^2, whereas the radar cross section of the B-52 is 100 m^2. The ATB is a strategic bomber whose design has fully incorporated stealth technology; its radar cross section is said to be an order of magnitude smaller than that of the B-1.

With the development of stealth technology, the U.S. Air Force has shifted the funding from the AGM-86B conventional air-launched cruise missile to the development of the new ACM stealth cruise missile. The new missile can be launched from the ground, from underwater, or from the air; its effective range is approximately 10,000 km with a hit accuracy of 16 m (circular probable error). By using proper profile design and stealth materials, it can successfully evade enemy radars and missiles.

In the area of fighter aircraft, the U.S. Air Force has deployed the F-19 stealth fighter since 1981; its mission is to attack enemy air defense and radar bases and to conduct strategic/tactical surveillance. A new Air Force plan is to develop the ATF advanced tactical fighter, which is a top-secret stealth aircraft for the 1990's; its radar cross section will be lower than 0.1 m^2, which corresponds to a 0.35-m-diameter metallic ball.

It is safe to predict that within the next decade, stealth technology will be sufficiently mature to be implemented not only on aircraft and missiles, but also on satellites, ships, tanks and motor vehicles. In addition to the United States, the Soviet Union has also been secretly conducting research in stealth technology for over 20 years. There are speculations that the Soviet Union already possesses an "optimally designed" stealth aircraft. [Passage omitted]

III. The Principles and Implementation of Anti-Radar Stealth Technology

The physical basis for detecting targets by radar is the scattering of electromagnetic waves by the target; a quantitative measure of detectability is the effective scattering cross section (or simply radar cross section σ). Based on the radar equation, the relationship between the maximum effective range of the radar R and the radar cross section σ is

$$R = K\sqrt[4]{\sigma} \qquad (1)$$

where K is a constant determined by such radar parameters as the wavelength, the antenna gain, the transmitter power, and the receiver sensitivity. Clearly, in order to reduce the effective radar range R, one must reduce the radar cross section of the target, as indicated by curve A in Figure 1. If the radar cross section is reduced by two orders of magnitude, then the effective radar range will be reduced to 32 percent of its original value.

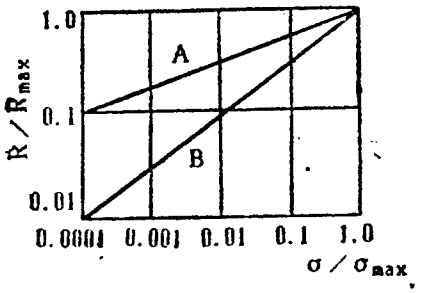

Figure 1. Relationship Between Effective Radar Range and Radar Cross Section

The stealth effect can be enhanced by combining stealth technology with active or passive interference. For example, the effective radar range for an aircraft carrying active jamming devices becomes

$$R_0 = K_0\sqrt{\frac{\sigma}{P_f G_f}} \qquad (2)$$

where K_0 is a constant determined by radar parameters, P_f is the jammer power, and G_f is the gain of the jammer antenna. Thus, instead of the one-fourth power relationship of equation (1), the effective radar range becomes proportional to the square root of the radar cross section, as indicated by curve B of Figure 1. Now when the radar cross section is reduced by two orders of magnitude, the effective range will be reduced to only 10 percent of its original value. By increasing the jammer power and antenna size, the stealth and combat capabilities of the target can be further enhanced. For passive interference such as chaff of infrared decoys, it is possible for a target with a small radar cross section to avoid detection over a much longer period, thus increasing the probability of error for the intercepting missile.

Simulation results show that for a defensive system with single-shot missile capability, the survivability of a stealth aircraft can be enhanced by a factor of two [i.e., increased 100 percent]. As a result of the drastic decrease in radar range, the warning time for the defense is greatly reduced; when the stealth aircraft penetrates the defense at supersonic speeds, it would be difficult for the enemy to take the proper defensive action within a short time interval of only one to two minutes.

The commonly used techniques to reduce the radar cross section include stealth profile design, use of radar-absorbent materials, and loading techniques.[2]

Stealth profile design involves optimization of the shape, size, material and structure of the aircraft to reduce its radar cross section in a specified direction. This optimization process should be carried out by considering other requirements such as aerodynamic characteristics, radar tracking, and guidance characteristics. Electromagnetic scattering is highly dependent on the geometric shape of the scattering body; for example, a 40-cm corner reflector has the same radar cross section as a heavy tank. Therefore, the first principle in profile design is to minimize corner reflection and mirror reflection or edge diffraction. Some of the effective profile design practices include: fusing the wing with body, fusing the cockpit with the fuselage, using delta wings, variable-sweep wings or swept forward wings, using embedded engines, V-shaped tails and hidden hangers for weapon support, and removing appendages and pertruding objects; these design measures have been used on the SR-71, the B-1, the ATB and the F-19 aircraft.

Profile stealth techniques also include special treatment of certain key scattering points. For example, the air inlet and exhaust of an aircraft are strong scattering sources. Such scattering can be suppressed by using back-pack type or S-shaped inlet design, by adding guide vanes, and by shielding the compressor blades. Another strong scattering source is the radome and the antenna. Their radar cross section can be reduced by using conical or specially shaped antenna covers, by controlling passive scattering and secondary radiation from the parabolic antenna, and by using phased-array multifunctional antenna or camouflaged antenna embedded in the aircraft body.

At present, the most effective stealth technique is the use of radar-absorbent materials. There are two major categories of radar-absorbent materials: surface coating material and structural composite material. By using surface coating materials containing ferrite or carbon-based ferrous compound, it is now possible to achieve an attenuation of more than 20 dB in the reflected energy. By using polonium-210 and curium-242 isotope absorbent materials, it is also possible to achieve attenuation of 10 dB or more. The disadvantages of radar-absorbent material are that it is difficult to maintain bonded to the coated surface; it adds to the weight of the aircraft; and it is sensitive to frequency, polarization and the angle of incidence.

Structural composite material is made of a combination of radar-absorbent material and non-metallic composite material; it not only has the capability to absorb radar waves, but is also lightweight and strong. It can be used to construct aircraft fuselages and wings with greatly reduced radar cross sections. The absorbent compound can be distributed according to the principle of impedance variation or in the form of a layered or sandwiched structure. It is estimated that by the end of this century, 50 percent of the materials used in building military aircraft will be new absorbent composite materials.

The loading techniques include both passive and active loading; the objective is to introduce auxiliary scattering sources (with appropriate amplitude and phase) to cancel the existing scattering energy from the target. This technique is effective in cancelling non-mirror type scattering, but its practical implementation is limited because of frequency band and adaptive loading constraints.

To achieve good evasion capability against radars requires the integration of many different technologies beyond stealth technology, including active and passive electronic interference techniques, radiation-seeking missiles, and high-energy laser or particle-beam weapons. According to current estimates, profile design can achieve a reduction of 5-8 dB in radar cross section, radar-absorbent materials can achieve a 7-10 dB reduction, and other measures (e.g., impedance loading, antenna covers, etc.) can achieve a 4-6 dB reduction. By combining these different techniques, it is possible to achieve a reduction of 20 dB in the radar cross section of stealth aircraft.

IV. Radar Cross Section Analysis and Measurement Techniques

The key issue in stealth and counter-stealth technologies centers around the radar cross section. During the 1960's and 1970's, a significant amount of theoretical and experimental research was carried out in the United States, and a large number of papers, reports and books were published on the subject.[2-8]

The theoretical definition of the radar cross section is:

$$\sigma = \lim_{R \to \infty} 4\pi R^2 \left| \frac{E_s}{E_i} \right|^2 \tag{3}$$

where E_i is the electric field strength on the target surface due to the incident radar wave, and E_s is the total electric field strength at the radar receiving antenna produced by the scattered energy from the target. The scattered electric field is generated by the induced current or electric charge when the electromagnetic wave passes an obstacle in its path. It includes the reflected and refracted field which obey the law of geometric optics, and the diffracted field which deviates from geometric optics. Therefore, the radar cross section depends on the shape, size, material, and structure of the target as well as the frequency, polarization, and angle of incidence of the radar wave. For a large target with complex shape, the overall scattered field strength is the superposition (vector sum of the phases) of the field strengths of the individual scattering centers:

$$\sigma = \left| \sum_{m=1}^{M} \sqrt{\sigma_m} \exp(j\phi_m) \right|^2 \tag{4}$$

where M is the total number of scattering elements, σ_m and ϕ_m are the radar cross section and the corresponding phase of the mth element. It

is the complexity and random nature of this phase summation that leads to the scintillation phenomenon and statistical behavior of the radar cross section.

In principle, the analytical methods used in solving electromagnetic scattering problems can be applied to calculate the target radar cross section.[2] But for a large target with complex shape, the boundary conditions become so complicated that it is impossible to obtain an accurate solution of the wave equation. Also, the integral equation method and the moment method are limited by computer capacity due to the excessive number of elements involved. Currently, the most effective methods are the various high-frequency approximation methods. The ray theory,[9] which is based on a combination of the geometric-optics method, the geometric-diffraction method, the multiple-ray method, and the multiple-ray expansion method, is a simple and practical method. In addition, the physical-optics method, the physical-diffraction method, the equivalent-current method, and the surface-traveling-wave method have also been used to calculate the scattered fields of certain types of targets. But many other challenging problems such as analysis of the scattered fields of large cavities (e.g., air inlet), non-conducting structures (e.g., antenna covers, absorbent materials), and antennas remain unsolved because of the difficulty in simulating the problem and the prohibitive computational cost. For this reason, one must develop new and simpler analysis techniques.

Radar cross section measurement techniques are used to provide experimental verification of the theoretical calculations; they can also be used directly to study and optimize radar cross section design. Measurement techniques include: full-scale dynamic measurement, full-scale outdoor static measurement, and scale-model measurement in microwave darkroom. Measurements can be performed using continuous waves, pulsed waves, and frequency-modulated continuous waves. Because of the weakness of the scattered field, background interference will have a severe effect on the measurement accuracy of radar cross section. For this reason, the radio-frequency cancellation technique, the time separation (range gating) technique, the spatial separation (angle filter) technique, and the Doppler signal technique are used to suppress background interference. Another effective way to study stealth technology is to use a high-resolution radar to separate the scattering centers of a complex target by forming one-dimensional, two-dimensional, or three-dimensional images.

V. Counter-Stealth Technology

In order to defend against the ever-increasing number of stealth aircraft, counter-stealth theories and techniques are also being developed; but they have not reached the same degree of maturity as stealth technology. At present, counter-stealth detection primarily centers around the use of new radar systems or new electromagnetic scattering theories to exploit the weaknesses that exist in stealth technology. For example, some of the techniques used to detect and identify stealth targets are: establishing a very-wide-band radar defense network (e.g., laser radar, millimeter-wave radar and short-wave over-the-horizon radar), the use of a dual-station

or multistation radar system, the use of down-looking early-warning airplanes or balloons, developing passive electronic sensors (passive radars), improving radar performance by using advanced signal processing systems and super-low-sidelobe antennas, the use of adaptive systems to achieve coherent superposition of the scattering centers of a large target, and the use of the impulse method or the singular expansion method to treat inverse scattering problems. But these theories and methods are still in the exploratory stage; they will not be ready for practical implementation for some time to come.

VI. Concluding Remarks

After more than 20 years of research, aircraft stealth technology has now reached the stage of practical implementation. It will undoubtedly have a major impact on weapons development in this century and on ways of conducting future warfare. It will also stimulate development in such technical fields as aeronautics, astronautics, electronics, computers, mechanical engineering, materials science, and chemical engineering. However, additional in-depth research is still required to solve many challenging problems in the theory and techniques of stealth and counter-stealth technologies.

References

1. J. B. Schultz, "Defence Electronics," 1983, No 3, 65-72.

2. E. F. Knott, et al., "Radar Scattering Cross Section," Electronics Industry Publishers, 1988 (translated and edited by Ruan Yingzheng et al.).

3. J. W. Crispin et al., "Methods of Radar Cross Section Analysis," Academic Press, 1968.

4. R. Mittra, AD755854, 1972.

5. G. T. Ruck et al., "Radar Cross Section Handbook," Plenum Press, 1970.

6. C. G. Bachman, "Radar Targets," D. C. Health and Company, 1982.

7. A. E. Fuhs, AD/A125576, 1982.

8. J. E. Terry, AD426080, 1964.

9. Lin Weigan, Ruan Yingzheng, "A Review of Ray Theory," DIANZI KEXUE XUEBAO [JOURNAL OF ELECTRONIC SCIENCE] (to be published).

Coherent Effects in Intense Laser-Field Induced Autoionization

40090036b Beijing WULI XUEBAO [ACTA PHYSICA SINICA] in Chinese Vol 37 No 11, Nov 88 pp 1760-1766

[English abstract of article by Yao Guanhua [1202 7070 5478], et al., of Shanghai Institute of Optics and Fine Mechanics, Chinese Academy of Sciences]

[Text] The authors have investigated in detail the influence of second-order ionization processes on the photoelectron spectrum, etc., which has previously been ignored in studies of intense laser-field induced autoionization. It is found that, in the region of laser intensity currently discussed in the literature, many physical features have been altered significantly. (1) Under certain conditions, the line-narrowing effect disappears. (2) The original photoelectron peaks are greatly reduced. (3) In agreement with the most recent experimental findings on multiphoton ionization, high-order photoelectron peaks increase drastically with an increase in laser intensity, and they dominate the original peaks for sufficiently high intensities.

References

1. Boyer, K., et al., J OPT SOC AM, Vol B1, 1984 p 3.
2. Harris, S.E., et al., J OPT SOC AM, Vol B4, 1987 p 547.
3. Fano, U., PHYS REV, Vol 124, 1961 p 1866.
4. Lambropoulos, P., et al., PHYS REV, Vol A24, 1981 p 379.
5. Rzazewski, K., et al., PHYS REV LETT, Vol 47, 1981 p 408.
6. Coleman, P.E., et al., J PHYS B, Vol 15, 1982 p L235.
7. Agarwal, G.S., et al., PHYS REV LETT, Vol 48, 1982 p 1164.
8. Agarwal, G.S., et al., PHYS REV, Vol A29, 1984 p 2552.
9. Haus, J.W., et al., OPT COMMUN, Vol 46, 1983 p 191.
10. Rzazewski, K., et al., PHYS REV, Vol A27, 1983 p 2026.
11. Heitler, W., "The Quantum Theory of Radiation," Clarendon Press, Oxford, 1954.
12. Autler, S.H., et al., PHYS REV, Vol 100, 1955 p 703.
13. Kruit, P., et al., PHYS REV, Vol A28, 1983 p 248.
14. Johann, U., et al., PHYS REV, Vol A34, 1986 p 1084.
15. Rzazewski, K., et al., PHYS REV, Vol A46, 1983 p 191.

Generation of Squeezing Light in Laser Cavity

40090036c Beijing WULI XUEBAO [ACTA PHYSICA SINICA] in Chinese Vol 37 No 11, Nov 88 pp 1767-1774

[English abstract of article by Zhang Weiping [1728 5898 1627], et al., of Shanghai Institute of Optics and Fine Mechanics, Chinese Academy of Sciences]

[Text] The generation of squeezing light depends on the nonlinear optical processes. Its intensity is usually low due to the limitations of the conversion efficiency. In this paper, the general conditions for producing squeezing light are given. According to these conditions, the conclusion is obtained that a laser cavity with a nonlinear medium and a gain medium can simultaneously amplify the light intensity and reduce the quantum fluctuation of one quadrature phase component of the light field.

References

1. Walls, D.F., NATURE, Vol 306, 1983 p 141.
2. Caves, C.M., PHYS REV, Vol D23, 1981 p 1693; Yuen, H.P., Shapiro, J.H., IEEE TRAN INFORM THEORY, Vol IT-24, 1978 p 657; Shapiro, J.H., Yuen, H.P., et al., IEEE TRAN INFORM THEORY, Vol IT-25, 1979 p 179.
3. Lu, E.Y.C., LETT NUOVO CIMENTO, Vol 2, 1971 p 1241; LETT NUOVO CIMENTO, Vol 3, 1972 p 585.
4. Wolinsky, M., Carmichal, H.J., OPT COMMUN, Vol 55, 1985 p 138; Yurke, B., PHYS REV, Vol A29, 1984 p 408.
5. Slusher, R.E., Lollerg, L., et al., PHYS REV LETT, Vol 25, 1985 p 2409; Shelby, R.M., Levenson, M.D., et al., PHYS REV LETT, Vol 57, 1986 p 691; Wu, Lingan, Kimble, H.J., et al., PHYS REV LETT, Vol 57, 1986 p 2520.
6. Yamamoto, Y., Machida, S., et al., PHYS REV, Vol A34, 1986 p 4025.
7. Glauber, R.J., PHYS REV, Vol 130, 1963 p 2529; ibid, Vol 131, 1963 p 2766; Sudarshan, E.C.G., PHYS REV LETT, Vol 10, 1963 p 277.
8. Drummond, P.D., Gardiner, C.W., J PHYS A, Vol 13, 1980 p 2353.
9. Reid, M.D., Walls, D.F., PHYS REV, Vol A28, 1983 p 339.
10. Louisell, W.H., "Quantum Statistical Properties of Radiation," Wiley, New York, 1973.
11. Drummond, P.D., Walls, D.F., PHYS REV, Vol A23, 1981 p 2563.
12. Gardiner, C.W., "Handbook of Stochastic Methods," Springer, Berlin, 1983.

Optical Absorption Property of TiO_2-Doped Vycor Glass

40090036h Beijing WULI XUEBAO [ACTA PHYSICA SINICA] in Chinese Vol 37 No 11, Nov 88 pp 1876-1881

[English abstract of article by Ling Ping [0407 1627], et al., of Shanghai Institute of Ceramics, Chinese Academy of Sciences]

[Text] The structure and optical absorption property of TiO_2-doped Vycor glasses are studied. The experimental results indicate that the optical absorption of the glasses is determined by anatase microcrystals in the glasses. The absorption edge shifts to long (or short) wavelengths with the increasing (or decreasing) of the microcrystal size. Anatase microcrystal of a diameter of about 80 Å shows the same absorption edge as that of bulk crystal.

References

1. Huang Xihuai, JOURNAL OF THE CHINESE SILICATE SOCIETY, Vol 1, 1962 p 98.
2. Zhou Yuhua, et al., JOURNAL OF THE CHINESE SILICATE SOCIETY, Vol 4, 1965 p 66.
3. Infrared Glass Group, NEW INORGANIC MATERIALS, Vol 5, 1977 p 1.
4. Huang Xihuai, et al., JOURNAL OF THE CHINESE SILICATE SOCIETY, Vol 3, 1964 p 193.
5. Lei Weiguo, et al., ACTA PHYSICA SINICA, Vol 35, 1986 p 1537.
6. Lei Weiguo, et al., JOURNAL OF THE CHINESE SILICATE SOCIETY, Vol 15, 1987 p 1.
7. Furukawa, T., White, W.B., PHYS CHEM GLASSES, Vol 20, 1979 p 69.
8. JCPDS card, 1982, 21-1272.
9. Sakka, S., Kamiya, K., "Physics of Non-Crystalline Solids," Proceedings of the 5th International Conference, Montpelier, 5-9 July, 1982, C9-235.
10. Brus, L.E., J CHEM PHYS, Vol 80, 1984 p 4403.

Generation of Short Pulse of 30 fs From Simple Colliding-Pulse Mode-Locking Dye Laser With Double Coated Stack Mirrors

40090037a Shanghai GUANGXUE XUEBAO [ACTA OPTICA SINICA] in Chinese Vol 8 No 11, Nov 88 pp 961-965

[English abstract of article by Wang Qingyue [3769 3237 2588], et al., of the Department of Precision Instruments, Tianjin University]

[Text] The dispersion produced by an ordinary single stack cavity mirror is analyzed. This kind of mirror has difficulty compensating for the upchirp of the pulses in the cavity. A kind of double coated stack mirror, with the appropriate amount of dispersion of $\ddot{\phi}(\omega) = 1.3 \times 10^{-28}$ sec^2 for upchirp compensation, is designed and used as the cavity mirror, enabling pulses as short as 30 fs to be generated directly from a simple colliding-pulse mode-locked (CPM) dye laser without additional dispersive elements in the cavity.

References

1. Dietel, W., Fontaine, J.J., Diels, J.C., OPTICS LETT, Vol 8 No 1, Jan 1983 p 4.
2. Valdmanis, J.A., Fork, R.L., Gordon, J.P., OPTICS LETT, Vol 10 No 3, Mar 1985 p 131.
3. Rudolph, W., Wilhelmi, B., APPL PHYS B, Vol 35 No 1, Jan 1984 p 37.
4. Martinez, O.E., Fork, R.L., Gordon, J.P., OPTICS LETT, Vol 9 No 5, May 1984 p 156.
5. Fork, R.L., Green, B.I., et al., APPL PHYS LETT, Vol 38 No 9, May 1981 p 671.
6. Silvestri, S.D., Laparta, P., Svelto, O., OPTICS LETT, Vol 9 No 8, Aug 1984 p 335.
7. Dietel, W., et al., OPT COMMUN, Vol 50 No 3, Jun 1984 p 179.
8. Yawashita, M., Ishikawa, M, Terizuka, K., OPTICS LETT, Vol 11 No 8, Aug 1986 p 504.
9. Wang Qingyue, Zhang Ruobing, Zhao Xinmiao, OPTICS COMMUN, to be published.
10. Wang Qingyue, et al., OPTICS COMMUN, to be published.
11. Wang Qingyue, et al., ACTA OPTICA SINICA, Vol 6 No 4, Apr 1986 p 320.

Deeply Thermo-Stable Telescopic Resonator

40090037b Shanghai GUANGXUE XUEBAO [ACTA OPTICA SINICA] in Chinese Vol 8 No 11, Nov 88 pp 966-974

[English abstract of article by Lu Baida [0712 4102 6671], et al., of the Department of Physics, Sichuan University, Chengdu]

[Text] In this paper, the deeply thermo-stable characteristics of telescopic resonators with G parameters satisfying the condition $G_1G_2 = 1/2$ are theoretically discussed in detail. An exact expression for the telescopic defocusing which can compensate for thermal disturbance is derived analytically. It is shown that the simplified approximation formulae for defocusing in References 4 and 5 can be deduced easily from this exact formulation if the appropriate assumptions are adopted. Computer simulation and numerical calculation are carried out to confirm the authors' theoretical results, and curves describing the variation of beam sizes with telescopic resonator parameters are given.

References

1. Steffen, J., et al., IEEE J QUANT ELECTRON, Vol QE-8 No 2, Feb 1972 p 239.
2. Lörtscher, J.P., et al., OPT & QUANT ELECTRON, Vol 7 No 6, Nov 1975 p 505.
3. Hanna, D.C., et al., OPT COMMUN, Vol 37 No 5, 1981 p 359.
4. Hanna, D.C., et al., OPT & QUANT ELECTRON, Vol 13 No 6, Nov 1981 p 493.
5. Lu Zukang, et al., "Papers from 1985 Annual Meeting of the China Optical Society," 1985 p 101 (ACTA OPTICA SINICA pending publication)
6. Lu Baida, ACTA OPTICA SINICA Vol 7 No 2, Feb 1987 p 105.
7. Lu Baida, "Laser Optics," Sichuan University Press, 1986 pp 258, 274.

Image Superresolution With Source Encoding Technique*

40090037c Shanghai GUANGXUE XUEBAO [ACTA OPTICA SINICA] in Chinese Vol 8 No 11, Nov 88 pp 984-990

[English abstract of article by Guo Binjun [6753 2430 0971], et al., of Shanghai Institute of Optical Instruments]

[Text] In this paper, a source encoding technique is presented for achieving a superresolution image. The experimental demonstrations show that the superresolution can be obtained easily by using this new technique. The method overcomes several drawbacks of other methods and demonstrates a new approach for the further study of practical applications of superresolution technology.

* Project supported by the National Natural Science Foundation of China.

References

1. Lee, S.H., "Optical Information Processing," Springer-Verlag, Berlin, Heidelberg, New York, 1981, Chapter 1.
2. Tan Weihan, et al., ACTA OPTICA SINICA, Vol 1 No 6, Nov 1981 pp 509-515.
3. Tsujiuchi, J., et al., "Optical Information Processing," Machine Industry Press, Beijing, 1983, Chapter 3.
4. Zhuang, S.L., Yu, F.T.S., APPL OPT, Vol 21 No 14, Jul 1982 pp 2587-2593.
5. Yu, F.T.S., Zhuang, S.L., et al., APPL PHYS, Vol B27 No 1, Jan 1982 pp 99-104.
6. Zhuang Songlin, et al., ACTA PHYSICA SINICA, Vol 5 No 4, Apr 1985 pp 439-446.

Computer Simulation Method to Change Wavefront of Lasers*

40090037d Shanghai GUANGXUE XUEBAO [ACTA OPTICA SINICA] in Chinese Vol 8 No 11, Nov 88 pp 991-997

[English abstract of article by Li Yongping [2621 3057 1627], et al., of the Department of Physics, University of Science and Technology of China, Hefei]

[Text] Using the phase plate calculated and designed by two-discrete FFT with dimensionless parameters and computer simulation, the fundamental mode Gaussian beam can be converted into a rectangular shape and the elliptical wavefront can change into a circular symmetrical shape. The relationship between the theoretical simulation and experimental parameters has been derived. Results of the simulation show that the experimental equipment is simple by using the data obtained in the authors' method and the efficiency of the energy transform is high.

* Project supported by the National Natural Science Foundation of China.

References

1. Lee, W.H., OPTICAL COMMUN, Vol 36 No 6, Mar 1981 pp 469-471.
2. Ih, C.S., et al., ACTA PHYSICA SINICA, Vol 35 No 2, Feb 1986 pp 220-226.
3. Liang Xiangchun, et al., ACTA OPTICA SINICA, Vol 5 No 8, Aug 1985 pp 761-764.
4. Rhodes, P.W., APPL OPT, Vol 19 No 20, Oct 1980 pp 3545-3553.
5. Goodman, J.W., "Fourier Optics," Science Press, 1979 pp 33-84, 88-110, 10, 12.
6. Brigham, E.O., "Fast Fourier Transforms," Shanghai Science Press, 1979 pp 165-183.
7. Zhou Bingkun, et al., "Laser Principles," National Defense Press, 1980 pp 348-359.
8. Yu Zuliang, "Computer Controlled Holograms," Qinghua University Press, 1984 pp 31-45.

Speckle Photography With Radially Scanning Aperture

40090037e Shanghai GUANGXUE XUEBAO [ACTA OPTICA SINICA] in Chinese Vol 8 No 11, Nov 88 pp 1018-1023

[English abstract of article by Chen Bingquan [7115 3521 3123], et al., of the Department of Physics, Suzhou University]

[Text] In this paper, a new speckle photography-radially scanning aperture method is proposed, and theoretical analysis and experimental results are presented. This method has the advantage that the whole dynamic process of an object can be recorded on one speckle photogram. The deformation information in the direction of the x and y axes and of 45 degrees at any moment can be obtained in the form of isothetic fringes by whole field filtering.

References

1. Hung, Y.Y., Rowlands, R.E., et al., APPL OPT, Vol 14 No 3, Mar 1975 p 618.
2. Dainty, J.C., "Laser Speckle and Related Phenomena," Chinese edition, Science Press, Beijing, 1981 pp 193-195.
3. Gu Jie, et al., ACTA OPTICA SINICA, Vol 7 No 5, May 1987 pp 394-399.
4. Chiang, F.P., Khefen, R.P., APPL OPT, Vol 18, 1979.
5. Jiang Jinhu, et al., ACTA OPTICA SINICA, pending publication.
6. Chen, J.B., Chiang, F.P., J OPT SOC AM A, Vol 1 No 8, 1984 pp 845-849.

Influence of Stimulated Raman Process on Fundamental Solitons in Fibers

40090037f Shanghai GUANGXUE XUEBAO [ACTA OPTICA SINICA] in Chinese Vol 8 No 11, Nov 88 pp 1048-1052

[English abstract of article by Qu Linjie [2575 2651 2638], et al., of the Department of Precision Instruments, Tianjin University]

[Text] With the aid of computer simulation, the authors have studied the energy spectrum evolution of the fundamental solitons propagating in fibers caused by Raman self-pumping. The authors find that the self-frequency shift effect will be accompanied by a bandwidth change and energy spectrum distortion of the solitons whose durations are shorter than the subpicosecond level.

References

1. Mitschke, F.M., Mollernauer, L.F., OPT LETT, Vol 11 No 10, Oct 1986 pp 659-661.
2. Gorden, J.P., OPT LETT, Vol 11 No 10, Oct 1986 pp 662-227.
3. Shen Yuanrang, "Principles of Nonlinear Optics," Science Press, Beijing, 1987, Vol 2 pp 201-211.
4. Mollenauer, L.F., Gorden, J.P., et al., IEEE J Q E, Vol QE-22 No 1, Jan 1986 pp 157-173.
5. Stolen, R.H., PROCEEDINGS OF THE IEEE, Vol 68 No 10, Oct 1980 pp 1232-1236.

650 nm Continuous Wave (CW) He-Ne Raman Laser

40090034a Shanghai ZHONGGUO JIGUANG [CHINESE JOURNAL OF LASERS] in Chinese Vol 15 No 11, 20 Nov 88 pp 648-651

[Article by Huang Zhiwen [7806 2784 2429] and Zhao Suitang [6392 4840 1016] of Department of Physics, Beijing University; and Jin Haoran [6855 3185 3544] of Department of Radio Electronics, Beijing University]

[Abstract] Through experiments, the 650 nm laser line of a six-wavelength CW He-Ne laser was verified as corresponding to stimulated Raman scattering emission in the cavity. The characteristics of Raman scattering emission were studied and its gain coefficient is given. The experimental arrangement is shown in the following diagram:

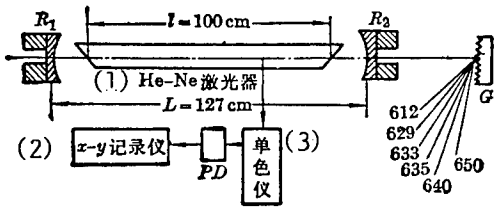

Discharge current I = 16 mA; d = 2.3 mm.

Key:
1. Laser
2. Recording instrument
3. Monochrometer

Five other figures show a space division six-wavelength laser, laser modes (633 and 650 nm), variation of laser power with cavity length, magnet positions and placement sequence, as well as curves indicating the variation of laser output power versus number of magnet blocks. The authors are grateful to Zhao Kegong [6392 0344 0501] director of the

China Metrology Academy for consultation, to Professor Zheng Luomin [6774 2867 3046] for his proposal of the stimulated Raman process, and to Associate Professor Wang Qingji [3769 1987 0679] for his discussions. Excellent quality lenses were supplied by the First Shanghai Glass Instrument Plant. References: 7, 3 in Chinese and 4 in English. The paper was received for publication on 17 June 1987.

Wide-Band Focusing System for Laser Beams

40090034b Shanghai ZHONGGUO JIGUANG [CHINESE JOURNAL OF LASERS] in Chinese Vol 15 No 11, 20 Nov 88 pp 656-659, 651

[Article by Li Junchang [2621 0193 2490] of Laboratory for Laser Applications, Kunming Institute of Technology]

[Abstract] A simple, feasible optical device was studied theoretically; the device can focus a monomode Gaussian laser beam (TEM_{00}) into a band-shaped light spot of varied sizes. A uniform energy distribution exists along the lengthwise direction of the light spot. The optical system is shown in the following diagram:

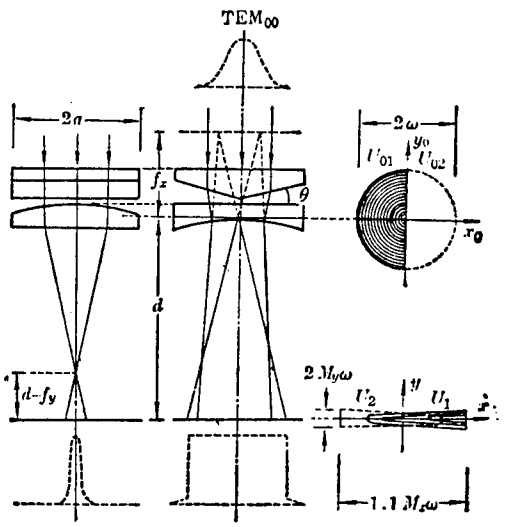

ω is the radius of incident Gaussian light beam. M_x is the lateral-direction amplification ratio of the system along the x-direction of the light field (My along the y-direction).

Three other figures show the energy distribution of the interferogram along the x-axis, the strength distribution of band-shaped light spots on an iterated addition plane, and a comparison of energy distribution on the x-axis calculated by diffraction integration and geometric optics. The paper was received for publication on 28 April 1987.
References: 5, in English.

Experimental Research on Spatial Coherence of Laser Light Passing Through a Multimode Fiber

40090034c Shanghai ZHONGGUO JIGUANG [CHINESE JOURNAL OF LASERS] in Chinese Vol 15 No 11, 20 Nov 88 pp 669-673

[Article by Dong Xiaoyi [5516 1321 5030], Sheng Qiuqin [4141 4428 3830], Zhang Jianzhong [1728 1696 1813], and Song Wentao [1345 2429 3447] of Institute of Modern Optics, Nankai University]

[Abstract] The average spatial coherent characteristics of laser light transmitting through a multimode optical fiber may be determined by measuring the contrast of speckle patterns projected from a multimode fiber. A method for measuring spatial coherent characteristics of laser light passing through a multimode optical fiber is given.

The principle of the experimental arrangement is shown in the following schematic diagram:

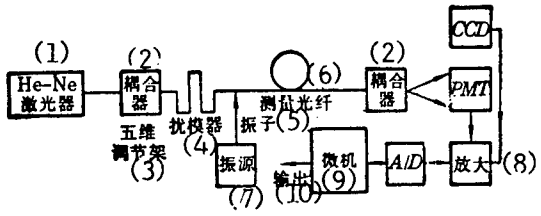

Key:

1. Laser
2. Coupler
3. Five-dimension adjustment frame
4. Mode interference device
5. Oscillator
6. Measuring optical fiber
7. Oscillation source
8. Amplification
9. Microcomputer
10. Output

Two tables list the data from measuring different lengths of optical fiber. Two other figures show the measuring procedures, corrected data and a comparison between theoretical calculations and actual measurements. The paper was received for publication on 11 May 1987.

REFERENCES

[1] Dedlovskiy, M. M., Radiotekhnika i Elektronika [Radio Engineering and Electronics], 25, 481 (1980).

[2] Abduployev, S. S., Kvan(tovaya) Elektr(onika) [Quantum Electronics], 12, 157 (1985).

[3] Dong Xiaoyi, et al., ZHONGGUO JIGUANG [CHINESE JOURNAL OF LASERS], [to be published].

[4] Takahara H., OPT. ACTA, 29, 441 (1982).

[5] Dong Xiaoyi, YINGYONG JIGUANG [APPLIED LASERS], 2 (3), 6 (1982).

[6] Epworth, R. E., LASER FOCUS, 17 (9), 109 (1981).

[7] Spano, P., OPT. COMMUN., 23, 265 (1980).

[8] Dong Xiaoyi, WULI [JOURNAL OF PHYSICS], 15, 439 (1986).

[9] Dong Xiaoyi, ed., GUANGBO DIANZIXUE [SPECTRAL ELECTRONICS], Chapter VI, Nankai University Publishing House, 1987.

Sealed Mini-TEA CO_2 Lasers With Metal Envelope

40090041a Shanghai YINGYONG JIGUANG [APPLIED LASER] in Chinese Vol 8 No 6, Dec 88 pp 258-262

[English abstract of article by Pan Chengzhi [3382 2110 1807], et al., of Beijing Vacuum Electronics Research Institute]

[Text] Sealed mini-TEA CO_2 lasers with metal envelopes produced by vacuum technology and their performances are reported. The total active volume of this kind of laser is ϕ 60 x 230 mm, while the energy outputs of the multi-mode and single mode are 60 and 30 mJ, respectively. The pulse width (FWHM) is $\leq$50 ns, the peak power output is $\geq$1 MW, and the divergence angle is approximately 2 mrad. The continuous working life is more than 10^7 shots per gas filling under the condition that the single pulse energy output is 20 mJ and the repetition rate is 5 pps.

References

1. Chang, T.Y., REV SCIENT INSTRUM, Vol 44, 1973.
2. Marchetti, R., et al., JAP, Vol 54, 1985 p 5672.
3. Pan Chengzhi, et al., LASERS AND INFRARED TECHNOLOGY, Vol 18, 1988 p 19.
4. Andrews, K.J., et al., J PHYS SCIENTIFIC INSTRUMENTS, Vol 8, 1975 p 493.

High-Resolution TeO_2 Acousto-Optic Deflector for mm-Wave Radio Spectrometer

40090041b Shanghai YINGYONG JIGUANG [APPLIED LASER] in Chinese Vol 8 No 6, Dec 88 pp 267-270

[English abstract of article by Xu Binghuo [6079 3521 3172], et al., of Shanghai Institute of Ceramics, Chinese Academy of Sciences]

[Text] This paper introduces a high-resolution TeO_2 deflector for a mm-wave radio spectrometer. The authors have developed a mm-wave acousto-optic radio spectrometer using these devices. It has 17.5 KHz frequency resolution, a 13 MHz bandwidth and the system drift is ±0.03 channel per hour.

References

1. Uchida, Naoya, PHYS REV, Vol B4, 1971 p 3736.
2. Yano, T., APPL PHYS LET, Vol 26, 1975 p 689.

Briefs

Phased-Array Radar Design Finalized--China's first all-solid-state three-coordinate phased-array radar, independently designed and developed by Research Institute 14 of the Ministry of Machine-Building & Electronics Industry, recently passed design finalization in a trial operation [jian fei 2914 7378] held at a certain place in China, indicating yet another new advance in Chinese radar technology. Institute 14's research on this technologically complex all-solid-state electromechanical scanning three-coordinate radar was begun in April 1980 at the request of the Commission of Science, Technology and Industry for National Defense. Based on the requirements of modern military tactics, the institute's researchers have utilized quite a few new technologies, such as an all-solid-state high-power transmitter, a phased-array antenna feedline, pulse compression, a high-purity frequency source for the frequency spectrum, low-angle altimetry, phased monopulse goniometry, digital signal processing [see JPRS-CST-89-004, 2 Feb 89, p 75] and data processing, an intelligent display terminal, automatic command and control software, etc. The high degree of radar system digitization and automation are fully brought into play in the performance of this radar system. During the design-finalization testing of the radar, main functions such as target detection, tracking range, measurement precision, and communications coordination were checked; all of their parameters met the main tactical and technical specifications for a command system. [Text] [40080125a Beijing ZHONGGUO DIANZI BAO in Chinese 17 Jan 89 p 1]

Weather-Radar Digital Control, Processing System--The model 711 weather-radar digital control and processing system, jointly developed by Nanjing University's Atmospheric Sciences Department and the Systems Engineering Division of Research Institute 14 in the Ministry of Machine-Building & Electronics Industry, recently passed technical accreditation held by the State Meteorological Administration. The basic performance indicators of this system meet advanced international standards for comparable systems. Consisting of an antenna controller, a signal averaging device/data processing unit, and a product filing/transmission unit, the system uses a microcomputer with an 8031 single-chip processor for antenna control. Over 200 meteorological, military, and merchant-marine institutions nationwide have already installed the radar. [Summary] [40080125b Beijing ZHONGGUO DIANZI BAO in Chinese 24 Jan 89 p 2]

New Mid-to-Low-Altitude Radar--At a technical evaluation for a new mid-to-low-altitude radar meeting advanced international standards of the eighties, prominent radar specialists from Beijing and elsewhere commented that the new system noticeably improves China's low-altitude defensive capabilities, and that it

will be a critical item for China's military forces in the nineties. The new radar, developed over a two-year period by the Binhu [3453 3275 "Lakeshore"] Machinery Plant in Wuhan, was certified at the state level at the end of last year. [Text] [40080125c Beijing ZHONGGUO DIANZI BAO in Chinese 27 Jan 89 p 1; see also JPRS-CST-88-020, 28 Sep 88, p 67]

New Fiber-Optic Temperature Sensor--The first domestic fiber-optic-sensing temperature-detection/alarm system, the GWB-1, developed by the Shanghai Fiber-Optic Communications Engineering Company, passed technical certification on 11 May 1988 at Refinery No 1 of the Gaoqiao petroleum facility in Shanghai Municipality. This system, which generates an acousto-optic alarm for oil explosions and fires throughout a pipeline, has the following specifications: (1) temperature measurement range: 0-100°C, (2) adjustable alarm temperature, (3) measurement error (in the 60-100°C range): ±1.5°C, (4) temperature response time: less than 40 seconds, and (5) continuous operation time: greater than or equal to 30 hours. [Summary] [40080117a Shanghai DIANZI YU ZIDONGHUA [ELECTRONICS & AUTOMATIZATION] in Chinese Vol 17 No 5, Sep-Oct 88, p 45]

8-mm GaAs Beam-Lead Schottky Barrier Mixer Diode

40080074a Beijing BANDAOTI XUEBAO [CHINESE JOURNAL OF SEMICONDUCTORS] in Chinese Vol 9 No 6, Nov 88 pp 570-577

[Article by Wang Liangchen [3769 5328 5256], Fang Puming [2455 3184 2494], and Zheng Dong [6774 2639] of the Institute of Semiconductors, Chinese Academy of Sciences; manuscript received 31 Jul 87; sponsored by the National Natural Science Foundation]

[Text] Abstract: With the aid of CAD [computer aided design] technology, the geometric parameters of a planar 8-mm GaAs beam-lead Schottky barrier mixer diode are designed and optimized based on the transmission line model (TLM) of a planar capacitor by Pucel and a planar resistor by Berger. Effects of key dimensions of the device on the total capacitance and series resistance were determined. The fabrication technology was similar to that of a GaAs MESFET [metal semiconductor field-effect transistor] and the geometric parameters of the device were carefully controlled. Typically the double sideband noise figure of the fabricated device was 4.8 dB at 35 GHz.

I. Introduction

In the development of millimeter-wave integrated circuits, needle-type Schottky mixer diodes with a nonplanar vertical structure were not compatible with the integrated circuit technology. Planar beam-lead mixer diodes are key devices in monolithic integrated circuits and there is an urgent need for this type of receiver in China.

In terms of design and fabrication, a planar mixer is far more complex than a vertical mixer. The main reason is that the device is not only flat but must also operate in the millimeter-wave frequency band. Therefore, the material structure, isolation technology and geometric dimension of the planar mixer are all different from those of a nonplanar mixer.

We used CAD technology in designing the geometric parameters of the planar mixer (to be published elsewhere). The calculation of the planar capacitance was based on the method given by Pucel[1] and the calculation of planar resistance was based on the TLM method by Berger.[2] Design and test results showed that, in order to achieve a high-performance, low-noise planar mixer, it is essential to reduce the series resistance and the distributed

capacitance of the device and to ensure the proper junction capacitance. Ion implantation masking is an important step in the fabrication of totally planar mixer diodes. If mesa isolation instead of proton implant isolation is used in the fabrication process, a greater difficulty will be encountered.

We have produced mixer diodes using both isolation methods. The finger Schottky anode was surrounded by a horseshoe-shaped cathode. The fabrication technology was similar to that of a GaAs MESFET and the metallized lead was thickened by gold plating. Typical double-sideband noise figure of a single-ended 8-mm GaAs planar mixer diode was 4.8 dB at 35 GHz.

II. Device Design

1. Planar Layout and Equivalent Circuit of the Device (Figure 1)

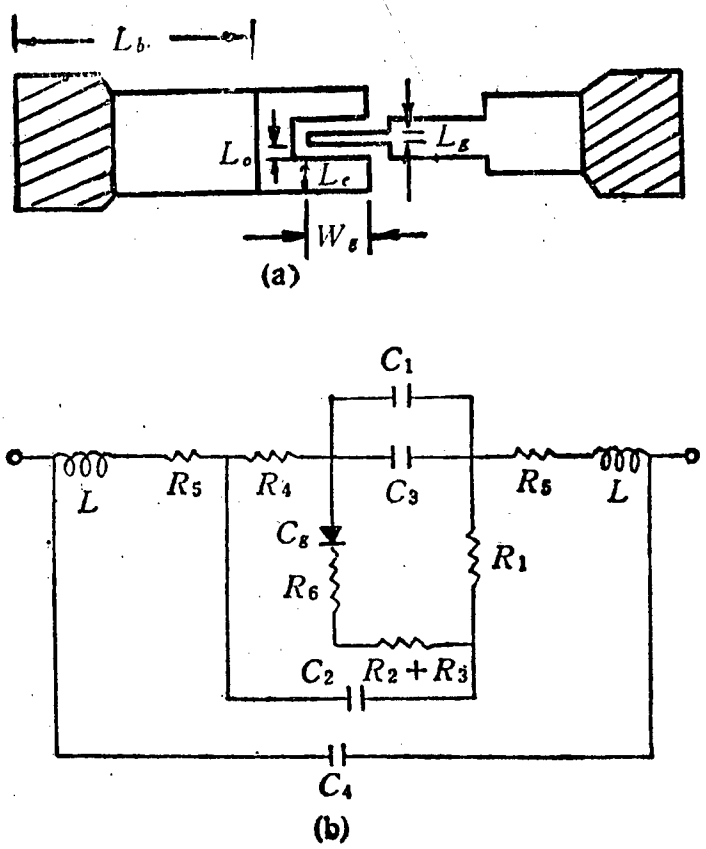

Figure 1. Plain view and equivalent circuit of the mixer diode

The planar layout and the equivalent circuit of the device are given in Figure 1 where R_1 is the resistance of the ohmic contact zone, R_2 is the resistance of the horseshoe-shaped epitaxial layer between the anode and the cathode, R_3 is the resistance of the N^+ layer under the Schottky junction, R_4 is the resistance of the Schottky metal, R_5 is the lead resistance, and

R_6 is the resistance of the undepleted N layer. Also in Figure 1, C_j is the junction capacitance, C_1 is the lead capacitance, C_2 is the ramp capacitance of the mesa isolation, C_3 is the capacitance of the horseshoe between the anode and the cathode, C_4 is the capacitance of the bond zone, and L is the lead inductance.

2. Capacitance

(1) The junction capacitance is given by

$$C_j = \frac{\varepsilon\varepsilon_0 L_g W_g}{W_d} \tag{1}$$

where L_g is the length of the Schottky junction metal (see Figure 1(a)), W_g is the width of the Schottky junction metal, W_d is the width of the depletion layer (W_d is taken to be the thickness of the N-type GaAs in a perforated model), ε is the relative dielectric constant of GaAs, and ε_0 is the dielectric constant of free space.

Considering the finger shape of the Schottky metal and the contribution of the fringe capacitance,[3] the following correction term was introduced:

$$C_{ij} = \frac{2}{\pi}\varepsilon\varepsilon_0 W_{g_1}\left[\frac{2}{K_n}\log_e\left(1+\frac{1}{K_n}\right)-\left(\frac{1}{K_n}-1\right)\log_e\left(\frac{1}{K_n^2}-1\right)\right] \tag{2}$$

where

$$W_{g_1} = W_g + L_g/2$$
$$K_n = 1 - T_{sh}/B_h$$
$$B_h = 2W_d + T_{sh}$$

and T_{sh} is the thickness of the finger-shaped metal.

We computed the change in the junction capacitance C_j due to changes in the depletion layer width under zero bias and under a bias of 0.6 V. The results are shown in Figure 2. There was obviously a large difference in the two capacitances. Since the device was operated under a positive bias, the geometric dimensions were computed for a positive bias.

(2) Capacitance between leads and bonded zone

We calculated these two capacitances using the case a approximation planar capacitance given by Pucel (see Figure 3). In this case, $L_1 = L_2 = L >> G$ and the capacitance is:

$$C = \varepsilon_0(1+\varepsilon)W\frac{K(\sqrt{1-k^2})}{K(k)} \tag{3}$$

where K is an elliptical integral of the first kind:

$$K(k) = \int_0^{\frac{\pi}{2}} \frac{d\phi}{\sqrt{1 - k^2 \sin \phi}} \qquad (0 \leqslant k \leqslant 1)$$

where

$$k = \sqrt{(2L + G)G/(L + G)^2}$$

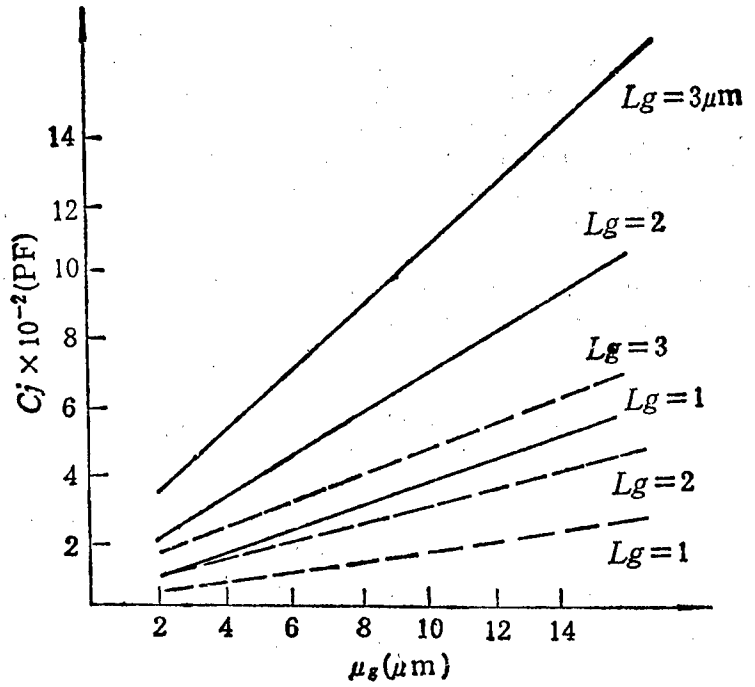

Figure 2. C_j and W_g curves for different biases
—— +0.6 V; ---- 0.0 V

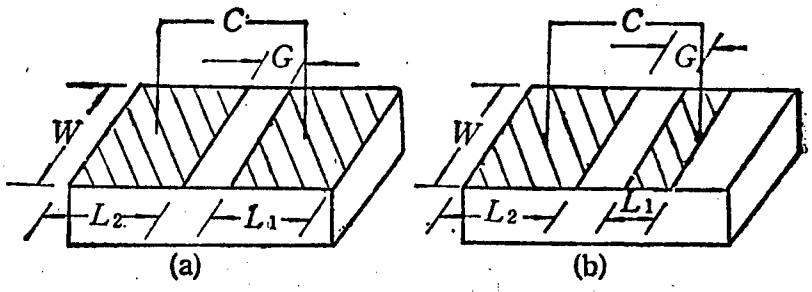

Figure 3. Schematic diagram of the planar capacitor

(3) Horseshoe-shaped capacitance between Schottky metal and ohmic contact

The capacitance was computed according to case b of Pucel's planar capacitance. Here, $L_2 >> G$, $L_1 \sim G$, and the capacitance is

$$C = \varepsilon_0(1+\varepsilon)W\frac{K(\sqrt{1-k^2})}{K(k)}$$

where K is again the elliptical integral of the first kind and k has the following value:

$$k = \sqrt{\frac{G}{G+L_1}}$$

For the planar mixer diode of Figure 1, we choose

$$k = \sqrt{\frac{L_0}{L_0+L_g}}$$
$$W = 2W_g + L_g$$

For structures using mesa isolation, the ramp capacitance of the finger-shaped metal can also be computed using the b-type capacitance approximation.

3. Resistance

(1) Under a positive bias, the contribution of the nondepleted N-layer GaAs to the series resistance is

$$R_s = \frac{T_N - W_d}{L_g W_g Q N_d \mu_N} \tag{4}$$

where μ_N is the electron mobility, Q is the electron charge, T_N is the thickness of the N-layer GaAs, N_d is the impurity concentration in the N layer, and W_d is the depletion-layer width at +0.6 V bias. For a metal-semiconductor barrier, W_d is computed with the following formula:

$$W_d = \sqrt{\frac{2\varepsilon\varepsilon_0(V_{bi} - V - 2KT/Q)}{QN_d}} \tag{5}$$

(2) Resistance of the ohmic contact zone

We calculated the resistance of the ohmic contact according to the Berger planar model:

$$R_i = Z_0 \coth(\alpha L_C) \tag{6}$$

where

$$Z_0 = \frac{\sqrt{R_S R_C}}{L_{eq}} \qquad (L_{eq} = 2W_g + L_g + 2L_0)$$

$$\alpha = \sqrt{R_S/R_C}$$

$$R_S = \frac{1}{T_{NP} N_d Q \mu_N}$$

In the above equation, R_S is the surface resistance and R_C is the ohmic contact resistance. The value of R_C of the experimental specimen was determined according to the TLM model of Berger. T_{NP} is the thickness of the N^+ layer.

(3) Resistance of the horseshoe-shaped epitaxial layer between the ohmic contact zone and the anode:

$$R_2 = \frac{L_0}{N_d Q \mu_N L_{eq} T_{NP}} \tag{7}$$

(4) Resistance of the Schottky metal junction

Since the signal is transmitted from one end of the anode to the other, the finger-shaped metal section should be regarded as a distributed network. Its resistance, different from the dc value,[4] is given by

$$R_4 = \frac{1.39 \times 10^{-6} W_i}{L_g \cdot T_{sho}} \tag{8}$$

where W_i is the total length of the metal finger, T_{sho} is a correction to the thickness of the metal finger considering the skin effect.

$$T_{sho} = d(1 - e^{-T_{sh}/d}) \tag{9}$$

$$d = \sqrt{\frac{2}{\omega H \sigma}}$$

where T_{sh} is the thickness of the metal finger, d is the skin depth, and ω is the angular frequency. H is the magnetic permeability. For nonmagnetic metals the permeability is taken to be the same as that of vacuum $\mu_0 = 4\pi \times 10^{-7}$ henry/sec.

In the resistance calculation we concentrated on the effects of the above resistance on the series resistance and gave second consideration to lead resistance and the resistance of the N^+ layer under the anode.

4. Results

Values of the calculated capacitances and resistances are shown below:

Capacitance (pF)		Resistance (Ω)	
$C_{j0.6V}$	= 0.045	R_1	= 0.51
C_{j0V}	= 0.020	R_2	= 2.6
C_1	= 0.0099	R_4	= 0.24
C_3	= 0.0013	R_6	= 2.26
C_4	= 0.018		

Total capacitance C_{to} = 0.0492 pF. Total resistance R_{to} = 5.61 Ω.

The cutoff frequency of the device is

$$f_{co} = \frac{1}{2\pi R_{so} C_{jo}} = 576.7\text{GHz}$$

III. Fabrication

Fabrication of planar mixer diodes generally takes three different approaches: (1) Generating N^+ and N layers with selective epitaxial growth and then achieving ohmic contact and Schottky junction in the growth zone.[5] The drawback of this method is the incompleteness and unevenness of the crystal growth near the edges of the growth zone. (2) The planar (actually quasi-planar) mixer diodes can be fabricated with the mesa isolation method similar to the fabrication of a MESFET. (3) Totally planar mixer diodes may be produced by proton ion injection.[6] Our technique for fabricating 8 mm GaAs planar mixer diodes was based essentially on the third method.

On an S.I-GaAs substrate, a 1-2 x 10^{18} cm^{-3} N^+ layer and a 1 x 10^{17} cm^{-3} N layer were grown using gas phase epitaxy. The thickness of the N^+ layer was decided based on the reduction of the series resistance and the ease of fabrication. The thickness of the N layer was about 0.2 μm. The Schottky metal used was Cr, the ohmic contact metal was Au-Ge-Ni, and the thick metal stripping technique was used. The films were silicon nitride (or silicon dioxide) deposited at low temperatures. The leads were thickened by metallization and the substrate was finally etched away and stripped off.

Ideally the mixer diode should have $n \leq 1.10$, a reverse bias of $V \leq 9$ volts (10 μA).

A flow chart of the fabrication process is shown in Figure 4.

IV. Testing

Noise figure of the mixer diode was measured using a gas discharge noise source. Figure 5 shows a block diagram of the testing system; it was actually a hyterodyne receiver.

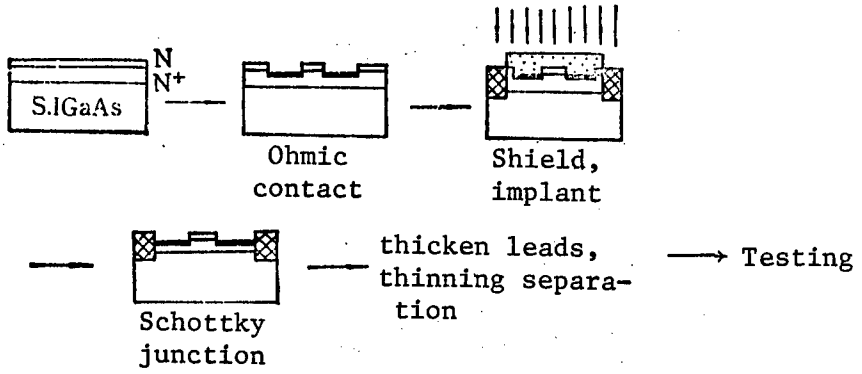

(a) Proton implant separation

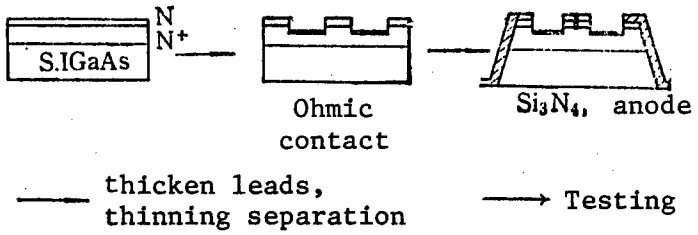

(b) Mesa isolation

Figure 4. Fabrication process of planar mixer diode

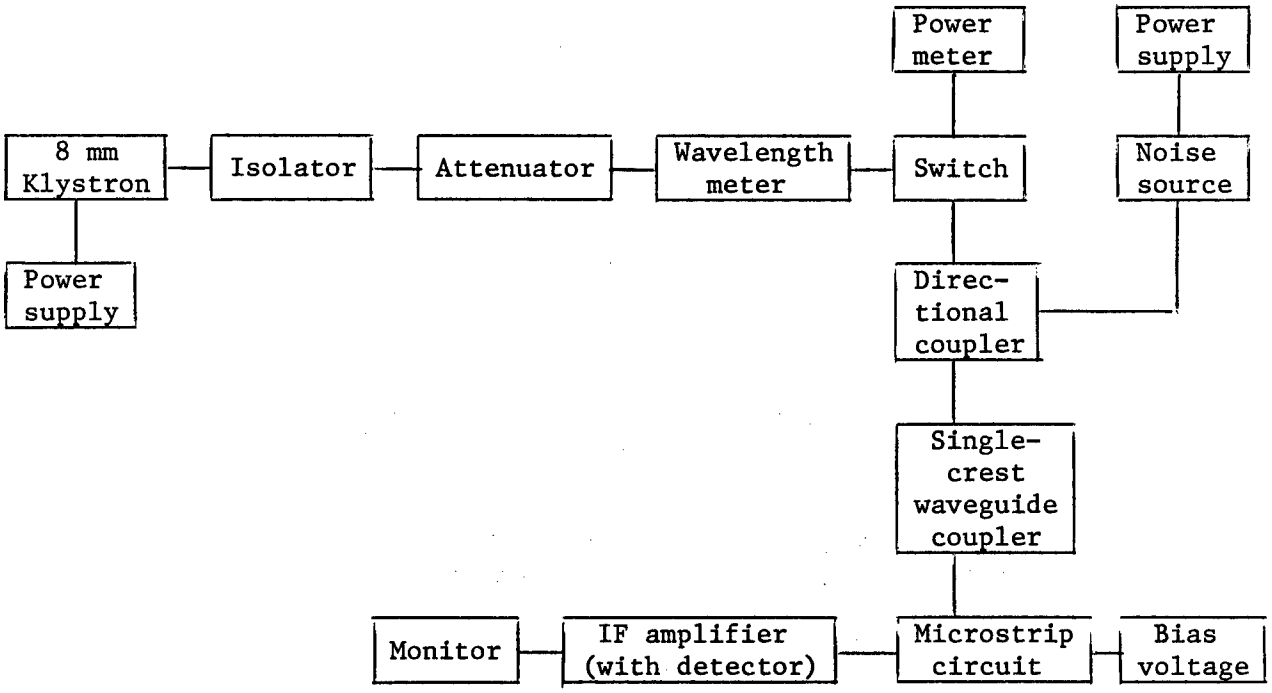

Figure 5. Block diagram of the testing system

The gas discharge tube in the system was a standard noise source and provided radio frequency signals for the measurements. An 8-mm klystron acted as a local oscillator, and the intermediate frequency after mixing was amplified by a 50-500-MHz low-noise broadband IF amplifier. The detector output was displayed on a microammeter. The single-ended testing circuit for the mixer was built on a quartz substrate and was connected to the system by a single-crest waveguide.

The noise figure is given by

$$N_F = ENR - 10\lg(Y-1) + \Delta$$
$$\approx ENR - 10\lg(Y-1)$$

where ENR = 17.846 ± 0.15 dB and Y is the multiplier factor.

Figure 6 shows the test results. The double-sideband noise figure of a single-ended mixer at 35 GHz was 4.8 dB.

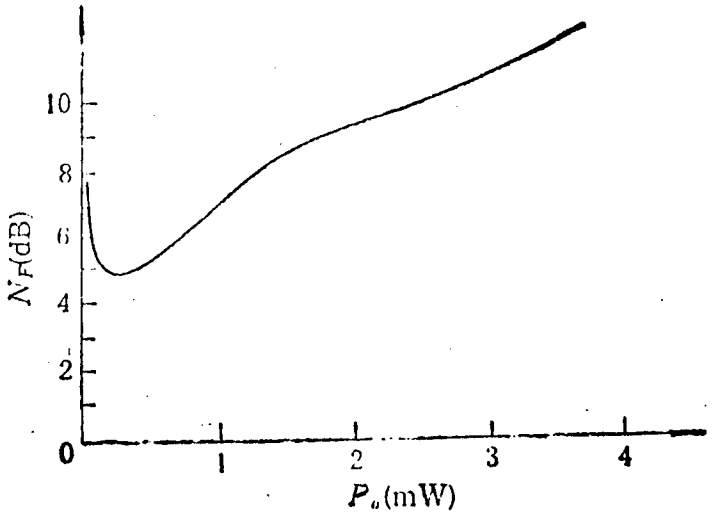

Figure 6. Double-sideband noise figure N_F as a function of P_O at 35 GHz and a bias current of 0.38 mA

V. Discussion

1. Performance tests of the device showed that the dimensional design of the device was quite reasonable. It should be possible to improve the performance of the planar mixer even more and to achieve even higher frequency by further optimization of the geometric parameters.

2. Among the total capacitance of the device, control of the junction capacitance is important. In the optimization of L_g and W_g, no particular attention needs to be given to the capacitance C_3 of the horseshoe, but the lead capacitance C_1 and the capacitance of the junction zone are important

constituents of distributed capacitance. This capacitance can be reduced by minimizing the area of the leads.

3. Major contributions to the total series resistance of the device are the resistance R_6 of the nondepletion layer and the resistance R_2 of the horseshoe epitaxial layer. Effective ways to reduce the series resistance are reducing the size of L_0 and controlling the thickness of the N and N^+ layers.

4. Reducing L_0 decreases the series resistance but at the same time increases the horseshoe capacitance. However, the latter changes slowly (see Figures 7 and 8), so L_0 still should be decreased in order to raise the cutoff frequency.

5. The testing system and the matching of the circuit with the testing rig should be improved in order to evaluate the performance of the mixer diode more reliably. In addition, a broadband IF amplifier was used in this work; the test results would have been different if a narrow-band amplifier were used.

The authors thank Wang Li [3769 5461], Gao Cuihua [7559 5050 5478], Wang Ruilin [3769 3843 2651], Zhang Jinchang [1728 6651 2490], Yu Qing [0080 3237], Shao Cuanyuan [6730 0356 6678], Liang Hong [2733 4767], and Tian Jing [3944 7234] for their assistance in the fabrication of the device.

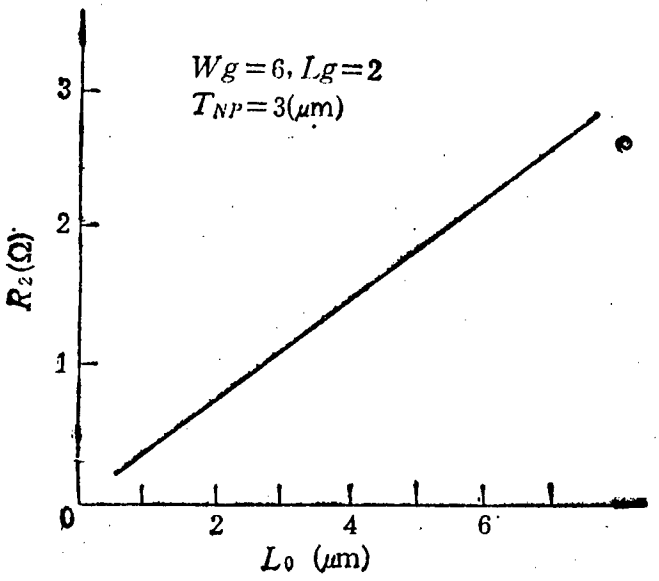

Figure 7. Horseshoe resistance R_2 as a function of L_0

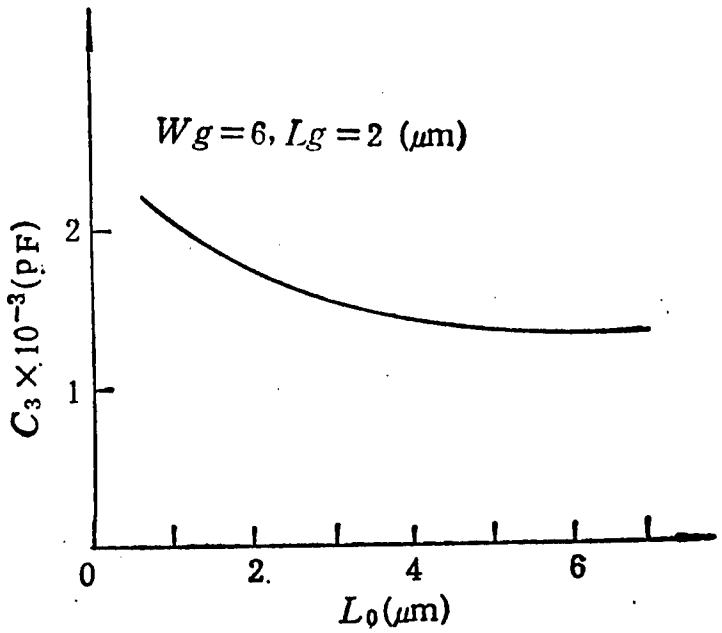

Figure 8. Horseshoe capacitance C_3 as a function of L_0

References

[1] R. A. Pucel, H. A. Haus, and H. Statz, Advances in Electronics and Electron Physics, Vol 38, pp 145-265 (Academic Press, New York, 1975).

[2] H. H. Berger, Solid State Electronics, p 145, 1972.

[3] H. Howe, Stripline Circuit Design (Dedham, MA. Artech, 1973).

[4] H. Fukul, Bell Systems Technical Journal, 58, 771 (1979).

[5] "Selective Epitaxial Growth of GaAs," Supplement to BANDAOTI TONGXUN [SEMICONDUCTOR COMMUNICATIONS], Special Issue on GaAs Schottky Mixer Diodes, Vol 10, p 117, 1972.

[6] N. J. Cronin and V. J. Law, "Planar Millimeter-Wave Diode Mixer," IEEE Trans. on Microwave Theory and Techniques, MTT-33, September 1985.

Novel Silicon Oxidation Method for VLSI--Two-Step HF Enhanced Oxidation

40080074b Beijing BANDAOTI XUEBAO [CHINESE JOURNAL OF SEMICONDUCTORS] in Chinese Vol 9 No 6, Nov 88 pp 640-647

[Article by Long Wei [7893 0251], Xu Yuansen [1776 0337 2773], and Zheng Yangshu [6774 7402 9452] of Shanghai Institute of Metallurgy, Chinese Academy of Sciences; manuscript received 21 Jul 87]

[Text] Abstract: A new silicon oxidation method that improves the oxidation rate by at least one order of magnitude by adding only a few thousand ppm of HF [hydrogen fluoride] to pure oxygen gas is reported. After rapid HF-doped oxidation at 800°C and subsequent annealing at the same temperature in pure oxygen, a 200Å-thick high-quality thin-film gate oxide exhibiting good uniformity of thickness can be obtained. Breakdown voltage measurements lead to a defect density of about $2/cm^2$ and intrinsic breakdown events of about 99 percent [as opposed to the 1 percent exhibiting low-voltage breakdown]. The interface charge densities are very low and the Si/SiO_2 interface is nearly atomically flat as revealed by TEM [transmission electron micrographs] at 2 million times magnification. These superior properties of the SiO_2 thin film hold great promises for VLSI [very large scale integrated circuit] applications.

I. Introduction

In the development of VLSI, it is desirable to lower the fabrication temperature, particularly the oxidation temperature, in order to overcome such problems as impurity redistribution in silicon at high temperature, silicon wafer warping, and thermally induced defects. However, silicon oxidizes very slowly below 900°C in dry oxygen and produces low quality Si/SiO_2 interfaces; conventionally almost all oxidations are done at about 1000°C. Ways to lower the oxidation temperature and increase the oxidation rate are therefore of considerable interest in current VLSI research.

In order to enhance the oxidation rate, low-temperature techniques such as high-pressure oxidation,[1] plasma-enhanced oxidation,[2] photo-enhanced oxidation,[3,4] and NF_3-enhanced oxidation[5] have been proposed. These methods have not been widely applied, not because of industry's reluctance to accept new technology but because of shortcomings that exist in these methods. For example, the convection currents in the pressurization process

of the high-pressure oxidation method lead to temperature inhomogeneities in the oxidation furnace and thickness nonuniformity in the oxidized layer[1] (especially thin gates). In plasma-enhanced oxidation, the high-energy and chemically active constituents in the plasma zone may cause equipment corrosion. Sputtering and gas phase reaction may deposit undesirable materials, and the oxidation layer will contain radiation damage and be of low quality.[2] The mechanism of photo-enhanced oxidation is still not clear and the quality of the oxidized layer using this method is not yet satisfactory.[3,4] When NF_3 is used to enhance the oxidation rate, the gas system still contains hazardous and corrosive materials and the resulting quality of the oxidized layer is far below that of oxidation layers obtained at high temperature.[5]

Authors of this paper found that a minute amount of HF added to dry oxygen greatly increased the oxidation rate of silicon. The oxidized layers that contained fluorine were then annealed in pure dry oxygen to reduce and even remove the fluorine atoms in order to achieve a high-quality oxidized layer. The two-step method therefore consisted of a rapid growth of oxide at low temperature (800°C) with HF doping, followed by annealing in pure dry oxygen. This method not only overcomes the obstacle of slow oxidation rate at low temperature but also avoids the problem of low oxide quality obtained with the other methods mentioned above. This paper describes the two-step method for growing high-quality silicon dioxide layers at 800°C and presents the research results.

II. Experimental Method

HF-doped oxidation was carried out in an ordinary diffusion furnace. The HF gas was obtained by passing dry oxygen over MOS-pure HF acid. The experimental setup is shown in Figure 1. The HF reagent was heated with a small electric heater. The temperature was controlled with a water bath and a temperature transducer to within ±0.5°C.

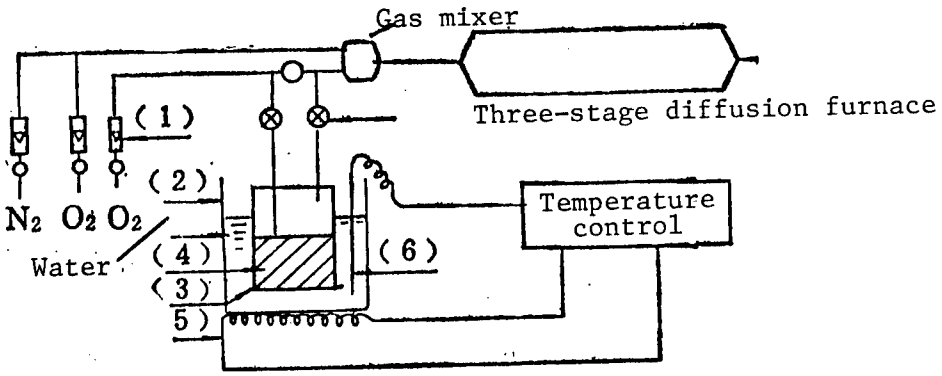

Figure 1. HF oxidation system

(1) Gas flowmeter; (2) quartz beaker; (3) polytetrafluoroethylene bottle; (4) 40 percent HF solution; (5) small electric furnace; (6) temperature transducer

P-type or N-type (100) silicon wafers ([resistivity] of 6-10 Ω-cm) were carefully cleaned chemically and then loaded onto boats and into the furnace immediately after cleaning. After a waiting period of 30 seconds for the temperature to stabilize while the wafers were protected by dry oxygen gas, a small amount (a few hundred to a few thousand ppm) of HF was introduced. Oxides grew rapidly on silicon in the O_2/HF atmosphere. The HF source was then shut off and the wafers were annealed in pure oxygen. Polycrystalline silicon was deposited on the wafers at low temperature immediately after the oxide growth and annealing. After doping and photoetching, MOS structures were formed to measure the quality of the oxide layers.

The oxide thickness was measured with an ellipsometer. The breakdown voltage was defined as the voltage when the conduction current through the SiO_2 film reached 3 μA, with the silicon substrate in the accumulation state. The area for capacitance measurement was 6×10^{-3} cm^2 and each wafer had 300 MOS patterns etched on it.

III. Experimental Results

Figure 2 shows the strong oxidation enhancement by HF. The oxidation rate was greatly increased after the introduction of a minute amount of HF. With HF, the oxidation rate at 800°C can be as fast as that at 1000°C in dry oxygen. For example, growing an oxide 300 Å thick at 800°C took more than 10 hours in dry oxygen, but required only 35 minutes with HF doping. With HF, oxidation can easily be done at the lower temperature of 800°C; this is undoubtedly desirable in the manufacture of VLSI.

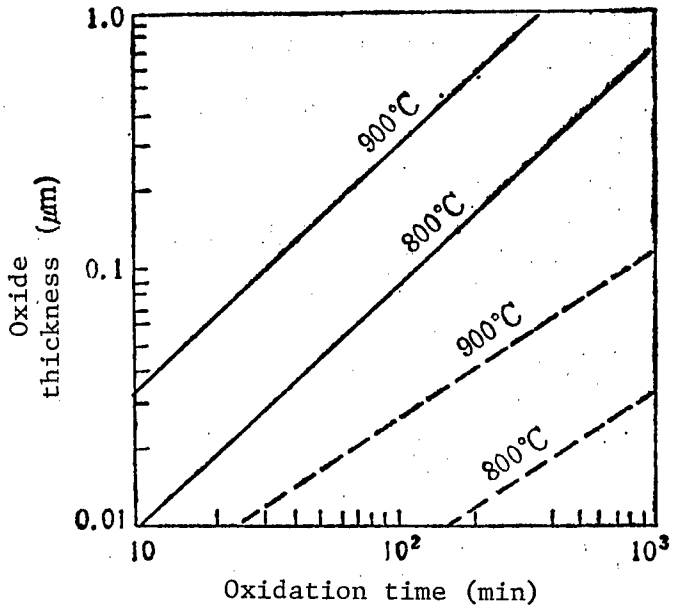

Figure 2. Comparison of oxidation rates in HF oxidation and pure oxygen oxidation. Results show a remarkable enhancement by HF.
—— 2000 ppm HF; ---- dry oxygen

The rapid growth behavior is shown in Figure 3. Experimental data agreed well with the linear-parabolic equation that describes oxide growth in pure oxygen. This showed that HF doping did not change the growth behavior of the oxide. By fitting linear and parabolic curves to the experimental results obtained at different temperatures, the rate constants were found (see Table 1). The linear rate constant increased over that for dry oxygen by 14-20 times, and the parabolic constant was enhanced by 60-90 times. These enhancements were much greater than the effects of water moisture in oxygen. In our system the amount of water moisture introduced while adding HF was about 2000 ppm; this amount of water moisture could not have increased the value of K_L by more than 30 percent,[6] and the observed increase in K_L was 45 times greater.

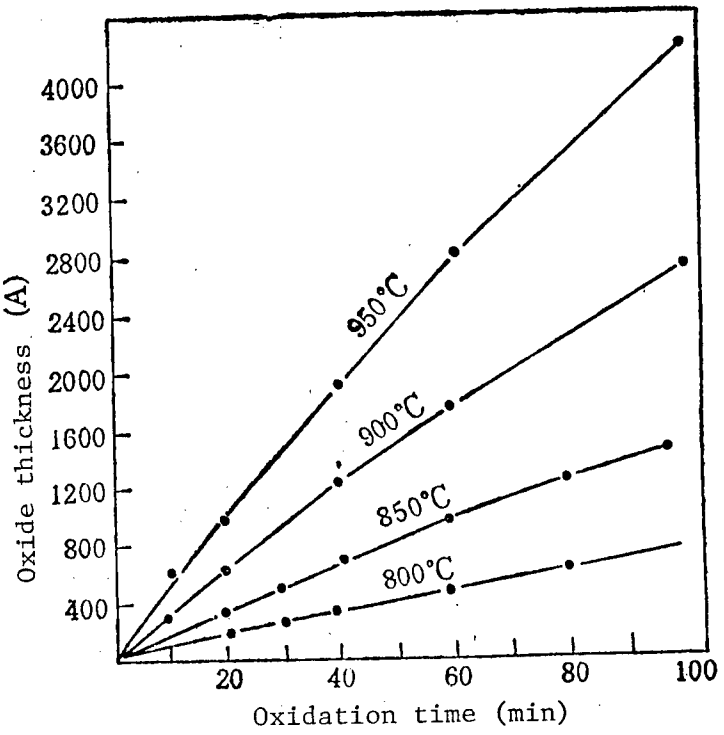

Figure 3. HF oxidation at 2000 ppm follows the ordinary linear-parabolic behavior. Dots are experimental data and lines are theoretical curves.

The density of the oxide was determined by measuring the refractive index n and using the Lorentz-Lorenz relationship: $\rho = K(n^2 - 1)/(n^2 + 1)$. The data in Table 2 show that the density of the oxide decreased with increasing concentration of HF. With HF, the oxide was less dense and contained more "free space."

Table 1. Comparison of HF Doped Oxidation Rate Constant With Pure Oxygen Oxidation

Temperature (°C)	Linear rate constant K_{LF} (μm/h)	Comparison with dry oxygen K_{LF}/K_{LD}	Parabolic rate constant K_{PF} ($\mu m^2/h$)	Comparison with pure oxygen K_{PF}/K_{PD}
800	0.053	20.5	0.038	95.6
850	0.115	20.6	0.065	57.3
900	0.210	16.8	0.207	61.7
950	0.342	14.2	0.469	64.6

Table 2. Effects of HF Concentration on the Refractive Index and Density of Oxide

Temperature	HF content in oxygen (ppm)	Oxide thickness (Å)	Refractive index (n)	Density $\rho(g/cm^3)$
900°C	700	577	1.485	2.306
	2000	387	1.474	2.261
	2650	455	1.430	2.079
950°C	1000	447	1.457	2.191
	2000	654	1.442	2.129
	2650	854	1.429	2.074

Note: Value of coefficient K is taken to be 8.0461 [per Ref. 7]

Auger electron spectroscopy (AES) and refractive index measurements were made on oxides grown with different annealing times. With increasing annealing time, the number of fluorine atoms in the oxide decreased and the density of the oxide increased. With 30 minutes annealing, the refractive index of the oxide grown at 950°C under 2650 ppm fluorine changed from 1.430 to 1.456 and the density of the oxide increased from 2.079 g/cm^3 to 2.186 g/cm^3. This showed that annealing in pure oxygen after oxidation gradually removed the fluorine atoms from the oxide and increased the density of the oxide.

Figure 4 shows the relative error of the silicon wafer thickness as a function of oxidation temperature. These data showed a trend: the higher the oxide temperature, the greater the thickness uniformity. This showed that HF-doped oxidation at low temperature can not only achieve an oxidation rate equal to that in pure oxygen at high temperature, but can also achieve better thickness uniformity. The better uniformity of thickness may be attributed to the lower temperature fluctuation of the diffusion furnace at lower temperatures than at higher temperatures.

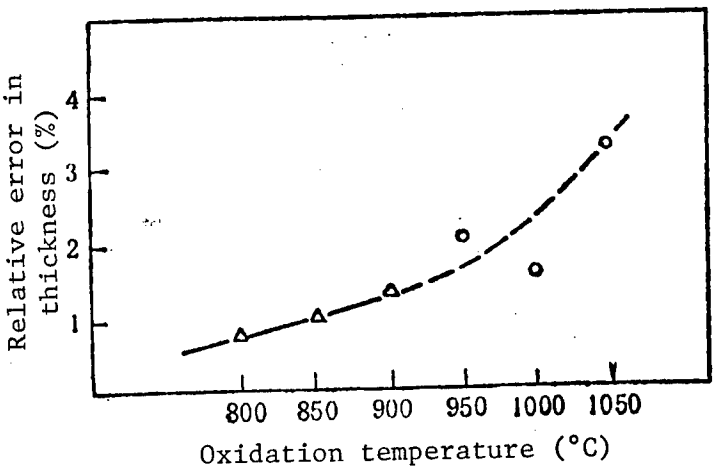

Figure 4. Uniformity of thickness is better at lower oxidation temperatures. o = pure dry oxygen; Δ = HF oxidation.

In this work, 200-Å-thick oxide layers were grown with the HF two-step low-temperature (800°C) method. C-V [capacitance-voltage] measurements made on the oxides showed that: (1) a typical value of the flat-band voltage was -0.85 V (P-type silicon substrate), (2) mobile charge density was less than 4×10^{10} cm^{-2}, (3) fixed charge density was less than 1×10^{11} cm^{-2}, and (4) the C-V curve showed no clear interfacial effect. These results indicated that the oxides obtained by HF-doped oxidation had very little interfacial charges and had good stability. They also indicated that the addition of HF did not introduce extra mobile charges nor noticeably increase fixed interfacial charges.

When a current flows through the oxide, traps in the oxide have a certain probability to capture electrons or holes and become charge centers. This will cause a shift in the C-V curve. Figure 5 shows this flat-band shift under large current injection ($J = 2.6 \times 10^{-4}$ A/cm^2). As can be seen, the flat-band shift of HF oxidation is less than that of high-temperature oxidation in pure oxygen. In other words, the trap density of oxides grown by HF oxidation is less than that of high-temperature oxides under large current injection. Since the trapping effect under the action of thermal electrons in the large current is a measure of the resistance against radiation, oxides made by the HF two-step method are more resistant to radiation.

It was discovered that oxides made with HF-doping only were not only low in density but were also poor in breakdown characteristics. We therefore used the method of pure-oxygen annealing together with HF-doped oxidation. Figure 6 shows the breakdown characteristics. When the annealing time was insufficient (e.g., 70 minutes), frequent medium field breakdown (6-8 MV/cm) was observed. This indicated the existence of defects such as half pinholes and local traps. With sufficient annealing time (e.g., 100 minutes), no medium field breakdowns were observed and the oxide showed intrinsic breakdown behavior. AES analysis showed that F atoms in the oxide decreased with annealing time. Results in Figure 6 therefore indicate that F atoms in SiO_2 may have damaged the original network structure in SiO_2 and introduced some

structural defects such as half pinholes and traps. As the annealing time increases, these defects gradually decrease and finally disappear.

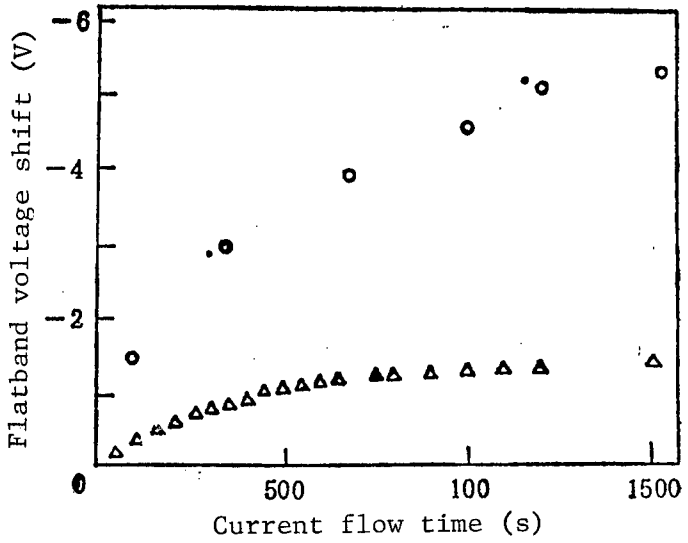

Figure 5. Flat-band voltage shift versus current injection time. o = thermal oxidation, Δ = HF oxidation; T_{ox} = 215 Å, J = 2.6 x 10^{-4} A/cm^2.

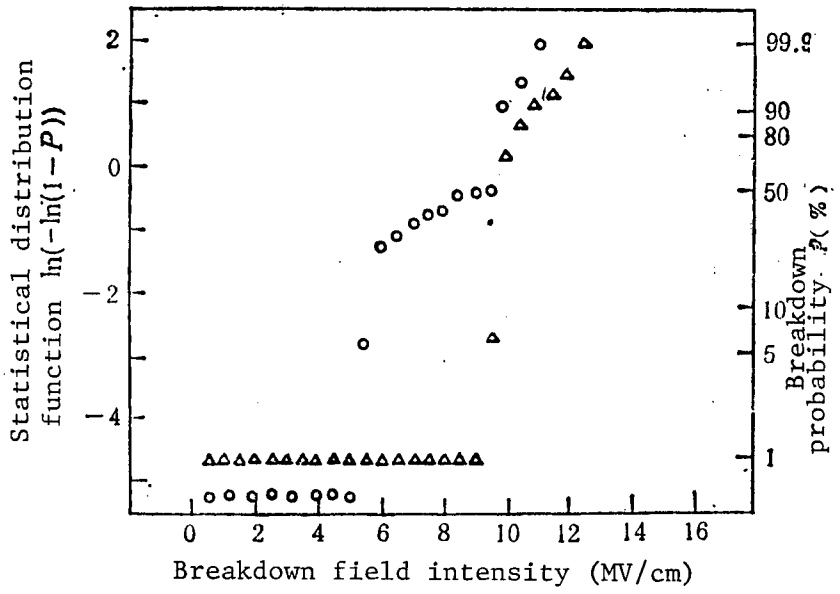

Figure 6. Effects of annealing time on dielectric breakdown. o = t_{ox} = 200 Å, annealing time = 70 minutes; Δ = t_{ox} = 215 Å, annealing time = 100 minutes.

The annealing conditions were carefully optimized and high-quality oxides were produced with the HF-doped two-step low-temperature procedure. Figure 7 shows the histogram of breakdown distribution in such oxides. Only 1 percent of the capacitors tested showed low-voltage breakdown and 99 percent showed intrinsic breakdown. The breakdown electric field exceeded 9.5 MV/cm. The results are similar to those obtained by HCl-doped oxidation (Figure 8) and the intermediate annealing thermal oxidation method (Figure 9). With HF doping and two-step oxidation, high-quality breakdown characteristics can be achieved at a low temperature of 800°C.

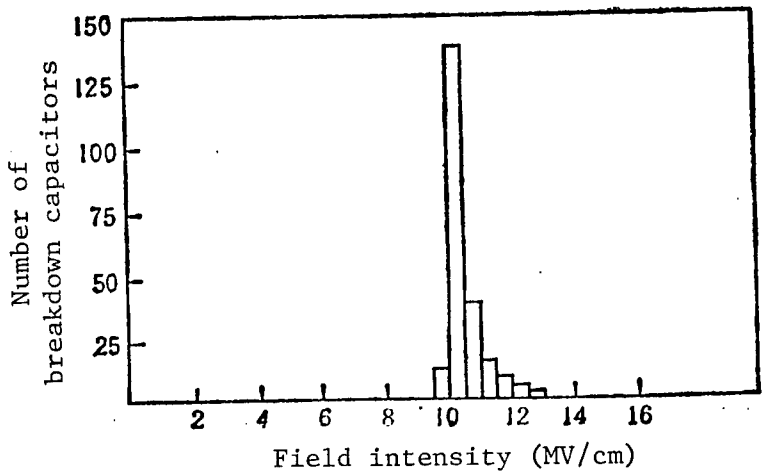

Figure 7. Breakdown distribution histogram of 215-Å-thick oxides grown with HF-doped two-step oxidation at low temperature (800°C). 800°C 30' + 100' annealing with 700 ppm HF.

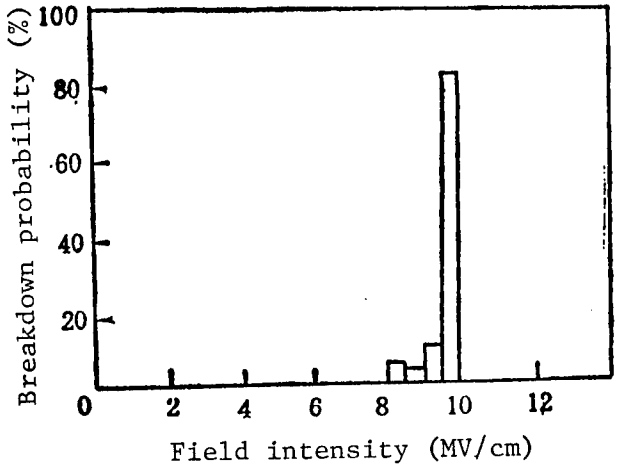

Figure 8. Breakdown characteristics of 150-Å-thick oxide grown with HCl-doped oxidation. 900°C, annealed for 1 hour.[10]

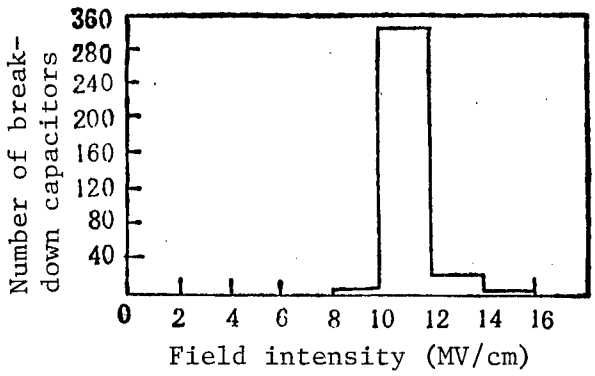

Figure 9. Breakdown characteristics of intermediate annealing oxides, 200 Å, 900°C, annealed for 100 minutes[11]

Based on the breakdown test results, the defect density ρ of the oxide can be obtained by applying the statistical formula[8] $\rho = -\ln(1-P)/A$. Here P is the percent of the capacitors that did not reach intrinsic breakdown and A is the area of the capacitor. The density ρ not only depends on structural defects such as pinhole and microcracks of the oxide, but also on other electrical imperfections. It is undoubtedly an important figure of merit for the oxides. Table 3 shows a comparison of the defect density in HF two-step oxides and in high-temperature oxides. Among the reported methods, the high-temperature two-step oxidation method of Vorst et al. produced the lowest defect density. The defect density of the HF oxides, only 2 cm^{-2}, is even lower than that of the Vorst method. It has been verified experimentally before that, in conventional oxidation, the lower the temperature the higher the defect density. Hence, HF doping not only retained the advantage of low-temperature oxidation, but also overcame the quality problem of low-temperature oxides and achieved oxide quality expected of high-temperature oxides.

Table 3. Comparison of Defect Density in HF Oxidation and in Other Oxide Methods

Technique	High temp, two-step, 900°C 1 hr anneal at 1050°C	HCl oxidation 900°C, anneal for 1 hr	HF, two-step at 800°C, 100 min anneal at 800°C
Oxide-layer thickness (Å)	86	150	215
Defect density ($1/cm^2$)	4	20	2

Transmission electron microscopic examinations were made on the cross-section of HF two-step oxides in the <110> direction. At 2 million times magnification, the Si/SiO_2 interface was observed to be quite smooth, as shown in Figure 10. Based on the magnification and the oxide dimension on the

micrograph, the oxide layer thickness was found to be 215-220 Å. This thickness agreed very well with the 215 Å result measured on an ellipsometer.

Figure 10. High-voltage electron microscope photo of the oxide layer interface [not reproducible]

IV. Discussion

1. After the oxide layer was grown with HF doping, we added an annealing step in pure oxygen at 800°C. This procedure differed from the conventional high-temperature oxidation method for modifying the interface because of the following reason. When HF was first introduced, there were many F and OH radicals in the oxide, existing in the form of ≡Si-F and H-O-Si≡. There were therefore many "broken bonds" in SiO_2. During the annealing in pure oxygen, F and OH may recombine and form HF:

$$\equiv Si - O - H + F - Si \equiv \rightleftharpoons \equiv Si - O - Si \equiv + HF\uparrow$$

This process gradually eliminates the "broken bonds" and repairs the silicon oxide network. The process naturally requires a certain length of time to complete. The purpose of using pure oxygen in annealing is more than just using oxygen as a protective gas. During annealing, there is a small amount of silicon oxide growth and it generates compressive stress at the SiO_2/Si interface. This stress presses the loose oxide layer and increases the probability of the reaction described above, thus making the silicon oxide denser. (This has been verified by refractive index measurements after annealing.)

2. Based on our measured results, two-step HF oxidation at low temperature can produce oxides of the same quality as that by two-step thermal oxidation at high temperature.[9] Other low-temperature oxidation methods did not produce oxides of such quality.

It is well known that the cleanliness of the oxidation system is one of the necessary conditions for producing high-quality oxides. Contaminations introduced in the oxidation process often lead to low-voltage breakdown. In other low-temperature methods, such as CF_4 doping or NF_3 doping, fluorine-containing gas must pass through a mass flow meter and other sensitive components before diluting. This often causes corrosion and contamination of the system, and results in low-quality oxides. In HF-doped oxidation, the HF molecules are carried out of a liquid source and the HF concentration can be adjusted by controlling the gas going into the source bottle. Gases with HF molecules no longer need to pass through any measurement devices and the fluorine concentration in the pipeline is too low (about 2000 ppm) to cause any corrosion. We have used the same quartz tube for more than 1 year and it still looks new. Also, the purity of the HF gas obtained from low-temperature evaporation is very high; the system can be kept very clean and high-quality SiO_2 layers can therefore be grown.

3. Low-temperature fabrication of VLSI [devices] is an important topic in modern microelectronics research. The success of HF-enhanced oxidation has made low-temperature (800°C) fabrication of VLSI [devices] more complete. In current VLSI fabrication technology, oxide growth and annealing after impurity doping are all done above 900°C. However, if laser or rapid thermal processing (RTP) are used in the activation of the impurities and in the elimination of implant damages, and HF oxidation at 800°C is used in growing all the oxide layers, then a low-temperature fabrication technology for IC's can be developed. Such a technology would have the following advantages:

(1) The quality of the oxide layer would be good and defects would be few in the silicon under the oxide. The surface mobility would be high.

(2) Large silicon wafers will not tend to curl, which favors higher accuracy in photoetching.

(3) Impurity redistribution would be negligible.

These characteristics are the goals in VLSI technology.

V. Conclusions

1. It was discovered in this research that when a small amount of HF (several hundred to several thousand ppm) was added into dry oxygen, the dry oxidation rate of silicon was increased by an order of magnitude at temperatures investigated (800-950°C). This discovery allowed the oxidation temperature in silicon device fabrication to be lowered to 800°C while still maintaining a satisfactory growth rate.

2. HF-doped oxidation at 800°C may be used in producing high-quality thin gate oxides in MOSVLSI. The specific steps are as follows. First the oxide layer is allowed to grow to almost the desired thickness in a dry oxygen atmosphere containing a small amount of HF. The second step is annealing in pure oxygen at the same temperature. The oxides produced with this method have good quality since the method avoids the usual long oxidation time associated with low-temperature growth that often leads to poor quality. It also produced oxides of uniform thickness, with high resistance to radiation damage, and negligible impurity redistribution.

3. The HF oxidation system has overcome the contamination problems plaguing other low-temperature techniques. It does not require special gas or equipment and the process is very simple. By suitably choosing the processing parameters, a number of needs can be met and the prospects for application are quite good.

The authors thank the assistance provided by the staff of the Integrated Circuit Laboratory, Shanghai Institute of Metallurgy. Comrade Ni Rushan [0242 1172 1472] provided high-voltage electron micrographs, and Comrade Yin Xinjuan [1438 2622 1227] and the Auger group helped analyze the F content.

References

[1] E. A. Irene, D. W. Dong, and R. J. Zeto, J. Electrochem. Soc., 127 (1980).

[2] A. K. Ray and A. Raisman, J. Electrochem. Soc., 128, 2424 (1981).

[3] E. M. Young and W. A. Tiller, Appl. Phys. Lett., 42, 63 (1983).

[4] I. W. Boyd, Appl. Phys. Lett., 42, 728 (1983).

[5] M. Morita, S. Aritome, M. Tsukude, and M. Hirose, IEDM, 144 (1984).

[6] E. A. Irene, J. Electrochem. Soc., 125, 1708 (1976).

[7] W. A. Plishkin and H. S. Lehman, J. Electrochem. Soc., 112, 1013 (1965).

[8] N. J. Chou and J. M. Eldridge, J. Electrochem. Soc., 120, 1140 (1973).

[9] A. Bhattacharyya and C. Vorst, J. Electrochem. Soc., 132, 1900 (1985).

[10] R. G. Cosway and S. Y. Wu, J. Electrochem. Soc., 132, 152 (1985).

[11] S. S. Cohen, J. Electrochem. Soc., 130, 929 (1983).

InP/InGaAsP Multi-Blocking Layer Buried Crescent Laser Emitting at 1.3 μm With Low Threshold Current

40080074c Beijing BANDAOTI XUEBAO [CHINESE JOURNAL OF SEMICONDUCTORS] in Chinese Vol 9 No 6, Nov 88 pp 665-667

[Article by Xiao Jianwei [5135 1696 0251], Bo Baoxue [5631 1032 1331], Yi Maobin [5902 5399 2430], Ma Yuzhen [7456 3768 3791], and Gao Dingsan [7559 7844 0005] of the Department of Electronics Science, Jilin University, Changchun; manuscript received 22 Dec 87]

[Text] Abstract: 1.3 μm InP/InGaAsP multi-blocking layer buried crescent lasers have been fabricated by a two-step LPE [liquid-phase epitaxial] growth process. Typical and minimum CW [continuous work] threshold currents are 20 mA and 10 mA, respectively. Stable fundamental transverse-mode operation has been obtained at three to five times the threshold current. The differential quantum efficiency per facet is about 20-30 percent.

Buried structure semiconductor lasers usually have very low threshold currents. The active region of the 1.3 μm InP/InGaAsP buried crescent (BC) laser is buried in the n-InP and p-InP layers grown from the V-shaped bottom of the (111) P sidewall. Eliminated are the far-field unevenness[1] and peak value drifting[2] often found in BH [buried heterostructure] lasers due to uneven burial boundary. Thus, BC lasers not only have very low threshold current but also extremely stable fundamental transverse-mode output; they are very promising semiconductor lasers. After we succeeded in developing BC lasers, we strove to improve the production rate and characteristics of low-threshold devices and developed the 1.3 μm InP/InGaAsP multi-blocking buried crescent laser. Figure 1 shows the end face structure and its scanning electron microscope (SEM) photo.

We used a double epitaxial method. The first epitaxial growth produced the n-p-n-p-n InP current blocking layer and the InGaAsP burial layer on the n^+-InP substrate. Other steps were similar to the manufacture of BC lasers.[3] The thickness at the center of the crescent-shaped active region is 0.2-0.3 μm, the width is 2-2.5 μm, and the length of the core cavity is 200-250 μm. Considering the needs for high-speed modulation, the device was installed on a silver-plated copper heat sink with the P side facing up.

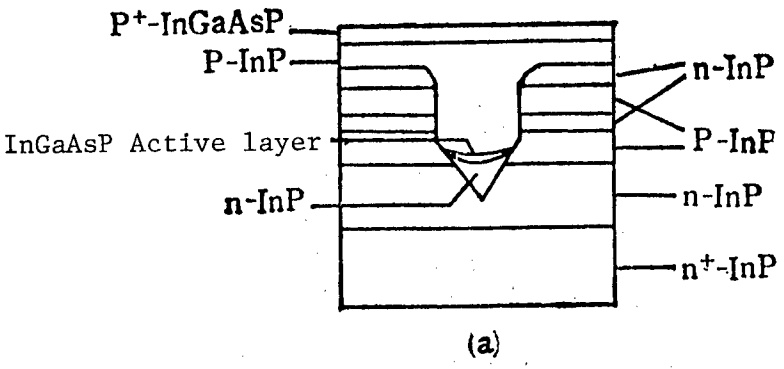

Figure 1. InP/InGaAsP multi-blocking buried crescent laser.
(a) Cross-section, (b) SEM photo [not reproducible]

The typical and minimum CW threshold currents for room-temperature operation of the 1.3 μm InP/InGaAsP BC laser are 20 mA and 10 mA, respectively. The temperature dependence of the P-I [power-current] curve is shown in Figure 2. T_o is about 35-45 K (near room temperature), and the maximum DC operating temperature is about 8-10°C lower than that for a reverse mounted device. Because of the low threshold, the room-temperature linear light power output of a forward-mounted device is still more than 8 mW. In the range of our measurements (3 to 5 times the threshold), the laser operates stably in the fundamental transverse mode and the far-field is very smooth. A good fraction of the devices produce a single longitudinal-mode output, as shown in Figure 3. The single-surface differential quantum efficiency of the device is generally in the 20-30 percent range. The far-field pattern of the multi-blocking BC laser is approximately circular, which facilitates direct coupling between laser and optical fiber and promotes coupling efficiency. The series resistance of the device is about 4-5 ohms. Using the C-V [capacitance-voltage] method, we measured a capacitance of 35 pF or so, with a minimum value of 28 pF. (The modulation frequency was 1 MHz, and the surface area of the device was 200 x 250 μm^2.) In the meantime, we also measured the capacitance of an oxide strip having the same area and the capacitance of a BC laser (they were about 120 pF and 55 pF, respectively). In comparison, the junction capacitance of the multi-blocking BC laser is noticeably reduced. Considering the response of the carriers, the capacitance of the device will still be much less[4] when the modulation frequency is in the GHz range.

Our experimental results showed that the fabrication process of the multi-blocking buried crescent laser is reproducible. We tested several batches of tubes using 50-percent duty cycle pulses; we found that about 50 percent of the tubes had a threshold current less than 25 mA. Since the thickness and width of the active region were not optimized, the threshold current of this type of laser can still be reduced further. We are currently improving the method to increase the output of the linear light power. Related high-frequency modulation characteristics will be reported in detail later.

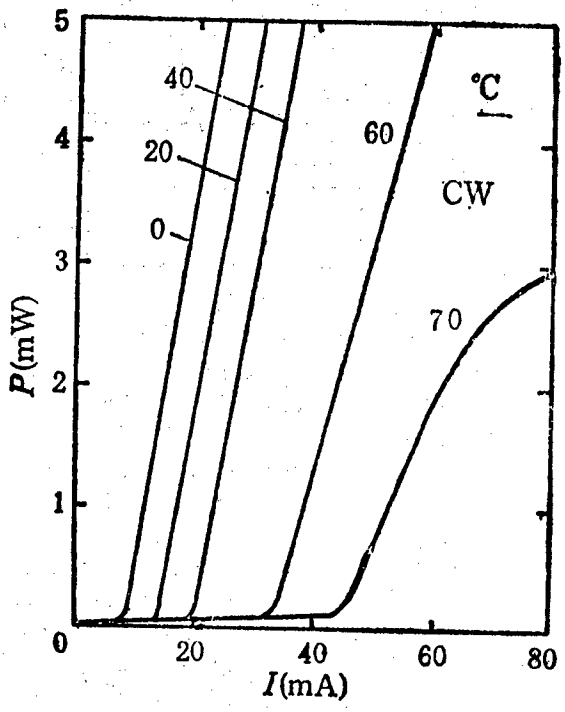

Figure 2. Temperature dependence of P-I characteristics of a typical multi-blocking buried crescent laser

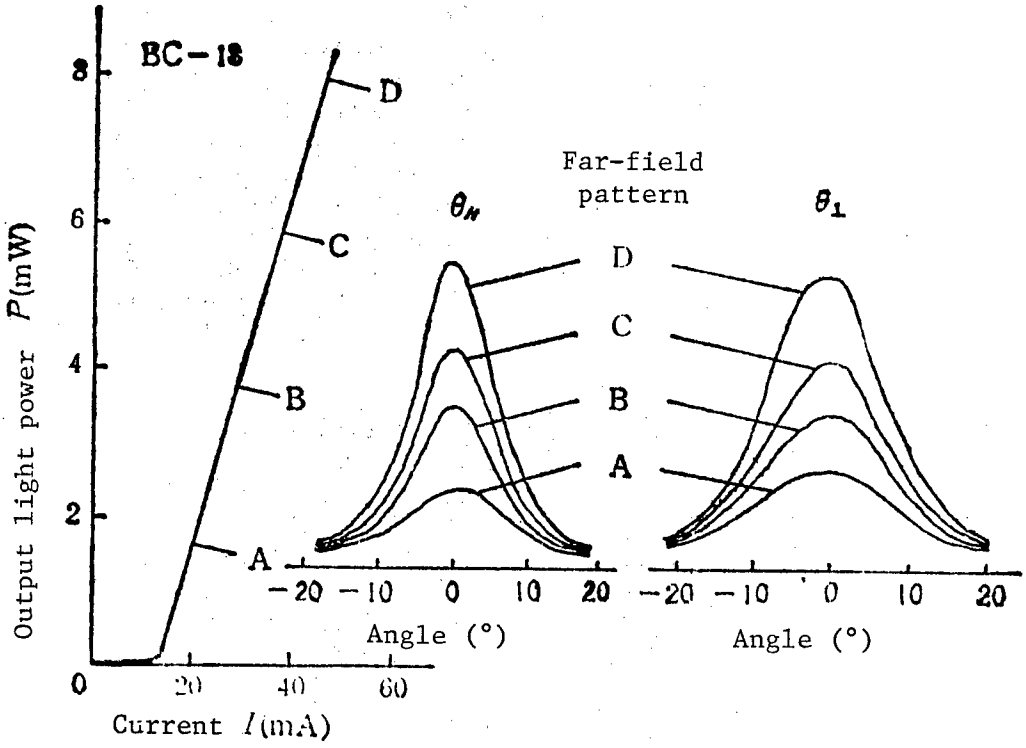

(a)

[Figure 3 continued on following page]

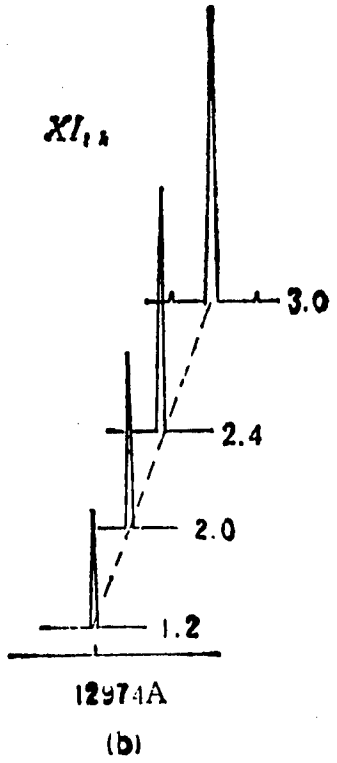

Figure 3. Far-field pattern (a) and spectral characteristics (b) of multi-blocking buried crescent laser

The authors thank Meng Qingju [1322 1987 1565], Zhao Yongsheng [6392 3057 3932], and Zhang Yuxian [1728 3768 6343] for providing the scanning electron micrographs.

References

[1] M. Hirao, S. Tsuji, K. Mizuishi, A. Doi, and M. Nakamura, J. Opt. Commun., 1 (1980).

[2] T. Muratan, E. Oomura, H. Higuchi, H. Namizaki, and W. Susaki, Electron. Lett., 16, 566 (1980).

[3] Xiao Jianwei et al., JILIN DAXUE ZIRAN KEXUE XUEBAO [JOURNAL OF JILIN UNIVERSITY, NATURAL SCIENCE], No 4, 119 (1987).

[4] K. Kamite, M. Yano, T. Tanahashi, H. Ishikawa, S. Yamakoshi, and H. Imai, Electron. Lett., 22, 407 (1986).

Stable Defects in Silicon Implanted With Hydrogen Ions

40080074d Beijing BANDAOTI XUEBAO [CHINESE JOURNAL OF SEMICONDUCTORS] in Chinese Vol 9 No 6, Nov 88 pp 674-675

[Article by Li Jianming [2621 1696 2494] of the Institute of Semiconductors, Chinese Academy of Sciences, Beijing; manuscript received 8 Jun 88]

[Text] Abstract: Thermal stability of defects in silicon implanted with H^+ has been studied. Stable defects were found in samples implanted with H^+, which were annealed at 600°C for a long time before annealing at high temperature. Stable defects were not found in samples that were directly annealed at high temperature. This shows that annealing of samples at 600°C for a long period of time is the key to the stability of defects.

Hydrogen atoms have the smallest volume and mass among all the atoms, they therefore have the highest thermal motion velocity. In heat-treating hydrogen-implanted silicon, hydrogen diffuses out easily. Many investigators have studied hydrogen in silicon and found that all the hydrogen escaped from silicon after heat treatment at 1000°C or higher. There is therefore an impression that hydrogen-related defects have extremely poor thermal stability.

In our experiments we used a type N <111> CZ [Czochralski process] silicon wafer. Its resistivity was 60-60 Ω-cm. The energy of the implanted hydrogen ions was 180 keV and there were two dosages: $2x10^{16}$ H^+/cm^2 and $5x10^{16}$ H^+/cm^2. After heat treatment at 600°C, a large number of bright spots appeared on the surface of the $5x10^{16}$ H^+/cm^2 sample. Optical microscopic examination revealed numerous small areas of surface fracture. At high dosage, the hydrogen ions coalesced into bubbles in their outward diffusion. Such bubbles were large in size and were near the surface; the stress of the expanding bubbles caused the surface to fracture. This phenomenon was not observed in the $2x10^{16}$ H^+/cm^2 samples after heat treating at 600°C. The samples were subsequently heat treated at 1180°C and one end was polished to an incline. After Sirtl etching and microscopic examination at 800X, defects were observed (see Figure 1).

Figures 2 and 3 (Plate 1) [not reproducible] show the etched incline plane after heat treatment at 600°C for 8 hours and 1 hour, respectively, and at 1180°C for 1 hour, followed by a two-step annealing. The thick white

vertical line marks the boundary between the surface and the incline, and the incline is to the right of the thick line.

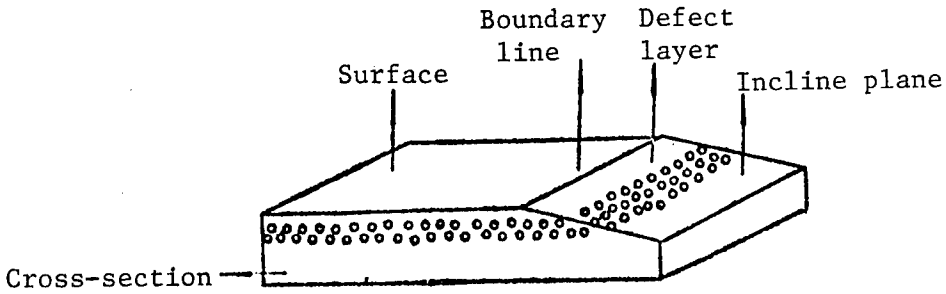

Figure 1. Schematic diagram of polished corner

Figure 2 clearly shows a band of etching pits on the inclined surface parallel to the boundary. This is the result of defect-induced preferential etching and it indicates the existence of a heavily defective layer under the surface. (The straight lines on the incline surface are polish marks.) Figure 3 shows less distinct etching pits on the incline and some etching pits on the flat surface. This shows that the defects under the surface are not severe and are located close to the surface or on the surface.

Stein[1] has done some pioneer work in hydrogen-implanted silicon. He discovered that most of the silicon-hydrogen bonds have already been broken at 600°C. Since the temperature was not very high, the outward diffusion of hydrogen was not vigorous. Many hydrogen atoms then coalesce into bubbles. These bubbles or groups of atoms have a large volume and cannot move easily in silicon. The existence of bubbles is a large defect in thermal stability, which explains Figures 2 and 3. It also seemed that after heat treating at 600°C for 1 hour, the hydrogen bubbles did not coalesce well, and some bubbles already existed on the surface. After 8 hours at 600°C, the bubbles coalesced much better and the surface was no longer pitted by the bubbles. This showed that long heat treating at 600°C helped to form large bubbles, which favored coalescing of the hydrogen bubbles. The same hydrogen-implanted silicon wafers annealed for one step at 1180°C did not show etching pits on the incline plane. This shows that in order to retain a greater quantity of hydrogen in silicon, the silicon must be treated at a lower temperature.

A high-voltage transmission electron microscope was also used in the study of hydrogen-implanted silicon. The samples were annealed at 600°C for 8 hours and then heat-treated at 1180°C for 1 hour. Figures 4 and 5 (see Plate 1) [not reproducible] show, respectively, the structure of the sample and the diffraction pattern of the crystalline lattice.

Figure 4 shows a number of voids caused by large bubbles in the sample. Figure 5 shows that the samples are polycrystalline. The presence of a large number of bubbles prevented the recovery of the single crystals and caused the sample to become polycrystalline.

One of the important applications of stable defects is defect trapping. Metal impurities have devastating effects on the devices. At high temperatures, impurities in the silicon roam about and are captured when they encounter defects. This causes the formation of defects on the back side of the silicon wafer and draws the impurities from the top surface to the back surface. If the removal of impurities is to be achieved before device fabrication, then the defects formed on the back side must have good thermal stability; otherwise, defects disappear during the high-temperature step of the fabrication process, and the trapped impurities will again be released into the device. Defects formed by ion implantation have very poor thermal stability. For lack of a better method, defects are formed on the back side of silicon after the device is fabricated. The devices are then heat-treated at moderate temperatures so that some impurities are removed without changing the structure of the device. By this time, however, some impurities have already stuck to the device and cannot be removed. The technique of ion implantation with impurity trapping has not yet been perfected. Plant 508 of the Ministry of Posts and Telecommunications manufactured the device first and then implanted hydrogen on the back of the silicon wafer. After heat treatment at 900°C, measurements showed that the quality of the device had improved.[2]

In summary, the hydrogen implant formed a stable impurity layer and permitted impurity trapping before fabricating the device. In the high temperature of manufacture, metallic impurities are tightly captured by the defects. This is very favorable for improving the quality of the device. This result holds promising prospects for the production of VLSI [devices].

References

[1] H. J. Stein, J. Electron. Mater., 4, 159 (1975).

[2] Yang Baoshan [2799 1405 1472], Proceedings of the Third National Three-Beam [ion beam, electron beam, photon beam] Conference (1984).

Infrared Digital System Developed To Detect, Analyze GaAs Defects

40080083b Beijing DIANZI KEXUE XUEKAN [JOURNAL OF ELECTRONICS] in Chinese Vol 10 No 6, Nov 88 pp 563-567

[Article by Zhang Fugui [1728 4395 6311], CAS Institute of Electronics, Beijing (manuscript received 17 December 1986, revised 5 June 1988): "Study of Morphological Distribution of Defects in GaAs Wafers by Infrared Digital Image Processing"]

[Text] Abstract: This paper describes a new method for studying defects in GaAs materials (as for example the property of absorbing EL2): we pass a 1.1-1.5-micron near-infrared beam through a section of GaAs material that is 4-8 mm thick and 50 mm in diameter. Then we use the Toshiba 8844 infrared pickup camera to capture the images, directly sending them to DATASUD, a computer image processing system. Images of non-uniform defects in the materials, that is, the distribution structural form (crisscrossed, latticed, globular, etc.) of the defects in the materials (EL2, dislocation, etc.) along a cross section can then be observed on screen. We provide in this paper some results obtained from the ZHIMAG (ZHang IMAGe) image processing software package designed for studying this kind of material, and from its application. ZHIMAG is also suitable for use in image processing of other types.

I. Introduction

There are two kinds of defects in semiconductor GaAs materials: one is the lattice dislocation defect; and the other is a defect from chemical impurities [1]. To meet the demands of uniformity in the substrates of IC's, it is extremely important to reduce and control fluctuations in the physical properties of the substrate. This is especially true for changes in substrate resistance brought on by changes in EL2 centers, which will directly affect the performance of IC's. There are already several methods for studying defects in GaAs materials:

(1) The dislocation counting method [2]. This is a slow method (often requiring several hours), and also rather tedious. The Sumitomo Company is using this method to set up a computer-aided system for automatic analysis and counting [3]. (2) The x-ray topology method [4]. Using this method, dislocation images can be obtained from x-ray sources or from

synchroaccelerators, but the materials used cannot be thicker than 1 mm. Because manufactured substrate for GaAs materials is 4-5 mm thick, this restricts the direct application of this technique, for one must first slice the material, then polish it. (3) The photoelectric measurement method, first used by M. Bonnet [5]. The basic method is to study the nonuniform distribution of the electrical properties of materials by measuring the conductivity and Hall effects of materials. Its deficiency is in its long measurement times.

The infrared transmitted imaging method proposed herein differs from the methods just described in not requiring the polishing or slicing of materials, and in its direct acquisition of infrared images. These images are composed of defects in the materials, and include all defects within the range 1.1-1.5 microns that can be detected by transducers. By using infrared laser sources we can quantitatively estimate EL2 at center densities and thicknesses. Because relative values for image gradation are indirectly related to EL2, it is possible to use them to study the "quenching" phenomenon of EL2 [6].

II. The Infrared Transmitted Imaging Method

The basic structure of the infrared transmitted imaging method is as follows: We pass a 1.1-1.5-micron near-infrared beam through a piece of GaAs (GaAs-SILEC) that is 4-8 mm thick and 50 mm in diameter, capture the image with a Toshiba 8844 pickup camera, then enter this into DATASUD, a computer image processing system. An image of nonuniform defects in the material is then displayed on a screen. By observation and analysis of the images, we can study the structural formation (crisscross, latticed, globular, etc.) of the distribution within a cross section of defects (EL2, dislocation, etc.) in materials.

Due to the effects of various kinds of interference in optical and electronic systems (such as thermal noise, the quality of photoelectric sensors), the quality of the image that is directly obtained in that manner is flawed. An infrared digital image processing technique was used to improve the quality of the image and to do quantitative analysis of the defects in the materials, which improves the signal-to-noise ratio and enhances image contrast. Following is a brief description of the infrared image collection devices and experimental conditions, and an introduction to the author's ZHIMAG image processing software package for studying the design of these materials. Finally, some results of application, as well as analyses thereof, are presented.

III. Experimental Apparatus

Processing devices for the gathering and analysis of infrared images of defects in GaAs materials are shown in Figure 1.

An infrared light source is used to generate a near-infrared light beam for excitation and testing. It consists of a 100-250-W halogen lamp and a low-voltage DC power source. The collimated light beam generated after prism focusing of the near-infrared beam (wavelength of 1.1-1.5 microns) passes

through a GaAs-SILEC cross-section 50 mm in diameter and 5 mm thick. The image of the defects is captured by the infrared pickup camera, a Toshiba 8844, and after it is digitized it is entered into the DATASUD image processor. The resolution of the image is 512 X 512 pixels, with 8-bit gradation. Finally, the ZHIMAG software package is used to display, process, and analyze it.

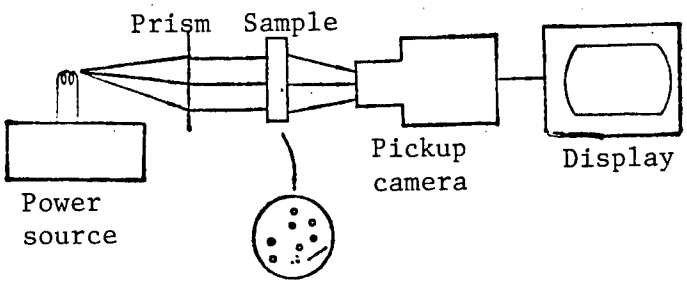

Figure 1. Processing devices for the gathering and analysis of infrared images of defects in GaAs materials

IV. A Description of the ZHIMAG Software Package

(1) Features of the ZHIMAG

(a) It uses a menu display for all image processing functions; (b) processing functions are selected by keyboard, from which they are immediately executed; (c) there is interactive selection of variable parameters; (d) control is by interrupt requests during the execution process; (e) there is an interactive process of execution with choice of multiple functions; (f) there is an option for batch file processing and data revision, and an interrupt option via keyboard or routines, with data entry by keyboard and output of the results.

(2) The Starting Process

For ease of use and direct entry into the ZHIMAG software package, a management file called a "kernel" can be automatically installed in the system upon boot-up.

(3) The Structure of the ZHIMAG System

The ZHIMAG is a looping structure that revolves around the management file "kernel," and this kernel is linked with the hardware components through the DOS system. In addition, it can open all files that constitute ZHIMAG.

(4) The ZHIMAG "Menu"

The "menu" enters all image-processing functions in a list, which is also displayed on the screen. Each image-processing function is supported by an ASCII code for selection at the keyboard. There is an automatic return to the "menu" after execution of a file.

(5) The ZHIMAG Processing Functions

The ZHIMAG processing subroutines were written in Motorola 68000 machine language. Users may select the same functions, but not the same application algorithm subroutine. ZHIMAG also includes special algorithm subroutines for use in the image processing of defects in GaAs materials.

In addition to the probability algorithm subroutines for calculating image density, we might also list the following processing functions: (a) pseudo-color processing; (b) enhancement of contrast; (c) spatial filtering; (d) image fast Fourier transforms and their analysis; (e) image segmentation; (f) image recognition; (g) boundary detection and tracing; (h) detection of image textural structure; (i) image analysis; and (j) analysis of the distribution of defects in GaAs materials.

(6) The ZHIMAG Image-Processing File Library Structure and Its Automatic Processing Procedure

After the image obtained with the pickup camera is digitized, it is entered into video RAM. The entire image-processing procedure may progress sequentially or can proceed concurrently. After the processing procedure is completed, all results can be sent to a television monitor for display or they can be recorded on disk.

V. Example of ZHIMAG Applications

Some image examples obtained during use of ZHIMAG are here given, as well as an analysis of some of the results.

[Translator's note: Figures 2-7 are reproductions of photographs and cannot be further reproduced in sufficient detail to be useful. The captions follow:]

Figure 2. Infrared transmitted image of GaAs material

Figure 3. Image of a homogenized histogram

Figure 4. A boundary-enhanced image

Figure 5. The image of Figure 2 enlarged 3X

Figure 6. An image of boundary detection using the differential method

Figure 7. An image after boundary tracing

Figure 2 shows the original infrared transmitted image in 512 X 512 pixels. We can observe from this image the lattice defects distributed throughout the entire image, and can see as well the EDZ defects in the bright areas and the "crisscross" defects at the center of the image.

Figure 3 is an image of a homogenized histogram. Expansion of the grey scale has produced an improvement in the contrast.

To make the lattice structure even clearer, we must enhance the original image, which is to say, after boundary detection we select an appropriate threshold value and then keep or transform each point in the image. In Figure 4 we compare the images both before and after enhancement, where the enhanced image is above the horizontal line and the original image is below it.

Figure 5 shows the original image enlarged 3X. We can more easily see the lattice defects (the darker portions) and the EDZ defects (the lighter portions). From this we can derive the following conclusion: the lattice corresponds to the EL2 high absorption areas, which surround the EDZ area where EL2 absorption is low. This conclusion conforms to the results obtained by Brozel [7] and Kikuta [8].

Figure 6 shows a boundary detection image obtained through the differential method. We used a differential algorithm on eight adjacent points in a 3 X 3 window. We may say that boundary detection can not only observe defects, but it can also segment and isolate different defects: for example, lattice defects (the bright areas) are composed of a series of enclosed curves, so that it surrounds the EDZ defects (the darker areas); in contrast, if the lattice is open, the line defects in that case (the darker areas) are SST and CST defects.

Figure 7 is a boundary trace image. We can see from Figure 6 that boundary detection can generate considerable boundary thickness. To keep boundaries to only one pixel in thickness, which is more accurate, we must use the boundary tracing algorithm.

VI. Conclusions

We have established by this work an image-processing software package called ZHIMAG, and have for the first time used it in the research of GaAs. There are several advantages for this technique:

(1) For industry this technique is nondestructive, and defects in materials can be detected and tested nearly in real time. This will allow improvement in the extraction technologies for materials, consequently realizing optimization of the manufacturing process; and (2) for the research of defects, the infrared transmitted images of GaAs materials are related to EL2 defects, which has a great effect on the electrical characteristics of materials. We can thereby study the reasons for manufacturing defects and device characteristics.

With the development and applications of ZHIMAG we have proved that this software package can automatically process images, can quantitatively analyze them, and can study by shape. It is also appropriate for any other kind of image processing.

References

1. Fugui Zhang, Morphologie des Distributions de Defauts Dans GaAs-SI par Imagerie Infra-Rouge Numerique, These de doctorat, Montpellier, France, 1986.

2. J. Logowski, et al., Semi-insulating III-V Materials, Conf., Kahneeta, U.S.A., 1984, 130-135.

3. N. Yoyoda, et al., Defect Recognition and Image Processing in III-V Compounds, Conf., La Grande Motte, France, 1985, 30-34.

4. M. P. Scott, Defect Recognition and Image Processing in III-V Compounds, Conf., La Grande Motte, France, 1985, 80-86.

5. B. Goutheraux, Les Mesures de Conductivite Electrique en Cartographie, These Paris VI, 1985, 120-140.

6. M. Asgarinia, L'etude Experimentals des Defauts Dans GaAs-SI, Report DEA, Montpellier, France, 1985, 50-56.

7. M. R. Brozel, et al., Three-Dimensional Image of the Distribution of 1 μm Absorption in Undoped SI-LEC GaAs and Related Compounds, Biarritz, France, 1984, 50-57.

8. T. Kikuta, et al., Microscopic Distribution of Deep and Shallow Levels Around Dislocations in Undoped SI-GaAs, GaAs and Related Compounds, Biarritz, France, 1984, 72-76.

Investigation of Structure, Electrical Properties of Non-Crystalline Ionic Conductors in Li_2O-Nb_2O_5-SiO_2 System

40090036a Beijing WULI XUEBAO [ACTA PHYSICA SINICA] in Chinese Vol 37 No 11, Nov 88 pp 1741-1751

[English abstract of article by Cui Wanqiu [1508 8001 4428], et al., of Wuhan University of Technology]

[Text] IR, WAXS and EXAFS are used to study the structure of the non-crystalline ionic conductors in the Li_2O-Nb_2O_5-SiO_2 system. From the analysis, it is known that Nb^{5+} ions exist mainly as (NbO_6) in the non-crystalline network. The non-crystalline structure varies with the Nb_2O_5 content. It consists of polycyclics formed by shared side (NbO_6) and (SiO_4) when the Nb_2O_5 content is low, and of shared apex (NbO_6) when the Nb_2O_5 content is higher. The results of conductivity measurement are used to study the relationships of the structure and electrical properties. The non-crystalline material with Li_2O of about 0.45 and Nb_2O_5 of 0.3 has the highest conductivity.

References

1. Glass, A.M., Lines, M.E., Nassau, K, Shiever, J.W., APPL PHYS LETT, Vol 3, 1977 p 249; Glass, A.M., Nassau, K., Negran, T.J., J APPL PHYS, Vol 49, 1978 p 4808.
2. Jazouli, A.E., Brochu, R., Viala, J.C., ANN CHIM FR, Vol 7, 1982 p 285.
3. Tatsumisago, M., Hamada, A., Minami, T., Tanaka, M., J NON-CRYST SOLIDS, Vol 56, 1983 p 423.
4. Yasui, I., Ohta, E., Hasegana, H., Imaoka, M., J NON-CRYST SOLIDS, Vol 52, 1982 p 283.
5. Cui Wanqiu, et al., article pending publication.
6. Xu Shunsheng, "Advances in X-ray Diffraction," Science Press, Beijing, 1986 pp 101-142.
7. Lu Kunquan, WULI XUEZHAN, Vol 5 No 1, 1985 p 125.
8. Nagatani, K., et al., KUGYO KYOKAISHI, Vol 88 No 5, 1980 p 271.
9. Abrahams, S.C., Reddy, J.M., Bernstein, J.L., J PHYS CHEM SOLIDS, Vol 27, 1966 p 977.
10. Catehouse, B.M., ACTA CRYST, Vol 17, 1964 p 1545.
11. (Jingerui), W.D., et al., "Ceramics Guide," China Architectural Industry Press, Beijing, 1982 p 55.

Analysis of Dimensionality of $Y_1Ba_2Cu_3O_7$ Crystal Lattices

40090036f Beijing WULI XUEBAO [ACTA PHYSICA SINICA] in Chinese Vol 37 No 11, Nov 88 pp 1829-1836

[English abstract of article by Shen Shunqing [3088 7311 3237], et al., of the Department of Physics, Fudan University, Shanghai]

[Text] By using the transforming generating function technique, the authors have calculated the escape probability of random walk on the $Y_1Ba_2Cu_3O_7$ lattice and have obtained its asymptotic expression in the weak coupling limit. A comparison of the expressions of the escape probability and the dimensions in the isotropic model yields a relationship between the dimensionality and the layer coupling in $Y_1Ba_2Cu_3O_7$. Theoretical calculation indicates $Y_1Ba_2Cu_3O_7$ is very close to a three-dimensional system.

References

1. Bednorz, J.G., Muller, K.A., Z PHYS, Vol 64, 1986 p 189.
2. Chu, C.W., et al., PHYS REV LETT, Vol 58, 1987, p 405; Zhao Zhongxian, et al., SCIENCE BULLETIN, Vol 32, 1987 p 412.
3. Yu, J., Freeman, A.J., Xu, J.H., PHYS REV LETT, Vol 38, 1987 p 1035.
4. Mattheiss, L.F., PHYS REV LETT, Vol 58, 1987 p 1028.
5. Hohenberg, P., PHYS REV, Vol 158, 1967 p 383.
6. Cava, R.J., et al., PHYS REV LETT, Vol 58, 1987 p 1676.
7. Schuller, I.K., et al., INTER J OF MOD PHYS, Vol B1, 1987 p 821.
8. Montrol, E.W., Weiss, G.H., J MATH PHYS, Vol 6, 1965 p 107.
9. Zheng Dafang, et al., ACTA PHYSICA SINICA, Nov 88.
10. Feller, W., "An Introduction to Probability Theory and Its Applications," Vol 1, 2nd ed, John Wiley and Sons, New York, 1957.
11. Barber, M.N., Ninham, B.W., "Random and Restricted Walks," Gordon and Breach, New York, 1970.
12. Tozer, S.W., et al., PHYS REV LETT, Vol 59, 1987 p 1768.
13. Bedell, K.S., Pines, D., PHYS REV, Vol B37, 1988 p 3730.

Structural Instability in High-T_c Superconductor $La_{2-x}Ba_xCuO_4$

40090038a Beijing DIWEN WULI XUEBAO [CHINESE JOURNAL OF LOW TEMPERATURE PHYSICS] in Chinese Vol 10 No 4, Dec 88 pp 253-256

[English abstract of article by Shuai Zhigang [1596 1807 0474], et al., of the Department of Physics, Fudan University, Shanghai]

[Text] Based on the two-dimensional tight-binding model Hamiltonian quantity including electron-phonon interaction, the Peierls instability of the Cu-O layer in the high-T_c superconductor BaLaCuO is studied. It is shown that La_2CuO_4 can be in the semiconductor ground state with an energy gap of 0.6 eV. The oxygen displacement is 0.07 Å. A charge transfer (ΔQ = 0.26 e) exists between the Cu atoms. Regarding the doping of the divalent elements Ba and Sr, the details involved in suppressing instability by lowering the Fermi surface are investigated.

References

1. Bednorz, J.G., Muller, K.A., Z PHYS, Vol B64, 1986 p 189.
2. Takagi, H., et al., to be published.
3. Sato, M., et al., SOLID STATE COMMUN, Vol 62, 1987 p 85.
4. Mattheiss, L.F., PHYS REV LETT, Vol 58, 1987 p 1028.
5. Yu, J., Freeman, A.J., Xu, J., PHYS REV LETT, Vol 58, 1987 p 1035.
6. Jorgensen, J.D., et al., PHYS REV LETT, Vol 58, 1987 p 1024.
7. Ye Ling, et al., private communication.
8. Fu, C.L., Freeman, A.J., Sub. to PHYS REV LETT, 1987.
9. Sinha, S.K., Harmon, B.N., PHYS REV LETT, Vol 35, 1975 p 1515.
10. Tanaka, S., et al., Preprint.
11. Freeman, A.J., Yu, J., Fu, C.L., Sub. to PHYS REV, 1987.

Far-Infrared Reflection Spectra of High-T_c Superconductor $YBa_2Cu_3O_{9-\delta}$

40090038b Beijing DIWEN WULI XUEBAO [CHINESE JOURNAL OF LOW TEMPERATURE PHYSICS] in Chinese Vol 10 No 4, Dec 88 pp 267-270

[English abstract of article by Ye Hongjuan [0673 4767 1227], et al., of the Infrared Physics Laboratory, Shanghai Institute of Technical Physics, Chinese Academy of Sciences; Miao Baicai [4924 2672 2624], et al., of the Physics Department, Fudan University, Shanghai]

[Text] The far-infrared reflection spectra of the high-T_c superconductor $YBa_2Cu_3O_{9-\delta}$ (T_c = 90K) have been measured in the temperature range of 4.2 - 200K. The authors have observed six distinct structures (S_1, S_2, N_1, N_2, N_3 and N_4) in the frequency range of 30-360 cm^{-1}. S_1 and S_2 appear only in the superconducting state, while the other four exist in both superconducting and normal states. According to the temperature effect, the authors believe that S_1 and S_2 are associated with the superconducting energy gap, while the structures N_1 to N_4 are the TO phonon reflection bands.

References

1. Bednorz, J.G., Müller, K.A., Z PHYS, Vol B64, 1986 p 189.
2. Wu, M.K., et al., PHYS REV LETT, Vol 58, 1987 p 908.
3. Zhao, Z.X., et al., KEXUE TONGBAO, No 6, 1987.
4. Walter, U., et al., PHYS REV, Vol B35, 1987 p 5329.
5. Schlesinger, Z., et al., PHYS REV, Vol B35, 1987 p 5334.
6. Sulewski, P., et al., PHYS REV, Vol B35, 1987 p 5330.
7. Kirtley, J., et al., PHYS REV, Vol B (to be published).
8. Genzel, L., et al., SOLID STATE COMMUN (to be published).
9. Moreland, J., Clark, A., Ku, H., preprint.

Investigation of Instability of Oxide Superconductors $MBa_2Cu_3O_{7-y}$

40090038c Beijing DIWEN WULI XUEBAO [CHINESE JOURNAL OF LOW TEMPERATURE PHYSICS] in Chinese Vol 10 No 4, Dec 88 pp 284-286

[English abstract of article by Cao Liezhao [2580 3525 0340], et al., of the Department of Physics, University of Science and Technology of China, Hefei]

[Text] In this paper, the instability of the oxide superconductor samples $GdBa_2Cu_3O_{7-y}$ and $EuBa_2Cu_3O_{7-y}$, which have been stored in the air for a long time, is studied. It is pointed out that the decay of their superconducting properties is caused by their decomposing into $BaCO_3$, CuO and Gd or Eu oxide due to their reaction with water vapor and CO_2 gas in the air.

References

1. Cao Liezhao, et al., CHINESE JOURNAL OF LOW TEMPERATURE PHYSICS, Vol 9, 1987 p 248.

Research on Y-Ba-Cu-O Superconducting Thin Films at Liquid Nitrogen Temperatures

40090038d Beijing DIWEN WULI XUEBAO [CHINESE JOURNAL OF LOW TEMPERATURE PHYSICS] in Chinese Vol 10 No 4, Dec 88 pp 287-291

[English abstract of article by Li Yuan [2621 0337], et al., of the Department of Information Physics, Nanjing University; Zhang Shiyuan [1728 0013 6678] of the Department of Physics, Nanjing University; Fan Depei [5400 1795 1014] of the Solid State Microstructure Laboratory, Nanjing University; Du Dean [2629 1795 1344], et al., of the Center of Materials Analysis, Nanjing University]

[Text] The Y-Ba-Cu-O superconducting thin films on several kinds of substrates of single crystal ZrO_2, YSZ and polycrystalline $SrTiO_3$ have been prepared successfully by means of rf reactive magnetron sputtering. The zero resistance temperature obtained is 81 K. The thickness of the films is about 1-2 μm.

In this paper, the composition of the films, the substrates, R-T curves, X-ray diffraction patterns and the heat treatment process of the films are described.

References

1. Bednorz, J.G., Muller, K.A., Z PHYS, Vol B64, 1986 p 189.
2. Wu, M.K., et al., PHYS REV LETT, Vol 58, 1987 p 908.
3. Zhao, Z.X., et al., KEXUE TONGBAO, Vol 32, 1987 p 412.
4. Zheng Jiaqi, et al., "Proceedings of the Beijing International Workshop on High Temperature Superconductivity," Beijing, 29 June - 1 July 1987.
5. Zhao, B.R., et al., CHINESE PHYS LETT, Vol 4 No 6, 1987.
6. Bao, Z.R., et al., KEXUE TONGBAO, Vol 32, 1987 p 1291.

Weak-Link Characteristics in High T_c Oxide Superconductivity

40090038e Beijing DIWEN WULI XUEBAO [CHINESE JOURNAL OF LOW TEMPERATURE PHYSICS] in Chinese Vol 10 No 4, Dec 88 pp 292-297

[English abstract of article by Cao Xiaowen [2580 2400 2429], et al., of the Institute of Plasma Physics, Chinese Academy of Sciences, Hefei]

[Text] The weak-link properties in high T_c oxide bulk superconductors have been characterized by various electromagnetic measurements, and their formation mechanism has been studied. The weak-link properties and the low j_c (B) and its anomalous behavior, as well as the Josephson effect on the large bridge, have been explained by a "soft" sponge model. The question involving how to raise the critical current density of oxide bulk superconductors is also discussed. It is concluded that the critical current density of $Y_1Ba_2Cu_3O_{7-\delta}$ bulk superconductors is mainly restricted by the Josephson weak links.

References

1. Bednorz, J.G., Müller, K.A., Z PHYSIK B, Vol 64, 1986 p 189.
2. Zhao Zhongxian, Chen Liquan, Yang Qiansheng, et al., KEXUE TONGBAO, Vol 32, 1987 p 412.
3. Chu, C.W., Hor, P.H., Meng, R.L., et al., PHYS REV LETT, Vol 58, 1987 p 405.
4. Wen Haihu, et al., International Conference on High T_c Superconductivity, Beijing, 1987; Cao Xiaowen, et al., unpublished.
5. Clarke, D.R., International Conference on High T_c Superconductivity, Beijing, 1987.
6. Cao Xiaowen, et al., SOLID STATE COMMUNICATIONS, submitted.
7. Chandhari, P., et al., preprint.
8. Dinger, T.R., et al., PHYS REV LETT, submitted.
9. Mastoo, J., PROC APPLIED SUPERCONDUCTIVITY, 535, 1972.
10. Mendelssohn, K., Moore, J.R., PROC ROY SOC, Vol A151, 1935 p 334, and Vol A152, 1935 p 34.
11. Cava, R.J., Batlogg, B., van Dover, B., et al., PHYS REV LETT, Vol 58, 1987 p 1676.
12. Engler, E.M., et al., preprint (1987).

13. Zhang Yuheng, et al., CHINESE JOURNAL OF LOW TEMPERATURE PHYSICS, Vol 8, 1986 p 298.
14. Fan Zhangxin, et al., All-China Symposium on Low Temperature Physical Properties, 1987.
15. Cao Xiaowen, et al., unpublished manuscript.

Influence of Oxygen Deficiency on Thermoelectric Power in Mixed Phase YBaCuO System

40090038f Beijing DIWEN WULI XUEBAO [CHINESE JOURNAL OF LOW TEMPERATURE PHYSICS] in Chinese Vol 10 No 4, Dec 88 pp 298-299

[English abstract of article by Ruan Yaozhong [7086 5069 6988], et al., of the Department of Physics, University of Science and Technology of China, Hefei]

[Text] The temperature dependence of thermoelectric power in a mixed-phase YBaCuO system has been measured. The results show that the thermoelectric power is negative at high temperatures and positive at low temperatures. It is suggested that the sample is influence predominantly by electrons at high temperatures and by holes at low temperatures, and the hole conduction behavior is directly correlated with the oxygen deficiency, i.e., the temperature region conducted by holes is wider when the sample has a greater amount of and more disordered oxygen vacancies.

References

1. Ruan Yaozhong, et al., CHINESE PHYS LETT (to be published).
2. Hundley, M.F., et al., (to be published).
3. Ruan Yaozhong, et al., (submitted to SOLID STATE COMMUNICATIONS).
4. Hettinger, J.D., et al., (to be published).
5. Wang, Z.Z., et al., (to be published).
6. Ruan Huizhong, et al., LOW TEMPERATURE PHYSICS (publication pending).
7. Jorgonsen, J.D., et al., (submitted to PHYS REV).

Factors Influencing Critical Current of Y-Ba-Cu-O Superconductor

40090038g Beijing DIWEN WULI XUEBAO [CHINESE JOURNAL OF LOW TEMPERATURE PHYSICS] in Chinese Vol 10 No 4, Dec 88 pp 300-305

[English abstract of article by Shi Kexin [0670 0668 0207], et al., of the Department of Physics and Institute of Solid State Physics, Nanjing University]

[Text] The effects of doping V on the superconducting oxide $YBa_2Cu_{3-x}V_xO_y$ have been studied. It is found that when $x \leq 0.6$, there is a decrease in the superconducting phase ratio of the volume and the grain size and an increase in J_c, the mass density and hardness of the samples. On the other hand, the sample synthesis conditions, critical temperature T_c and the superconducting phase structure are not sensitive to the x values. These suggest that the impurity V stays mainly in the grain boundaries and can improve the connection between the grains. In certain cases, it is more important to improve the grain connection than to increase the superconducting phase ratio.

References

1. Yu Zheng, et al., "Proceedings of the Beijing International Workshop on High Temperature Superconductivity (Supplement)," p 33.

Superconductivity on $GdBa_2Cu_3O_{7-\delta}$ Large Single Crystal

40090038h Beijing DIWEN WULI XUEBAO [CHINESE JOURNAL OF LOW TEMPERATURE PHYSICS] in Chinese Vol 10 No 4, Dec 88 pp 306-308

[English abstract of article by Fang Minghu [2455 2494 5706], et al., of the Department of Physics and the Department of Applied Chemistry, University of Science and Technology of China, Hefei]

[Text] In this paper, a series of single crystal samples with a maximum size of 7 x 3 x 2 mm^3 has been prepared with the fluxed method by substituting Gd for Y in full. The results of structural analysis show that they are orthorhombic 1-2-3 phase single crystals with space group P_{mmm}. The lattice parameters of the samples without any treatment are a = 3.88 A, b = 3.82 A and c = 11.68 A. The samples' superconductivity, which has been much improved since they were annealed in O_2, is discussed.

References

1. Zhang Qirui, et al., CHINESE JOURNAL OF LOW TEMPERATURE PHYSICS, Vol 9, 1987 p 245.
2. Sun Dunming, JOURNAL OF THE UNIVERSITY OF SCIENCE AND TECHNOLOGY OF CHINA, No 1, 1988.
3. Jorgensen, J.D., et al., submitted to PHYS REV LETT.
4. Fang Minghu, et al., submitted to SOLID STATE COMMUNICATIONS.
5. Brown, S.E., et al., to be submitted.

Effect of Ion Implantation on Superconductive Transition Temperature of MoN_x Thin Films

40090038i Beijing DIWEN WULI XUEBAO [CHINESE JOURNAL OF LOW TEMPERATURE PHYSICS] in Chinese Vol 10 No 4, Dec 88 pp 329-332

[English abstract of article by Che Yunyi [6508 7301 1837], et al., of the Department of Physics, Northeast University of Technology, Shenyang]

[Text] Using a combined technique of ion implantation and sputtering, superconductive thin films with a single phase of γ-Mo_2N and mixed phase of γ-Mo_2N and β-Mo_2N and γ-Mo_2N and δ-MoN have been prepared. The results show that the increase in T_c of the MoN_x thin films is limited by increasing the ion implantation dose and energy. However, the change in ion implantation methods produces an immediate effect on increasing the T_c of the films. By means of multi-layer films and the multi-ion implantation method, the maximum T_c of the films is 11.0 K.

References

1. Pictell, et al., PHYSICA, Vol 107B, 1981 p 667.
2. Ihara, H., et al., PHYS REV, Vol B32, 1985 p 1816.
3. Sekula, S.T., et al., J APPL PHYS, Vol 54, 1983 p 6517.
4. Linker, G., et al., J PHYS, Vol F14, 1985 p L115.
5. Lindhard, J., et al., MAT FYS MEDD, Vol 10, 1963 p 33.
6. Ihara, H., FUNCTIONAL MATERIALS, Vol 33, 1985 p 6.

Present Status, Future Prospects for China's Radio, Television Broadcast Technology

40080075 Shanghai DIANZI JISHU [ELECTRONIC TECHNOLOGY] in Chinese Vol 15 No 10, Oct 88 pp 2-5

[Article by Liu Songying [0491 2646 5391]]

[Excerpts] [Passage omitted] Today, the degree of proliferation and sophistication of a nation's radio and television broadcast technology has become a measure of its level of industrial development. In recent years, China's radio and television industry has been growing at a rapid pace. At the end of 1987, China had 386 radio stations with 624 medium- and short-wave transmitters; they reach 70.5 percent of the population. It also had 366 television stations with 721 high-power (greater than 1 kW) transmitters and relay towers and thousands of low-power transmitters; they reach 73 percent of the population. [passage omitted]

Wireless Broadcasting

Wireless broadcasting is a broadcasting technique which uses radio waves to transmit radio and television programs to the users. Such a system generally has three major components: the radio and television broadcast center, the transmission network, and the program distribution network. [passage omitted] At present, China uses the following types of wireless broadcasting: medium-wave amplitude modulation (AM) broadcasting, short-wave (SW) broadcasting, ultra-short-wave frequency modulation (FM) broadcasting, and meter-wave and decimeter-wave television broadcasting.

Medium-wave AM broadcasting is primarily used for domestic broadcasting; it covers the frequency range of 526.5-1605.5 kHz, with 120 bands each separated by 9 kHz. Since the 1960's, the number of medium-wave stations and the associated transmitter power have been increasing both in this country and abroad, producing increasingly higher levels of background interference. Although the transmitter power of domestic medium-wave stations has also increased, the receiving range has been

decreasing. In order to improve the quality of reception, a synchronized broadcasting technique has been used in China's medium-wave AM broadcasting starting 23 November 1978. With this technique, the same program is broadcast by two or more stations on the same frequency at different locations to provide relief to the problem of frequency crowding and interferences. This technique requires the use of single-frequency transmitters with frequency deviation less than 0.015 Hz in order to avoid interference and ensure quality of broadcast. To achieve such high-frequency accuracy, we use the synchronizing signal (15625 kHz) of the Central Television Station as the frequency standard for the whole nation. In the medium-wave synchronous broadcast network, each program of the Central Station uses 6 frequencies, and each program at the provincial or regional level uses 3 frequencies.

SW broadcasting relies on ionospheric reflection for transmitting radio waves; it covers a frequency band primarily reserved for foreign broadcasting. It is used to transmit program signals from the Central Station to the regional stations as well as to the remote regions. Generally, SW broadcasting uses high-power transmitters and directional, high-gain antennas in order to boost the field strength at the receivers. In recent years, Chinese-built high-power rotating SW antennas have been used by a number of stations to improve the utilization efficiency of transmitters; with a rotating antenna, each transmitter can broadcast in any direction. In the past, SW broadcasting had always used plate amplitude modulation; but more recently, China has begun to use the PDM (pulse duration modulation) technique, which provides higher overall efficiency and better electro-acoustic performance. We are also actively studying the new PSM (pulse step modulation) technique. The frequency band used in China's SW broadcasting is 2.3-26.1 MHz.

Ultra-short-wave FM broadcasting has many advantages including better electro-acoustic performance, superior tone quality, stronger interference-rejection capability, and wider service range. In developed nations, it is used extensively as a means for domestic broadcasting. China began using FM broadcasting in 1959, and since 1980, FM broadcasts have been received over most parts of the country. Eventually it will become China's primary mode of domestic broadcasting. In planning the development of an FM broadcasting network, our goal is to provide 4-5 different FM programs in most towns and villages, and possibly more programs in large cities under state jurisdiction. The frequency band used for FM broadcasting in this country is 87-108 MHz with a total of 210 channels each separated by 100 kHz.

In recent years, many radio stations in this country have started FM stereo broadcasting, which simultaneously emits sound signals in both left and right channels to give the listener a three-dimensional effect when receiving sound waves from two separate speakers. Based on a comparison of stereo-sound production standards used in other countries,

we have adopted the pilot frequency standard for China's stereo broadcasting.

In developing the FM broadcasting network, we will also actively promote the dual-programming technique, in which an FM transmitter can simultaneously broadcast two separate programs through a main channel and a secondary channel; the carrier frequency of the secondary channel is 67 kHz. A conventional FM receiver can only listen to programs on the main channel; however, a receiver with auxiliary equipment can select programs from either channel. By utilizing dual-programming techniques, one can increase the channel utilization rate, and provide an additional program without extra equipment. Furthermore, in regions where there is a concentration of minority ethnic groups speaking special dialects, dual-programming can be used to broadcast programs in different languages.

China's television broadcasting industry began in the 1950's. On 1 May 1958, the Central Television Station broadcast its first 2-channel black-and-white television program in the capital area; on 2 September regular broadcasting began. On 1 October 1973, the Central Television Station broadcast its first 8-channel color television program in the Beijing area; since that time, China's TV broadcasting has gradually converted from black-and-white to color. In 1982, the state formally approved the use of the PAL-D system as the standard for China's color TV broadcasting.

China's TV broadcasting is divided into two frequency bands: the meter-wave band (48.5-84 MHz; 167-223 MHz) and decimeter-wave band (470-566 MHz; 606-958 MHz). The meter-wave band has 11 channels, the decimeter-wave band has 68 channels; each channel occupies a bandwidth of 8 MHz. The 11 meter-wave channels and 36 of the decimeter-wave channels (13-48) are used exclusively for TV broadcasting; the other 20 channels are shared with other applications. The TV video signals use a residual side-band AM format with a bandwidth of 6 MHz; the accompanying audio signals use an FM format with a carrier frequency of 6.5 MHz. The TV network in this country is designed to take advantage of natural terrain to coordinate the locations of the trunk stations and the relay stations, and to combine transmitters of different power levels. In order to increase coverage, a large number of low-power differential relays have been installed around the trunk stations and relay stations. According to current plans, by the end of this century, 95 percent of the population in this country will have access to 4 simultaneous TV programs, and people in major cities and capitals will have access to 5 simultaneous programs.

The methods of transmission used in this country include: microwave relays, [coaxial] cable, optical cable, and communication satellites.

In the case of microwave-relay transmission, the TV signal is modulated onto a microwave carrier (300 MHz-300 GHz) using either analog or

digital format, and transmitted over the relay network. Since 1971, microwave has been used to transmit programs of the Central Television Station; since 1974, programs of the Central People's Broadcasting Station have also been transmitted via microwave trunk lines. Today, it is possible not only to transmit programs from Beijing to the capitals of different provinces (with the exception of Xinjiang and Tibet provinces) and cities under state control, but also to receive programs from these locations. This capability facilitates business transactions and the exchange of news photos. In the early 1980's, China had developed dedicated microwave equipment for the transmission of television programs, and the provinces and autonomous regions also began construction of microwave TV networks. By the end of 1987, a total of 37,362 km of dedicated microwave lines had been completed to connect the various nodal stations with the provincial TV broadcasting center; as a result, the quality of the TV network was significantly improved. The next step would be to increase the number of TV programs broadcast from the provincial capitals and to construct two-way transmission facilities.

Satellite TV broadcasting systems, unlike ground-based broadcast systems, are not affected by mountains or buildings; also, by using wide-band FM techniques, it is possible to achieve high-resolution pictures with low distortion and no ghost images. [passage omitted] There are two types of ground reception systems: individual reception and centralized reception. In the case of individual reception, a private television set equipped with a satellite receiver and a small antenna (50 cm) can directly receive satellite-transmitted programs; in the case of centralized reception, the transponded signals are received by a ground station, which in turn re-transmits the signals to the users within a certain radius or sends the signals to a cable TV system. Currently, China's satellite broadcasting system primarily uses centralized reception; it is expected to be converted to individual reception by the year 2000. The communications satellite launched in 1988 (at 87.5 degrees east longitude, frequency band 3.7-42 GHz) can broadcast the two regular programs of the Central Television Station to the whole country; the two educational programs of the Central Station will be broadcast via the leased INTELSAT-V satellite (at 66 degrees east longitude). At the end of 1987, there were already over 4,600 satellite ground stations in this country.

The microwave relay system and satellite communications system are suitable for long-distance transmission of TV programs, whereas [coaxial] cables and optical cables are used for short-distance transmission. Optical-cable communication uses light waves to transmit information in optical fibers. [passage omitted] These features allow the signal quality to be better preserved in a television transmission system. Therefore, since the early 1980's, optical cable has been used in the Central Television Station and in a number of provincial and municipal stations for short-distance transmission (from the program

production center to the transmitting station); the future trend is clearly to replace [coaxial] cables with optical cables.

Wired Broadcasting

The large-scale development of a wired broadcasting system in China is designed not only to satisfy the broadcast needs of the general public but also to serve as a propaganda tool. At the end of 1984, an independent, nationwide wired broadcast network had been established. Wired broadcasting generally means the direct transmission of broadcast signals to user receiving equipment via a regional distribution network which consists of metallic wires or optical fibers. Currently, there are three different wired broadcasting systems in this country: 1. the Central Station's audio-frequency transmission system with centralized amplification. In this system, the Central Station performs the dual functions of program production and broadcasting, as well as power amplification and distribution. This system is primarily used in high-density regions such as urban areas and large industrial and mining complexes. 2. A second-level system which uses mixed audio-frequency and high-frequency transmission and distributed amplification. It is centered at the county station with branch stations located in towns and villages. Because this system suffers low transmission loss and is easy to manage, it is used by most county broadcast networks. 3. A third-level system which also uses mixed audio-frequency and high-frequency transmission and distributed amplification. It is based in counties, towns and villages, and has many advantages such as low transmission loss, high power, preservation of signal quality and low system voltage. The number of such systems is growing steadily. Because of the high construction cost and high maintenance cost of long-distance wired broadcasting systems, they are gradually being converted to FM transmission systems in recent years. With the rapid development of the electronic industry, China's wired broadcasting is advancing in the direction of multi-functional, multi-channel, high-quality, and stereo-sound systems.

Wired television is primarily used in a regional distribution network which relies on [coaxial] cables or optical fibers to deliver TV programs directly to private TV receivers; therefore it is also called cable television or closed-circuit television. Wired television can produce clearer pictures because it is not affected by shadow or ghost interference caused by large buildings. It can meet the needs of a wide range of TV viewers by providing not only transcribed programs from TV stations but also educational and arts programs aimed at different levels of TV viewers. It can also provide a solution to the growing problem of crowded channels and channel management due to the increasing number of wireless TV stations; a [coaxial] cable with a 300-MHz band can transmit almost 40 color TV programs simultaneously. In the late 1970's, wired television technology in China was sufficiently mature to produce complete sets of TV equipment and to promote the use of wired TV

transmission across the nation. Undoubtedly it will become a major part of China's broadcasting and propaganda network.

The next step in wired television development is two-way television: using the downlink signals (from television center to user) to transmit TV programs, and using the uplink signals (from user to television center) to transmit various data such as questions raised during a television lecture, TV shopping service, search request from a video library, monitoring the consumption of water, electricity and gas, and warning signals from security systems, fire detection systems and medical emergency systems.

Television Multiplex Broadcasting

In today's developing society, a large amount of data are used in both industrial production activities and commercial activities. In order to deliver the necessary financial information, weather information, traffic information, merchandise information, medical information, and sports and recreation information to thousands of families in a timely manner, TV multiplex broadcasting was developed. The so-called multiplex broadcasting is a new broadcasting scheme where conventional video and audio signals are multiplexed with other information by utilizing space slots in the frequency domain (e.g., adding subcarrier or carrier to the baseband) or in the time domain (e.g., using the blanking periods of horizontal and vertical retraces) to enhance the capacity of TV broadcast. With multiplex broadcasting, it is possible to increase the utilization of frequency resources without additional financial burden by using existing broadcast networks, TV centers and transmitting and receiving equipment. In recent years, China has made significant progress in this area of research, and is currently planning to implement the following three types of broadcast systems:

Dual-Audio-Channel Television Broadcasting. In this case, an additional audio channel (secondary audio channel) is added to the existing audio channel (primary audio channel) to allow simultaneous transmission of two different languages or delivery of programs in stereo sound. China has decided to use a dual-carrier system where the carrier frequency of the secondary audio channel is 6.742 MHz.

Teletext Broadcasting. By using the character multiplex lines (lines 17,18/330,331) during the blanking period of vertical trace, it is possible to transmit additional texts and pictures in conjunction with existing TV programs. It can deliver approximately 10 different programs which contain simple texts and pictures used in the broadcasting of news, weather forecasts, market information, traffic information, financial information, and sport information; it can also deliver closed captions specially designed for hearing-impaired viewers. This information can be made available to anyone equipped with a relatively simple receiver unit. If necessary, the information can also be printed for closer examination. China has already completed

experiments of teletext broadcasting using the graphics system; currently, a study is under way to try out a code system teletext broadcasting. It is expected that within the next few years, a decision on a standard system will be made and actual broadcasting will begin in some of the large cities.

Multi-Program Still Picture Broadcast. In this case, many TV pictures and associated audio sound are broadcast on the same TV channel; for example, an analog system can simultaneously transmit 46 video channels and a 5-kHz-wide audio channel. This type of multiplex system is primarily used for educational TV. China has already conducted experiments in TV multiplex broadcasting and in satellite transmission, and has established specifications for multi-program still-picture broadcasting which are consistent with the PAL-D system.

New System for Satellite-Transmitted Television Programs

Satellite-transmitted television signals are transmitted using wide-band (27 MHz) FM. However, in today's color television system, the color signal and the brightness signal are frequency-division multiplexed (the color subcarrier is placed at the high end of the brightness signal), which is not ideally suited for an FM system. In an FM transmission system, noise increases with frequency; hence the signal-to-noise ratio (SNR) of the color signal which is transmitted by a high-frequency subcarrier will be lower than that of the brightness signal, and becomes the limiting factor of system quality. In addition, the presence of a subcarrier may produce intermodulation between the color signal and the brightness signal, and distortions in differential gain and differential phase. Therefore, in the early 1980's, a new TV system called MAC (multiplexed analog components) was developed; it uses time-axial compressed, time-division MAC coding. In a MAC system, the brightness signal and the color signal in the same line are time-axis compressed (according to a fixed compression ratio), and then time-division multiplexed in an effective line period. During transmission, the brightness signal is transmitted on every line whereas the color signal is transmitted only on alternate lines. The MAC system is further divided into types B, C, D_1, and D_2 according to the different multiplex modes of the audio, data and video transmissions. The use of the MAC system to transmit TV programs through satellite channels has many advantages. For example, by using time-division transmission of brightness and color signals, the problems of brightness and color intermodulation, distortions in differential gain and differential phase, and imbalance between the brightness and color SNR are eliminated, and enhanced picture quality can be achieved; by judiciously utilizing the line-blanking periods and digital code modulation, four-to eight companded high-quality audio channels can be accommodated; also, by using digital error-protecting synchronization techniques, good video synchronization can be ensured even at low RF carrier-to-noise ratios. Furthermore, the use of line-blanking sound transmission eliminates the audio subcarrier, and removes the bandwidth constraint on the brightness

signal; therefore, the resolution of the received picture in a MAC system can be enhanced by simply increasing the transmission frequency band. It is also relatively easy to implement interference and security measures on the video and audio signals. In 1986 and 1987, closed-circuit simulation and satellite transmission experiments of the B-MAC and D_2-MAC systems were conducted in Shanghai and in Beijing respectively. A study is currently under way to decide on the format of China's satellite-transmitted television programs.

Improvement of the Picture Quality of Color Television

The picture quality of today's color television broadcasts still cannot match the quality of 35 mm movie film. The main problems are the following: inadequate resolution, intermodulation between brightness signals and color signals, inter-line flickering, large-area flickering at high brightness levels, and violation of the constant brightness principle caused by creep and γ correction. With the proliferation of color television broadcasts, TV viewers are demanding higher quality programs and becoming increasingly intolerant of these shortcomings. Therefore, by taking advantage of new technological developments in electronics and telecommunications, the Japan Broadcasting Association (NHK) and other research organizations in some developed countries have been studying new television systems ever since the late 1960's. Many of these research efforts are bearing fruit today and some of them have already been implemented in practice.

The NHK has developed high-definition television (HDTV) with 1125 lines/60 fields and 2:1 alternate line scanning; its horizontal and vertical resolution is higher than that of the existing format by a factor of two, and the transmitted and reconstructed information content is 5 times that of existing television. The width to height ratio of the picture screen is 5:3, the appropriate viewing angle is 30°, and the recommended viewing distance is three times the screen height--so that the large-screen color picture would appear more realistic and more colorful; its picture quality is considered comparable to that of 35 mm film. Japan already has plans to begin HDTV broadcast via the BS-3 satellite by 1990. Unfortunately, HDTV is not compatible with the existing color TV format (cannot be received by existing receivers), and cannot be transmitted by ground network because of the wide bandwidth requirement. Hence, it is not likely that this country will have HDTV until after the year 2000; nevertheless, there is little doubt that it will be the next-generation color television. Currently, China is not only closely following the technical development abroad but also conducting its own research on HDTV parameters and standards in preparation for future implementation of HDTV in this country. [See "Design of Digital Filters Used in Compatible HQTV System," JPRS-CST-88-011, 22 Jun 88, pp 117-124.]

In an effort to improve the picture quality of color TV before year 2000, China is investigating designs which are compatible with the

existing format; e.g., the improved-definition television (IDTV) and extended-definition television (EDTV). With IDTV, the existing broadcasting system remains unchanged; only the receiver is modified by replacing alternate-line scanning with line-by-line scanning to improve picture quality. EDTV is a high-resolution system which is compatible with the existing format; in this system, the existing broadcasting system is modified to facilitate signal processing at the receiving end; specifically, in addition to line-by-line scanning in the receiver, it is also necessary to enhance the horizontal resolution by transmitting the resolution component of the brightness signal. The width-to-height ratio of the picture screen is 16:9.

Digital Television

Up to now, television signals have been transmitted by analog means, which generally suffer degradations in SNR and distortion during transmission. By using digitized TV signals, such degradations are eliminated; also, digitized signals are not affected by the recording and copying processes in an audio or video recorder. Therefore, not only the quality of program production is improved, but the preservation of the program can be extended to allow digital processing of the signals to enhance the technical quality and the artistic impression of the program. With the development of digital technology and VLSI circuits, digital equipment is being used extensively in television broadcasting centers. Digital visual effects (DVE) have also been used to enliven the pictures and to produce remarkable special effects. In addition to the conventional cutting/switching techniques, various translational and rotational cutting/switching techniques are now being used. By using different key-control techniques, it is possible to add white or color captions on the screen, to insert one picture frame into another, and to superimpose the picture of an actor or an announcer onto a background scene to give the illusion that he is performing or broadcasting at a live scene. By using digital techniques, it is possible to compress, to expand, to freeze, and to rotate the picture; it is also possible to show the trajectory of a moving object, and to display double images. The Central Television State also uses a digital still-picture storage unit to provide pictures for display during blank periods between two programs; it is a computer-controlled high-speed picture storage and monitor system which can file more than 3,000 pictures extracted from the signal sources onto a magnetic disk; during replay, any picture can be retrieved within half a second.

At present, there are still a number of difficulties to overcome before complete digitization of the TV broadcast system can be realized. One difficulty is the complicated process of recording digital signals because of its large bandwidth requirement. Although the United States and Japan have developed digital video recorders of component signals or composite signals in recent years, their high cost makes it impractical for large-scale use except in the Central Television Station. The second difficulty is the transmission of digitized signals, again caused

by the large bandwidth; many countries are currently studying the problem of bandwidth compression. The third and most important difficulty is the fact that all existing TV receivers must be replaced by new digital receivers. For these reasons, digitization of TV broadcast in this country will be limited to studio use in the foreseeable future, and may be realized in program transmission at a later date; but direct broadcast to the general public is not expected to happen until after year 2,000. Nevertheless, digitization of TV signals is an inevitable trend in the developmental process of broadcast television technology; we must keep up with this technology and strive to achieve this higher standard for China's television broadcasting industry.

Briefs

Highest-Capacity Fiber-Optic Trunkline--The nation's highest-capacity long-distance digital fiber-optic communications project--a 205-km optical cable providing 7680 circuits between Fuzhou and Nanping [Fujian Province]--is now under construction. The project, part of which uses materials imported from the FRG, will be divided into two phases, with the first (3840 circuits) scheduled to be completed by 1 October 1989. [Summary] [40080117b Beijing RENMIN RIBAO in Chinese 14 Jan 89 p 2]

DAMA Satellite System Technology Certified--On 16 November 1988, the basic technology (backbone units) for an SCPC [single carrier per channel] decentralized-control demand assignment multiple access (DAMA) system developed by the satellite division of the Ministry of Posts & Telecommunication's (MPT) Research Institute 1 passed technical certification. In addition to MPT specialists, the accreditation committee included representatives of the Commission of Science, Technology and Industry for National Defense; the Shanghai Long-Distance Telecommunications Bureau; and the Shanghai Satellite Earth Station. After an on-site functional demonstration of the two terminals comprising the backbone units, Lou Hairi [2869 3189 2480], Director of MPT's Institute of Posts & Telecommunications, commented that this technology filled a domestic void. [Summary] [40080117c Shanghai DIANXIN KUAIBAO [TELECOMMUNICATIONS INFORMATION] in Chinese No 12, Dec 88 p 32]

Fiber-Optic Coupler Patented--A new fiber-optic coupler developed by design engineers Lu Wenquan [4151 2429 0356] and Jin Wujun [6855 2976 0193] of the Guilin Laser Communications Research Institute received a patent at the end of last year and is now in batch production at the fiber-optic components plant run by the Guilin civil administration. This new improved coupler will mainly be used in laser medical instruments and in fiber-optic transmission units. [Summary] [40080129a Beijing ZHONGGUO DIANZI BAO in Chinese 27 Jan 89 p 1]

First DMW Trunkline in Southwest--The first digital microwave (DMW) trunkline in the Southwest--a major project of the [former] Ministry of Water Resources and Electric Power during the Sixth 5-Year Plan--is now [formally] operational. The Guiyang-to-Zunyi (Guizhou Province) 123.9-km line consists of six microwave stations and is basically oriented to high-quality digital telephone, but can also transmit data and sports information. A six-months-plus trial operation demonstrated that the system's overall design complies with recommended standards of the Consultative Committee on [International] Radio [CCIR]. The system was designed, built, and installed by the China Zhenhua [2182 5478] Electronic Industries Company's Red Flag Machinery Plant. [Text] [40080129b Beijing ZHONGGUO DIANZI BAO in Chinese 27 Jan 89 p 1]

Properties of Co-Adsorption of K With O on Ag(110) Surface Studied by XPS, UPS, EELS, LEED

40090036d Beijing WULI XUEBAO [ACTA PHYSICA SINICA] in Chinese Vol 37 No 11, Nov 88 pp 1785-1793

[English abstract of article by Wu Mingcheng [0702 7686 2052] of the Laboratory of Surface Physics, Fudan University, Shanghai]

[Text] The properties of co-adsorption of K with O on the Ag(110) surface have been investigated with X-ray photoelectron spectroscopy (XPS), ultraviolet photoelectron spectroscopy (UPS), electron energy loss spectrometry (EELS) and low energy electron diffraction (LEED). It is shown that, at low potassium coverages, there are two distinct oxygen species on the Ag(110) which are determined as the dissolved and chemisorbed atomic oxygen species. With K coverage increasing, the molecular oxygen is developed which is associated with sub-surface K. These oxygen species peaks can be clearly distinguished from UPS as well as XPS. The initial adhesive coefficient of the K precovered Ag surface for oxygen adsorption is enhanced. K and O display a mutual enhancement of surface to bulk transport. Monolayer K atoms form a (1 x 2) LEED pattern on the Ag(110) surface, which is consistent with the early results. The surface structure, however, transfers into a (2 x 1) ordered structure when oxygen is exposed to the surface. A model for the co-adsorption of K with O on the Ag(110) is proposed.

References

1. DePaola, R.A., Hrbek, J., Hoffmann, F.M., J CHEM PHYS, Vol 82, 1985 p 2484.
2. Crowell, J.E., Garfunkel, E.L., Somorjai, G.A., SURF SCI, Vol 121, 1982 p 303.
3. Surnev, L., Rangelov, G., Kiskinova, M., SURF SCI, Vol 179, 1987 p 303.
4. Ayyoob, M., Hegde, M.S., SURF SCI, Vol 133, 1983 p 516.
5. Kitson, M., Lambert, R.M., SURF SCI, Vol 109, 1981 p 60.
6. Döhl-Oelze, R., Sture, E.M., Sass, J.K., SOLID STATE COMMUN, Vol 57, 1986 p 323.
7. Wijers, C., Adriaens, M.R., Feuerbacher, B., SURF SCI, Vol 80, 1979 p 317.
8. Muscat, J.P., Newns, D.M., SURF SCI, Vol 84, 1979 p 262.
9. Wallden, L., Lindgren, S.A., SOLID STATE COMMUN, Vol 28, 1978 p 283.

10. Lindgren, S.A., Wallden, L., PHYS REV, Vol B22, 1980 p 5967.
11. Rao, C.N.R., Vishnu Kamath, P., Yashonath, S., CHEM PHYS LETT, Vol 88, 1982 p 13.
12. Raether, H., ed., "Excitation of Plasmons and Interband Transitions by Electrons," SPRINGER TRACTS IN MODERN PHYSICS, Vol 88, 1980 p 50.
13. Rovida, G., J ELECTRON SPECTROSC RELAT PHENOMENA, Vol 1, 1973 p 296.
14. Ehrenreich, H., Philipp, H.R., PHYS REV, Vol 128, 1962 p 1622.
15. Engelhardt, H.A., Menzel, D., SURF SCI, Vol 57, 1976 p 591.
16. Prince, K.C., Paolucci, G., Bradshaw, A.M., SURF SCI, Vol 175, 1986 p 101.
17. Jacobi, K., Scheffler, M., Kambe, K., Forstmann, F., SOLID STATE COMMUN, Vol 22, 1977 p 17.
18. Garfunkel, E.L., Somorjai, G.A., SURF SCI, Vol 115, 1982 p 441.
19. Surnev, L., Rangelov, G., Bertel, E., Netzer, F.P., SURF SCI, Vol 184, 1987 p 10.
20. Rösch, N., "Electrons in Finite and Infinite Structures," eds. P. Phariseau, L. Scheire, Plenum Press, New York, 1977 p 120.

Piezoresistive Properties of Boron-Doped PECVD μc-Si Films

40090036e Beijing WULI XUEBAO [ACTA PHYSICA SINICA] in Chinese Vol 37 No 11, Nov 88 pp 1794-1799

[English abstract of article by Guo Shuwen [6753 6615 2429], et al., of Shanghai Institute of Metallurgy, Chinese Academy of Sciences]

[Text] The piezoresistive properties of boron-doped PECVD microcrystalline Si films (μc-Si) deposited on SiO_2 coated Si, covar or quartz substrates have been investigated. The relationships between the gauge factor (GF) and doping concentrations, as well as the film thickness, etc., have been obtained experimentally. The maximum longitudinal GF of 25 and 20 are measured for Si and covar substrates, respectively. An expression for calculating the GF of p-type μc-Si is derived theoretically by using the splitting model of the heavy and light hole bands at $k = 0$ and the thermionic emission theory. The calculated dependences of GF on the doping concentrations, grain size and trap state density agree well with the experimental results, which offer a better understanding of the piezoresistive characteristics of μc-Si or poly-Si, and enable the design and fabrication of the μc-Si or poly-Si strain gauges to be optimized.

References

1. Jaffe, J.M., ELECTRONICS LETTERS, Vol 10, 1974 p 420.
2. Seto, John Y.W., J APPL PHYS, Vol 47, 1976 p 4780.
3. Schubert, D., et al., SENSORS AND ACTUATORS, Vol 11, 1987 p 145.
4. French, P.J., Evans, A.G.R., SENSORS AND ACTUATORS, Vol 8, 1985 p 219.
5. Germer, W., SENSORS AND ACTUATORS, Vol 7, 1985 p 135.
6. French, P.J., Evans, A.G.R., "Transducers '87," 1987 pp 379-382.
7. He Yuliang, et al., SCIENCE BULLETIN, Vol 27, 1982 p 1037.
8. Iqbal, Z., Veprek, S., APPL PHYS LETT, Vol 36, 1981 p 163.
9. Iqbal, Z., Veprek, S., SOLID STATE COMMUN, Vol 37, 1981 p 993.
10. Hamaski, T., et al., JPN J APPL PHYS, Vol 20 No 2, 1981 p L84.
11. Lu, Nicky Chau-Chun, et al., IEEE TRANS ELECTRON DEVICES, Vol ED-28, No 7, 1981 p 818.
12. Seto, John Y.W., J ELECTROCHEM SOC, Vol 122, 1975 p 701.

13. Tufle, O.N., Stelier, E.L., PHYS REV, Vol 133, 1964 p A1705.
14. Seto, J.Y.W., J APPL PHYS, Vol 46, 1975 p 5247.
15. Kanda, Yozo, IEEE TRANS ELECTRON DEVICES, Vol ED-29 No 1, 1975 p 64.
16. Wortman, J.J., Evans, R.A., J APPL PHYSICS, Vol 36 No 1, 1965 p 153.
17. Kanda, Yozo, JPN J APPL PHYS, Vol 6 No 4, 1967 p 475.

Study of Structural Relaxation of Metallic Glass $(Fe_{0.85}Ni_{0.15})_{84}B_{16}$ by Measuring Thermal Expansion, Resistance Under Zero Stress

40090036g Beijing WULI XUEBAO [ACTA PHYSICA SINICA] in Chinese Vol 37 No 11, Nov 88 pp 1855-1858

[English abstract of article by Yao Cishun [1202 1964 7311] of North China University of Technology, Beijing; Cheng Xian'an [4453 0341 1344] of the Department of Applied Mathematics and Physics, Beijing Institute of Aeronautics and Astronautics]

[Text] The dependence of the structural relaxation of the material on the annealing temperature T_a is studied by measuring the difference of thermal elongation $\Delta\ell$ or that of the electrical resistivity $\Delta\rho$ and that of the thermal expansion coefficient $\Delta\alpha$ between an as-quenched and an annealed sample. $\Delta\alpha/\alpha_0$ is measured by placing an as-quenched and an annealed sample in juxtaposition and heating them with iodine-tungsten lamps. The samples expand freely.

The experimental results are summarized by three curves, i.e., $\Delta\alpha/\alpha_0$ vs T_a, $\Delta\ell/\ell_0$ vs T_a and $\Delta\rho/\rho_0$ vs T_a, where α_0, ℓ_0, and ρ_0 are the linear expansion coefficient, the length and the resistivity of the as-quenched sample, respectively. The results obtained are discussed.

References

1. Neuhäuser, H., J PHYS E, Vol 18, 1985 p 1058.
2. Komatsu, T., J NON-CRYST SOLIDS, Vol 57, 1983 p 129.

Neutron Diffraction Study of $Y_2(Fe_{1-x}Si_x)_{14}B$

40090036i Beijing WULI XUEBAO [ACTA PHYSICA SINICA] in Chinese Vol 37 No 11, Nov 88 pp 1908-1909

[English abstract of article by Yang Jilian [2799 4949 1670], et al., of the Institute of Atomic Energy, Beijing; Yang Yingchang [2799 2019 2490], et al., Department of Physics, Beijing University]

[Text] The outstanding permanent magnetic material $Nd_2Fe_{14}B$ possesses a very high energy product. However, its Curie temperature is a little bit too low for practical application. Some elements were added to the material in order to raise the Curie temperature. Reference 9 and the authors' recent experimental results show that the Curie temperature can be raised by partially substituting silicon for iron in the material and in the $Y_2Fe_{14}B$. In order to understand the effect of silicon on magnetism, the occupancy of Si in $Y_2Fe_{14}B$ was studied by neutron diffraction. The neutron diffraction results show that silicon preferentially occupies the sites of c, j_1 and k_2. The magnetic interaction theory is applied to explain the experimental results.

References

1. Sinnema, S., et al., J MAGN MAGN MATER, Vol 44, 1984 p 333.
2. Cadogon, J.M., Coey, J.M.D., PHYS REV, Vol B30, 1984 p 7326.
3. Herbst, J.F., Yelon, W.B., J APPL PHYS, Vol 60, 1986 p 4224.
4. Croat, J.J., et al., APPL PHYS LETT, Vol 44, 1984 p 148.
5. Rietveld, H.M., J APPL CRYSTALLOGR, Vol 2, 1969 p 65.
6. Givord, D., et al., SOLID STATE COMMUN, Vol 50, 1984 p 497.
7. Herbst, J.F., et al., PHYS REV, Vol B29, 1984 p 4176.
8. Kahn, R.W., ed., "Physical Metallurgy," 1st edition, Science Press, Feb 1984 p 73.
9. Hu Boping, et al., ACTA PHYSICA SINICA, Vol 36, 1987 p 1363.
10. Givord, D., et al., SOLID STATE COMMUN, Vol 51, 1984 p 857.

Plasma Physics Institute Scores Success in Fusion Research

40080081a Beijing GUANGMING RIBAO in Chinese 23 Nov 88 p 1

[Article by reporter Xue Changci [5641 2490 6101]]

[Excerpts] Fusion of the hydrogen contained in 1 kilogram of sea water releases an amount of energy equal to that of 300 liters of gasoline. It may sound like fantasy, but science is getting closer to that goal, every day, according to an official of the Plasma Physics Institute of the Chinese Academy of Sciences.

Fusion research is basic scientific research. The Plasma Physics Institute of CAS is a small research institute of 460 people. Its annual budget is only 4 million yuan, which is really a drop in the bucket for enormously expensive fusion research. But the workers did not complain or wait for help to come. They used medium and small facilities to study the law of motion of high-temperature plasmas and established the HT-6M Tokamak system. The system employs advanced structure and a complete set of diagnostic equipments. It has reached the 1980's international standard of similar machines and was awarded the first prize in science and technology by the CAS. The Institute also developed a state of the art multichannel far infrared interferometer and achieved automatic data acquisition and processing. In 10 years they have built 8 megawatts of substations, 80 megawatts of dc flywheel pulse generators and a medium size electrophysical plant. With the exception of some purchased items, these facilities were basically domestically built, resulting in great savings of funds. Four hundred million yuan were saved on just the Takomak laboratory alone. Using these facilities, they produced valuable research results in science and technology. The study of the magnetic fluid properties of plasma in a helical field was praised by scientists of the world and received a first prize of the CAS. In the past 10 years the Institute received a total of two first prizes, 10 second prizes and 8 third prizes. The fusion research of the Institute not only is a leader in China, but has also received the attention of the international fusion field.

The Institute should take full advantage of the reform and open door policy and broadly develop international cooperation and exchange. One of the unique features of the Institute should be the training of a modern research team with international support. Fusion research is pursued by many countries in the world; developed countries spent great amounts of money and made early starts. These countries have accumulated a wealth of information. In the last few years the Institute has sent more than 80 researchers to work or pursue Ph.D. degrees in the laboratories of developed nations. More than 50 have returned to their posts. Almost all the main investigators that move the project forward have had 1 or 2 years of overseas experience. [passage omitted] The Institute has gained international trust by relying on its own research results. The Institute also insists that the people it sends overseas should serve research in the Institute. Personnel returning from abroad are not allowed to start new topics of research. Opinions of foreign experts are selected based on our own research goals. Based on our strength, we have earned the confidence of a number of countries. A dozen countries have invited our personnel to visit and work, and each year there are 50 scientists coming to the Institute to visit and work. The fusion laboratory of University of Texas in the United States requested the Institute to design and build vacuum chambers for them, and Brazil asked it to design medium and small Tokamaks. Some say that the Institute has a bigger name in foreign countries than in China. [passage omitted]

END